

EXPERIMENTAL USE OF SATELLITE-DE-
RIVED DATA IN NUMERICAL ANALYSIS
AND THE EFFECT ON A PRIMITIVE
EQUATION PREDICTION SCHEME

Thomas Joseph Mantei

United States Naval Postgraduate School



THESIS

EXPERIMENTAL USE OF SATELLITE-DERIVED DATA
IN NUMERICAL ANALYSIS AND THE EFFECT
ON A PRIMITIVE EQUATION PREDICTION SCHEME

by

Thomas Joseph Mantei
and
Charles Edwin Workman

Co-Thesis Advisors:

Harry D. Hamilton
Robert J. Renard

December 1971

Approved for public release; distribution unlimited.

Experimental Use of Satellite-Derived Data
in Numerical Analysis and the Effect
on a Primitive Equation Prediction Scheme

by

Thomas Joseph Mantei
Lieutenant Commander, United States Navy
B.S., Marquette University, 1962

and

Charles Edwin Workman
Lieutenant Commander, United States Navy
B.S., Yale University, 1954; M.A., University of Texas, 1961

Submitted in partial fulfillment of the
requirements for the degree of

MASTER OF SCIENCE IN METEOROLOGY

from the

NAVAL POSTGRADUATE SCHOOL
December 1971

ABSTRACT

The results of an experiment to test the utility of satellite-observed data for enhancing the accuracy and detail of numerical analyses and its effect on the attendant primitive equation (PE) prognoses is presented. The test, carried out in the framework of Fleet Numerical Weather Central's system, employed SIRS data and various quasi objective techniques to establish bogus pressure/height and wind data at sea level/500 mb over the North Pacific Ocean area. The resulting satellite-modified analyses for five synoptic times, in the period 10-12 March 1971, were used to generate PE prognoses from 1200 GMT 10 March and 0000 GMT 11 March 1971. Comparison with PE prognoses from analyses dependent only on conventional data indicated relatively more improvement at sea level than at 500 mb. The complex results are interpreted in terms of the initialization of the analyzed fields, known behavioral characteristics of the PE model, the mechanics of the modification procedures and the experience level of the analysts.

TABLE OF CONTENTS

I.	INTRODUCTION	-----	12
II.	BACKGROUND	-----	14
	A.	SUBJECTIVE ANALYSIS CHANGES FROM THE INTERPRETATION OF VIDEO AND INFRARED WEATHER SATELLITE OBSERVATIONS	----- 15
	B.	CLOUD-MOTION VECTOR WINDS	----- 15
	C.	STATISTICALLY DERIVED 500 mb HEIGHTS FROM SATELLITE-OBSERVED CLOUD PATTERNS	----- 18
	D.	SATELLITE INFRARED SPECTROMETER (SIRS) PRESSURE-TEMPERATURE SOUNDINGS	----- 20
III.	DATA SOURCES AND SELECTION OF STUDY PERIOD	-----	29
IV.	PROCEDURES AND RESTRICTIONS	-----	33
V.	CASE STUDIES OF MODIFICATIONS TO ANALYSES	-----	37
VI.	RESULTS	-----	62
	A.	ANALYSIS	----- 62
	B.	PROGNOSES	----- 68
	C.	VERIFICATIONS	----- 83
VII.	CONCLUSIONS AND RECOMMENDATIONS FOR FURTHER STUDY	-----	103
APPENDIX A	COMPUTER RECTIFIED PHOTOGRAPHS OF ATS-1 OBSERVATIONS; 1800 GMT 9-12 MARCH 1971	-----	105

APPENDIX B COMPARISON OF NORTHERN HEMISPHERE SIRS
 500 mb HEIGHTS AND FNWC MONTEREY 500 mb
 ISOHYPTIC ANALYSES FOR 9-14 MARCH 1971 ----- 109

APPENDIX C COMMENTS ON PROCEDURES USED TO DETERMINE
 BOGUS DATA ----- 112

BIBLIOGRAPHY ----- 114

INITIAL DISTRIBUTION LIST ----- 117

FORM DD 1473 ----- 118

LIST OF TABLES

<u>Table</u>		<u>Page</u>
I.	Sources of conventional and satellite data -----	31
II.	Evaluation of prognoses difference fields -----	85
III.	A comparison of SIRS 500 mb heights to FNWC Monterey 500 mb isohyptic analyses for the Northern Hemisphere, 9-14 March 1971 -----	111

LIST OF ILLUSTRATIONS

<u>Figure</u>		<u>Page</u>
1.	NESS cloud motion vector winds from ATS-1 and ATS-3 satellite photographs: 300 mb level, 0000 GMT 12 March 1971 -----	17
2.	Schematic representation of the relationship between a cloud pattern and features of the 500 mb relative vorticity field -----	21
3.	Geometrical construction for determining the diameter and amplitude of a cloud system -----	22
4a.	Worksheet for solution of the Nagle-Hayden regression equation to determine the 500 mb height at a spiral cloud center (SCC) -----	23
4b.	Worksheet grid compatible with FNWC 4-P-1 chart -----	24
5.	NMC update 500 mb SIRS coverage for 0000 GMT 12 March 1971 -----	27
6.	500 mb analyses: 0000 GMT 10 March 1971 -----	52
7.	Sea-level pressure analysis: 0000 GMT 10 March 1971 ---	52
8.	Video mosaic from ITOS-1: " " " " " ---	53
9.	500 mb analyses: 1200 GMT 10 March 1971 ---	54
10.	Sea-level pressure analyses: 1200 GMT 10 March 1971 ---	54
11.	Photo of ITOS-IR mosaic: " " " " " ---	55
12.	500 mb analyses: 0000 GMT 11 March 1971 ---	56
13.	Sea-level pressure analyses: 0000 GMT 11 March 1971 --	56
14.	Video mosaic from ITOS-1: " " " " " ---	57
15.	500 mb analyses: 1200 GMT 11 March 1971 ---	58
16.	Sea-level pressure analyses: 1200 GMT 11 March 1971 --	58
17.	Photo of ITOS-IR mosaic: " " " " " ---	59
18.	500 mb analyses: 0000 GMT 12 March 1971 ---	60
19.	Sea-level pressure analyses: 0000 GMT 12 March 1971 -	60
20.	Video mosaic from ITOS-1: " " " " " --	61
21.	500 mb 12 hr prognoses from 1200 GMT 10 March 1971 --	74
22.	Sea-level " " " " " " " " --	74

23.	500 mb 24 hr prognoses from 1200 GMT 10 March 1971	----	75
24.	Sea-level " " " " " " " "	----	75
25.	500 mb 36 hr " " " " " " " "	----	76
26.	Sea-level " " " " " " " "	----	76
27.	500 mb 48 hr " " " " " " " "	----	77
28.	Sea-level " " " " " " " "	----	77
29.	500 mb 12 hr " " 0000 GMT 11 March 1971	----	78
30.	Sea-level " " " " " " " "	----	78
31.	500 mb 24 hr " " " " " " " "	----	79
32.	Sea-level " " " " " " " "	----	79
33.	500 mb 36 hr " " " " " " " "	----	80
34.	Sea-level " " " " " " " "	----	80
35.	500 mb 48 hr " " " " " " " "	----	81
36.	Sea-level " " " " " " " "	----	81
37.	500 mb 48 hr PROG Differential " " " "	----	82
38.	500 mb 12 hr PROGS vs STACKANAL: 1200 GMT 10 March	----	90
39.	Sea-level " " " " " " " " " "	----	90
40.	500 mb 24 hr " " " " " " " " " "	----	91
41.	Sea-level " " " " " " " " " "	----	91
42.	500 mb 36 hr " " " " " " " " " "	----	92
43.	Sea-level " " " " " " " " " "	----	92
44.	500 mb 48 hr " " " " " " " " " "	----	93
45.	Sea-level " " " " " " " " " "	----	93
46.	500 mb 12 hr " " " " 0000 GMT 11 March	----	94
47.	Sea-level " " " " " " " " " "	----	94
48.	500 mb 24 hr " " " " " " " " " "	----	95
49.	Sea-level " " " " " " " " " "	----	95
50.	500 mb 36 hr " " " " " " " " " "	----	96
51.	Sea-level " " " " " " " " " "	----	96
52.	500 mb 48 hr " " " " " " " " " "	----	97
53.	Sea-level " " " " " " " " " "	----	97

54.	500 mb 12 hr PROGS vs BEST corres ANAL: 1200 GMT 10 March	-- 98
55.	Sea-level " " " " " " " " " "	-- 98
56.	500 mb 24 hr " " " " " " " " " "	-- 99
57.	Sea-level " " " " " " " " " "	-- 99
58.	500 mb 36 hr " " " " " " " " " "	--100
59.	Sea-level " " " " " " " " " "	--100
60.	500 mb 12 hr " " " " " 0000 GMT 11 March	--101
61.	Sea-level " " " " " " " " " "	--101
62.	500 mb 24 hr " " " " " " " " " "	--102
63.	Sea-level " " " " " " " " " "	--102
64.	Photo of ATS-1 observations about 1800 GMT 09 March 1971	--105
65.	" " " " " " 10 " "	--106
66.	" " " " " " 11 " "	--107
67.	" " " " " " 12 " "	--108

ABBREVIATIONS

ADP	Automated Data Processing
APT	Automatic Picture Transmission
ATS	Applications Technology Satellite
AVCS	Advanced Vidicon Camera System
CDA Station	Command & Data Acquisition Station
EPRF	Environmental Prediction Research Facility, Monterey, California
ESSA	Environmental Science Service Administration
FAMOS	Fleet Application of Meteorological Observations from Satellites
FNWC	Fleet Numerical Weather Central (Monterey)
FOFAX	Forecasters Facsimile Circuit
FWC	Fleet Weather Central
FWF	Fleet Weather Facility
IR	Infrared
ITOS	Improved TIROS Operational Satellite
NAFAX	National Facsimile Circuit
NASA	National Aeronautics and Space Administration
NEDN	Naval Environmental Data Network
NESS	National Environmental Satellite Service
NESC	National Environmental Satellite Center
NMC	National Meteorological Center

NOAA	National Oceanic and Atmospheric Administration
NWRF	Navy Weather Research Facility (redesignated EPRF)
NWSED	Naval Weather Service Environmental Detachment
PE	Primitive Equation prognosis model
SCC	Spiral Cloud Center
SINAP	Satellite Input to Numerical Analysis and Prediction
SIRS	Satellite Infrared Spectrometer
SRI	Stanford Research Institute
SSCC	Spin Scan Cloud Camera
TIROS	Television Infrared Observation Satellite

ACKNOWLEDGEMENT

The authors especially thank Dr. Robert J. Renard for his guidance, advice, and constant help during this thesis work. Commander Harry D. Hamilton, USN, is singled out for his technical support at every step of the research effort. Project FAMOS personnel, especially Mr. Fred Bittner and AG1 Robert Harbold, USN, spent many hours obtaining the necessary satellite data without which this thesis could not have been written. Mr. Roland Nagle of the National Environmental Satellite Service graciously supplied his latest predictor coefficients and working materials for the statistical 500 mb height derivations. Mr. Ted Hesse of PNWC Monterey handled the programming of the re-analyses and was an unfailing source of help. His assistance and friendship were invaluable to the authors. Lt (j.g.) Peter Hildebrand was responsible for generating the many Varian plotter maps used in this study. Lastly, the patience, moral support, and typing assistance of our wives are noted with deep appreciation.

I. INTRODUCTION

This thesis reports on a preliminary scheme for integrating four methods of converting satellite-observed data into conventional parameters for incorporation into the data base of an operational numerical analysis program. The four methods utilized are: 1) subjective changes to the current analyses based on the interpretation of video and infrared (IR) weather satellite observations; 2) cloud-motion vector winds from satellite time-lapse photographs; 3) statistically-derived 500 mb heights from satellite-observed cloud patterns; and 4) statistically derived pressure-temperature soundings from satellite infrared spectrometer (SIRS) radiance observations.

The data derived from these methods were used in the objective re-analyses of the Fleet Numerical Weather Central, Monterey (FNWC), sea-level pressure and 500 mb height fields at five synoptic times for the period 10-12 March 1971. Two dates were selected for making parallel numerical prognoses, with and without satellite data, by using the FNWC primitive equation (PE) model.¹

¹In the foregoing discussion, the following terms are used:
UNMOD ANAL--analysis derived from conventional data only.
MOD ANAL --analysis derived from conventional data and satellite
 observations.
UNMOD PROG--prognosis generated from the UNMOD ANAL.
MOD PROG --prognosis generated from the MOD ANAL.

Though the generation of quantitative data from the satellite observations was not accomplished in real time, the scheme followed may be adapted easily to the operational schedule at a major computer center which has access to satellite observations.

II. BACKGROUND

The major meteorological centers rely almost entirely on conventional synoptic data (i.e., surface observations, rawinsondes, airesps, etc.) for their operational numerical analysis and prediction schemes. The question of incorporating largely qualitative satellite video and radiance observations into this automated computer system is frequently referred to as the SINAP (satellite input to numerical analysis and prediction) problem [8] .

Conventional sources of data are frequently scarce over the Pacific and Atlantic Oceans. Here, satellite-observed cloud patterns attain their best development, and radiance measurements have their least contamination owing to the absence of hot or high terrain, snow or ice reflection, and so forth. Consequently, the thrust of satellite meteorology this past decade has been to quantify satellite information from these oceanic regions, particularly the North Pacific Ocean, because the poor conventional data base there can lead to erroneous numerical predictions in terms of accurate weather forecasts for North America.

Four methods for attacking the SINAP problem have received strong emphasis. The general background of these methods follows.

A. SUBJECTIVE ANALYSIS CHANGES FROM THE INTERPRETATION OF VIDEO AND INFRARED WEATHER SATELLITE OBSERVATIONS

Subjective changes to either manual or objective analysis have been undertaken since the first meteorological satellite video pictures were received in 1960. Global video coverage was realized with the launching of TIROS IX in 1965. Since 1964, infrared sensors have provided displays of cloud patterns similar to the video pictures, but with significant diagnostic differences. Global infrared nighttime coverage was made operationally available with the launching of ITOS I in 1970.

In general, the synoptic meteorologist interprets the position or intensity of important weather features from a visual study of current satellite pictures. He then changes the operational analyses by either manually re-analyzing the weather charts or by fabricating "bogus" pressure, temperature, or wind values to insert into a computer re-analysis scheme.

Numerous studies report the substantial progress made in the interpretation of synoptic-scale cloud patterns and the incorporation of the satellite data into subjective or objective (numerical) analysis schemes. The reader is especially directed to Refs. 1, 7, 12, 14, 17, and 26 for video interpretations and to Ref. 15 for infrared imagery interpretations. Terminology developed in these references will be used in this thesis.

B. CLOUD-MOTION VECTOR WINDS

Since the earliest satellite pictures of cloud patterns, meteorologists have attempted to obtain wind estimates from such features as

cirrus "blow-off" from cumulonimbus clouds, cirrus patterns associated with jet streams, apparent intensity of tropical storms, and so forth. Great impetus was given to this method with the launching of the geostationary Applications Technology Satellites, namely ATS-1, over the Pacific Ocean equator in November 1967. Time-lapse photographs are taken with the Spin-Scan Cloud Camera (SSCC) approximately every 25 minutes during daylight hours. From the geostationary altitude of approximately 19,000 nmi, the camera has a resolution of two miles at zero nadir angle, and views a geographical region from about 50 S to 50 N latitudinally and over 100 degrees of longitude along the equator. Consequently, excellent daylight video coverage of cloud systems is obtained over the oceanic tropical and subtropical areas where conventional data are normally sparse. Appendix A contains ATS-1 photographs taken at approximately 1800 GMT for 9-12 March 1971.

Utilizing methods developed primarily at the Stanford Research Institute (SRI) [19, 20, 21], NESS personnel produce wind estimates from film loops of ATS time-lapse photographs. An individual scan is superimposed on a map of appropriate scale and projection, particular cloud elements are selected and judged to be either upper level (near 300 mb) or low level (near 850 mb), and marked for study. These cloud elements are then followed on successive frames for at least one hour in order to obtain a wind estimate.

An example of the operational output of ATS wind data from NESS is shown in Fig. 1. These data are incorporated into the National

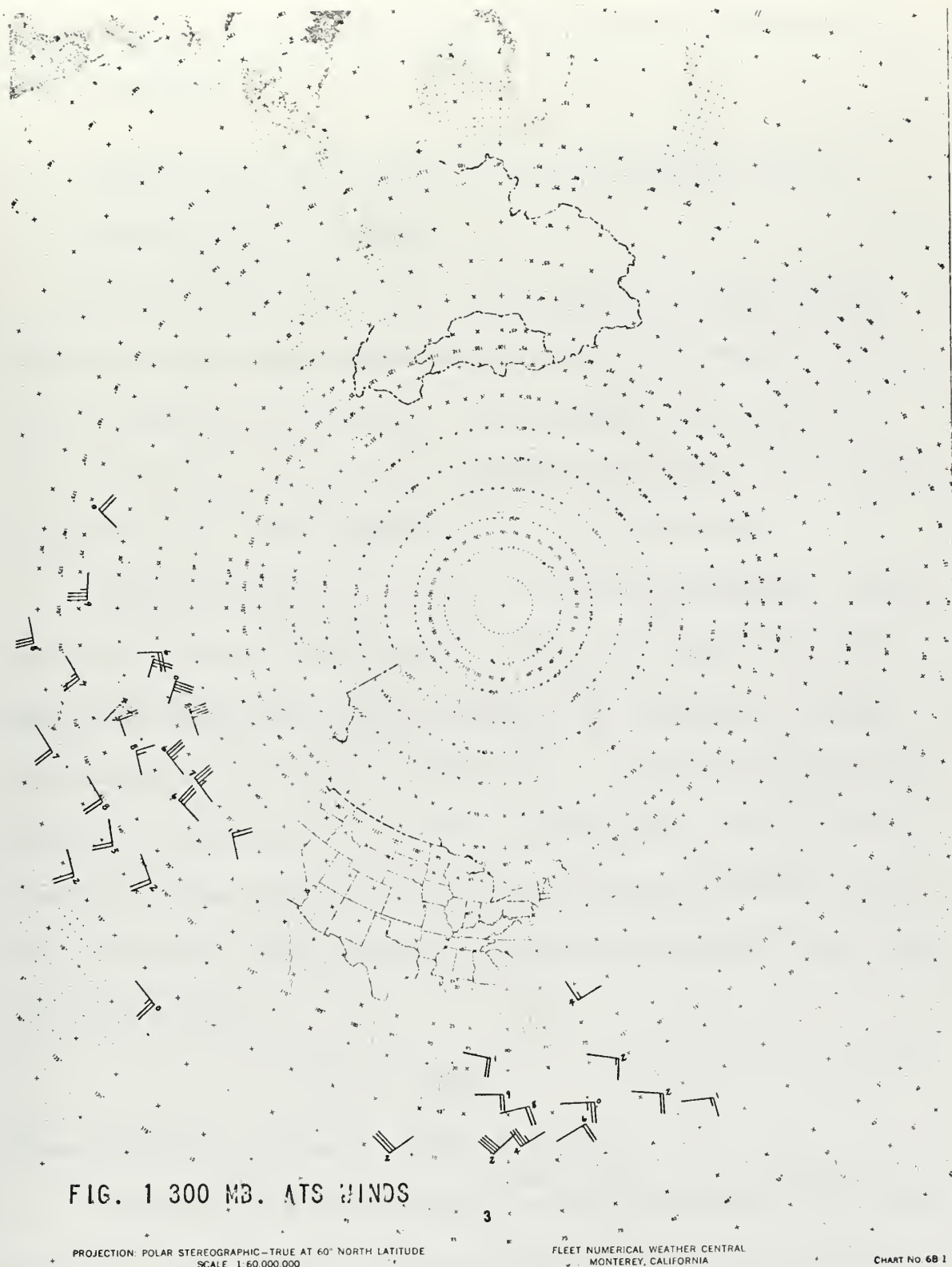


Fig. 1. 0000 GMT 12 March 1971 ATS winds

Meteorological Center's (NMC) 0000 GMT Northern Hemisphere and tropical analyses.

C. STATISTICALLY DERIVED 500 mb HEIGHTS FROM SATELLITE-OBSERVED CLOUD PATTERNS

In 1968, Nagle and Clark [5, 18] reported on a quasi-objective method of incorporating satellite-derived cloud pattern information into a 500 mb numerical analysis scheme. Subsequently, Nagle and Hayden [10] further refined this technique at NESS, developing operational procedures used by the NMC quality control group since 1969.

The NESS technique consists of the following procedures. The 12-hour 500 mb prognosis from 1200 GMT, which forms the "first guess" field for the subsequent 0000 GMT analysis, is subjected to a pattern-separation program developed by Holl [6]. Two of the several fields produced by this program are the SR or residual pattern, which may be considered a space mean field depicting the long-wave pattern, and the SD or disturbance field, depicting the short-wave features. These fields are additive, that is

$$Z = Z_{SR} + Z_{SD} \quad (1)$$

where Equations (1) through (5) refer to 500 mb.

Assuming the SR field is quasi-conservative with time and a perfect prognosis, the SR prognostic value accurately specifies the current (t_0) SR value. Obtaining the current 500 mb value then reduces to specifying the current SD value at the particular location:

$$Z_{t_0} = Z_{\text{SR 12 hr prog}} + Z_{\text{SD}_{t_0}} \quad (2)$$

(t₋₁₂ to t₀)

Over data-sparse oceanic regions, conventional observations normally will not adequately describe the fast-changing SD (t₀) short-wavelength disturbances. This SD value is obtained by statistically linking it to characteristic features of real-time, satellite-observed cloud patterns:

$$Z_{t_0} = Z_{\text{SR 12 hr prog}} + Z_{\text{SD}_{t_0}} \quad \begin{array}{l} \text{(derived from current} \\ \text{cloud pattern)} \end{array} \quad (3)$$

(t₋₁₂ to t₀)

The SD field approximates that of the geostrophic relative vorticity with algebraic sign reversed. Developing cloud systems on the synoptic scale are related to the vertical motion associated with the positive advection of vorticity in the upper troposphere [9] . Thus, a strong positive correlation has been obtained between negative centers in the SD field and centers of spiral (vortical) cloud patterns [5, 18, 10, and Mr. F. Bittner,² personal communication, 1971] . An adjunct of this relationship is the correlation of the zero line of the SD field (i.e., zero relative vorticity) with cloud patterns. Thus, superimposing the zero SD line upon the SR field immediately yields the current 500 mb height from the relationship

$$Z_{t_0} = Z_{\text{SR 12 hr prog}} + Z_{\text{SD}_{\text{Zero line}}} \quad (4)$$

(t₋₁₂ to t₀)

$$= Z_{\text{SR 12 hr prog}} \quad (5)$$

(t₋₁₂ to t₀)

²Mr. Fred Bittner of Project FAMOS. (This is the popular designator for the Naval Weapons Engineering Support Activity, Iverson Mall, 3737 Branch Ave., Room 307, Hillcrest Heights, Maryland).

Fig. 2 gives a schematic representation of many of these correlated relationships between the satellite-observed patterns and the 500 mb SD disturbance field.

The magnitude of the SD minimum value at the spiral cloud center (SCC) is obtained from the solution of a regression equation whose predictors are: a) latitude of the SCC, b) maximum diameter of the SCC cloud system, c) amplitude of the SCC cloud system, and d) the Laplacian of the SR field at the SCC. The method for measuring diameter and amplitude of the spiral cloud pattern is illustrated in Fig. 3. An alternate regression equation involving only the latitude of the SCC and the Laplacian of the SR field at the SCC also has been developed by Nagle and Hayden for situations where the amplitude and diameter of the cloud pattern are not readily obtained from the satellite picture.

Both of these regression equations are shown in worksheet form in Fig. 4. The predictor coefficients and constants in the worksheet were given to the authors by Mr. Nagle in June 1971. (These coefficients are derived from continuing statistical analyses of dependent case studies of the pattern-separated components of the NMC numerical 500 mb analysis and spiral cloud systems in the North Atlantic Ocean.)

D. SATELLITE INFRARED SPECTROMETER (SIRS) PRESSURE-TEMPERATURE SOUNDINGS

Satellite radiance measurements have been available to meteorologists since the launching of the first TIROS satellite in 1960. Although the potential of these observations has been widely studied, their incorporation

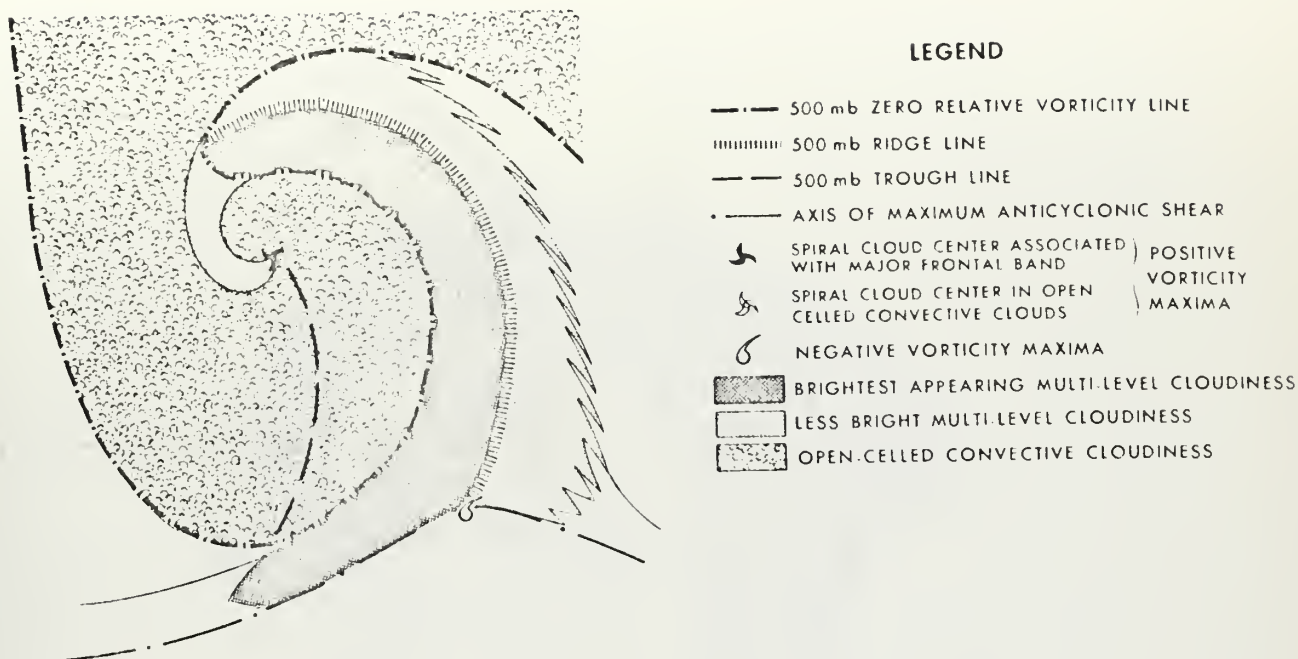
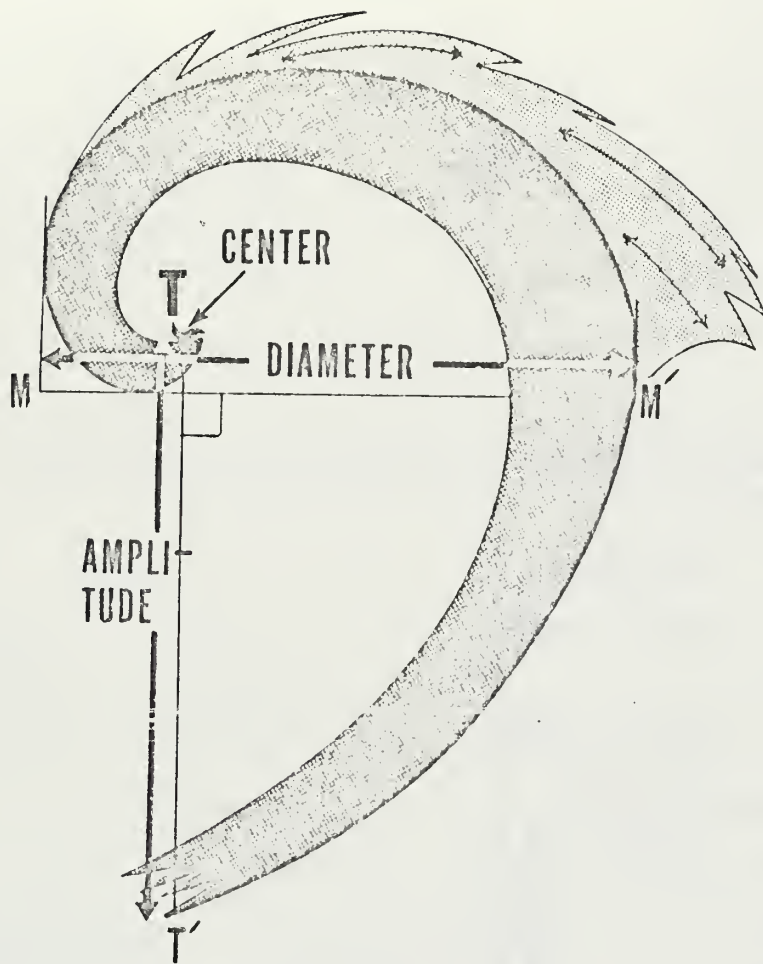


Fig. 2. Schematic representation of the relationships between cloud patterns and features of the 500 mb relative vorticity field [10] .

into the NMC numerical weather analysis scheme began experimentally in 1969 with the conversion of Satellite Infrared Spectrometer (SIRS) radiation measurements into pressure-temperature soundings [16] . This experimental work has since become a real-time effort for NESS personnel who now routinely process these SIRS observations for use by the quality control group of NMC in the Northern Hemisphere analyses for both 0000 and 1200 GMT (Mr. F. Bittner, personal communication, 1971). A brief summary of the conversion process follows:

The SIRS eight-channel radiometer observes the earth and its atmosphere every eight seconds along the north-south track of the NIMBUS satellite from an orbital altitude of approximately 600 nmi. Its field of view is 11.5 degrees, or a "square" of the earth's surface 120 nmi on a



SINAP WORKSHEET (Fig. 4) parameters:

- Ⓑ MAXDI = DIAMETER (MM')
- Ⓒ CDAMP = AMPLITUDE (TT')

Fig. 3. Geometrical construction for determining the diameter and amplitude of a cloud system [10].

SINAP WORKSHEET

Time/Date: _____ GMT/ _____ System: _____ Stage: _____

(A) LAT: _____ N LAPLACIAN-TYPE
LONG: _____ E/W COMPUTATION

(B) MAXDI: _____ °LAT

(C) CDAMP: _____ °LAT

S_1 : _____ m

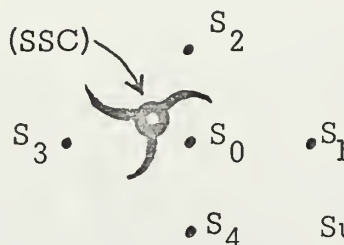
S_2 : _____ m

S_3 : _____ m

S_4 : _____ m

Sum = _____ m

A 1/2 in x 1/2 in grid (Fig. 4b)
overlay on the SR500 field with
 S_0 as the grid point nearest the
SSC specifies the LAPLACIAN
heights:



(D) LAPSR = $(S_1 + S_2 + S_3 + S_4) - 4 S_0 =$ _____ +/- m $4 \times S_0 =$ _____ m

(E) SSC = _____ m

REGRESSION COMPUTATION (SCC METHOD)

ALTERNATE COMPUTATION

(Poor Cloud Dev.)

	+	-
CONSTANT:	+21.5	
(A) x (-1.7):		
(B) x (-10.4):		
(C) x (-1.0):		
(D) x (-2.1):		

TOTALS: + _____ - _____

(F) SUM: _____ +/- m

(E) SR Value at SCC : _____ m

(F) SD Intensity at SCC : _____ m

(G) Z500 = SR + SD = E + F = _____ m

	+	-
CONSTANT		-53.5
(A) x (-1.03):		

(D) x (-1.65): _____

TOTALS: + _____ - _____

(F) SUM: _____ +/- m

(E) _____ m

(F) _____ m

(G) _____ m

Hydrostatic HT. Extrap. : (1) P_0 : _____ mb (2) T_{500} : _____ °C

(H) Base HT (Table IV) * : _____ m

(3) T_0 + : _____ °C

(I) TEMP corr. (Table V) * : _____ m

(4) ΔT = _____ °C

(J) 500HT = H + I = _____ m

*Tables from 500 mb height extrapolation method from Duthie, W.D., unpublished lab notes, Meteorology Dept., Naval Postgraduate School, Monterey, Calif.

Fig. 4a. Worksheet for Nagle-Hayden regression equation solution determining 500 mb height at a spiral cloud center (SCC) using satellite pictures and the SR500 field on a 1:30,000,000 scale (FNWC chart No. 4-P-1) polar stereographic projection, true at 60N.

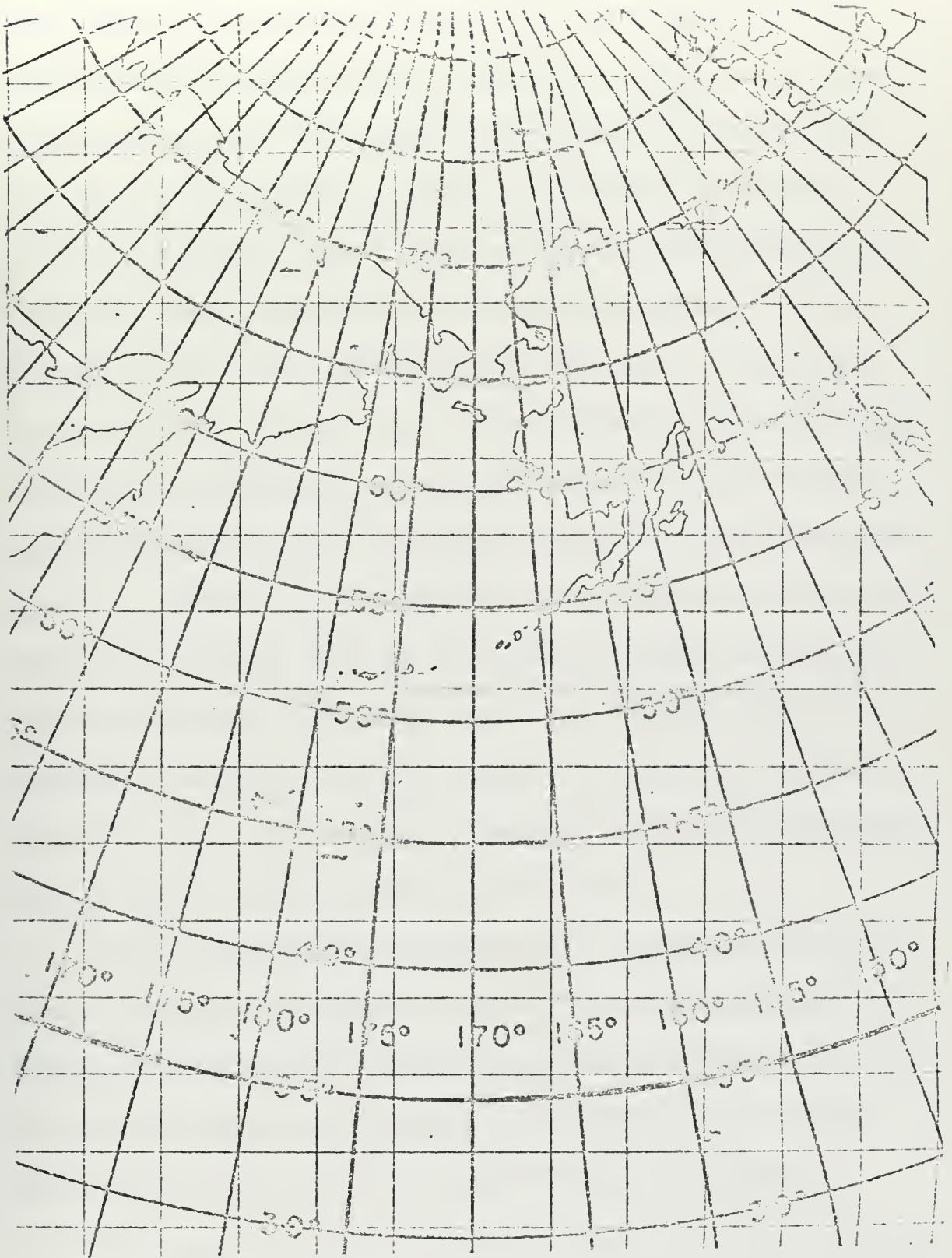


Fig. 4b. A 1/2 in X 1/2 in grid over an FNWC chart No. 4-P-1 and compatible with worksheet (Fig. 4a).

side. These readings are transmitted to CDA stations for relay to the NESS processing center at Suitland, Maryland. At NESS, the automated computer processing program compares three successive observations. From these, the one with the highest sum of radiances for all eight channels is selected. Since the earth's surface is usually warmer than cloud tops, this procedure tends to select cloud-free areas. On the average, an observation is selected every 48 seconds, or every three degrees of latitude, along the track of the satellite subpoint. Using all available radiance readings from the eight channels (channel readings containing excessive noise "spikes" are discarded), temperature profiles are then calculated by a least-squares multiple regression solution. Best results are, of course, obtained for the cloud-free cases when all eight channels are utilized. The solution is less satisfactory when clouds are present to "contaminate" channel readings.³ The poorest results are obtained for high cirrus overcast. Computations are considered unreliable for a cirrus coverage greater than 40 percent.

Having obtained the temperature profile, the heights of constant-pressure surfaces are computed through the hydrostatic relationship by using the 850 mb surface as the known reference level.⁴ The final result is a pressure-temperature sounding from 1000 mb to 10 mb in a format readily usable in the NMC conventional data processing program.

³With future high resolution scanning radiometers, it is expected that temperature profiles for cloudy conditions will be as accurate as the present cloud-free profiles. Methods are also being derived to account for the influences of high and hot terrain.

⁴Depending on the time of the SIRS observation, interpolation is made between the preceding 850 mb analysis and the 850 mb 12-hour prognosis to obtain the most accurate 850 mb height.

At NMC, the SIRS soundings are subjected to the same accuracy checks as conventional data; that is, any soundings differing by more than 200 m when compared with the 500 mb and 300 mb "first guess" heights are rejected in their entirety. Such rejected soundings are subjectively reviewed by a quality control group which may re-insert the sounding if it is deemed accurate. All accepted soundings are put into the objective analysis program. The SIRS soundings are given the same "weight" or significance as the conventional soundings.

NMC performs both an operational upper air analysis (at approximately 0000/1200 GMT + 3.5 hours) and an update analysis (0000/1200 GMT + 10 hours). The latter utilizes all the synoptic or near synoptic data received since 0000/1200 GMT. Thus, the SIRS soundings, which are being continuously processed, are usually entered into both analyses. Presently, the processing time delay at NESS dictates that only those SIRS observations taken in the interval from one to six hours prior to synoptic time (0000/1200 GMT) can be processed in time for incorporation into the operational analysis. The number of SIRS soundings entering the operational analysis is usually less than 30; whereas for the update version, the total (including those in the operational analyses) averages about 60 soundings. The comparable average figures for conventional radiosonde data are 500 and 575, respectively (March 1971 figures).

An example of the NMC update 500 mb SIRS coverage for 0000 GMT 12 March 1971 is shown in Fig. 5. The lack of data at lower latitudes is



Fig. 5. 0000 GMT 12 March 1971 500 mb SIRS data with the analyzed FNWC heights in parentheses.

partly a function of the wider spacing of orbital paths near the equator.

As the orbital paths converge in the polar areas, the coverage increases accordingly.⁵

⁵Future satellite spectrometers will also scan in a direction lateral to their orbital paths, providing data to fill in these wide gaps in the lower latitudes.

III. DATA SOURCES AND SELECTION OF STUDY PERIOD

The proposed interaction with the FNWC analysis and prediction scheme hinged on their retention (on magnetic tape) of the conventional synoptic data so that a re-analysis could be performed at a subsequent date using bogus reports fabricated from the satellite-derived information. FNWC agreed to save their update synoptic data during the month of March 1971, thereby establishing the month of the study period.

The National Environmental Satellite Service (NESS) was contacted by Mr. F. Bittner of Project FAMOS for use of their ATS film loops and photographs, AVCS video, and ITOS nighttime IR Northern Hemisphere mosaics. However, to ensure a good satellite data base from which to work, in the eventuality of the AVCS or ATS data from NESS not being available, a large number of satellite data sources were requested to provide their satellite material.

All shore-based Naval Weather Service Command activities in the North Pacific Ocean having satellite readout equipment were contacted for possible use of their gridded pictures. Lt. Cmdr. D. Edgren of NWSED, Moffett Field, Calif., contacted the Air Force Satellite Center, Sunnyvale, Calif., for their APT readouts. Cmdr. W. Willingham of FWF Suitland, Md., contacted the NMC for the operational SIRS soundings and nephanalyses. The response of all activities was gratifying and ensured that an excellent collection of satellite pictures was available.

The five upper air synoptic times from 0000 GMT 10 March through 0000 GMT 12 March 1971 were selected for the study period for two reasons:

- 1) neither satellite-derived bogus data from FWF Suitland nor SIRS data from NMC (via FWF Suitland) entered the FNWC analyses during this period.
- 2) substantial short period weather pattern changes were observed in the North Pacific Ocean.

The first reason ensured that the FNWC objective analyses were essentially void of subjective or satellite-influenced changes. To further this concept, the real-time surface cyclone boguses incorporated in the operational FNWC analyses from the FWC Pearl Harbor were deleted from the magnetic tape data retention. Thus, in the later re-running of this data, both an UNMOD ANAL containing only conventional data, and a MOD ANAL containing conventional and the authors' bogus insertions were generated.

The second reason was based on the premise that the weather pattern changes noted on the synoptic maps would be noticeable in the satellite data.

Table I lists the satellite and conventional data sources used in this research. The authors are indebted to each activity and the individuals in these organizations for their cooperation in making this data available to the Department of Meteorology, Naval Postgraduate School, Monterey, California.

TABLE I.

Sources of conventional and satellite data

A. Satellite Data

1. Video Pictures (ITOS-1, ESSA VIII) :
 - FWC Alameda
 - FWC Pearl Harbor
 - FWC Guam
 - FWF Kodiak
 - FWF Yokusuka
 - FWF Sangley Point
 - NPS Monterey
 - PMR Pt. Mugu
 - NWSED Moffett Field
 - NWSED Midway Island
 - NWSED Adak Is.
 - AFSC Sunnyvale
 - NESS, Suitland (Mosaics)
- *2. IR Nighttime Data (ITOS-1) :
 - NESS, Suitland (Mosaics)
- *3. ATS-1 Wind Computations and Film Loops :
 - NESS, Suitland
- *4. SIRS Soundings :
 - NESS, Suitland
 - NWSED Asheville (repository for NESS SIRS soundings)
- *5. Nephanalyses :
 - NESS, Suitland (also available from FOFAF and NAFAX circuits)
- *6. Pacific Operational Bogus Data and SINAP Maps :
 - NMC, Suitland

B. Conventional Data

1. Surface and Upper Air Synoptic Data:
FNWC Monterey
NMC, Suitland
2. Surface Analyses :
FNWC Monterey
FWC Alameda
FWC Pearl Harbor
NMC, Suitland (FOFAX and NAFAX circuits)
3. Upper Air Analyses :
FNWC Monterey
FWC Pearl Harbor (tropical)
NMC, Suitland (FOFAX and NAFAX circuits)
4. Pattern Separation Analyses (SR and SD Contour Fields):
FNWC Monterey

*Collected and forwarded by Project FAMOS

IV. PROCEDURES AND RESTRICTIONS

Quasi-operational ground rules were established for incorporating the satellite-derived data into the data base of the FNWC numerical analysis program. The primary rule was that all procedures be designed to improve the operational FNWC analyses (available at 0000/1200 GMT + 4.5 hours) in time for these improvements to enter the update analysis run (approximately 0000/1200 GMT + 10 hours). This implied that the following intermediate (0600/1800 GMT) surface analysis (produced at 0600/1800 GMT + 2 hours) was available to indicate developing trends; and the operational 0000/1200 GMT 500 mb SR pattern could be used instead of the previous 12-hour SR prognosis as used in the NESS version of the Nagle-Hayden technique.

Another important rule was that only satellite pictures in the synoptic time frame could be used. For example, APT photographs taken after the 1000 GMT cut-off time for the 0000 GMT analysis were not used in modifying the original analysis. In the actual research this rule was not a hindrance as most Pacific video satellite pictures are taken between 2000 GMT and 0200 GMT; thus, they are naturally restricted to usage in the 0000 GMT analysis. The only views available for the 1200 GMT synoptic period were the ITOS IR nighttime mosaics taken between 1000 GMT and 1600 GMT in the Pacific Ocean region.

The third operational rule was that conventional observations were considered reliable and inviolate unless clearly demonstrated otherwise.

Certain restrictions were placed on the re-analysis effort owing to the current (July 1971) programming practices at FNWC; namely, bogus inputs were permitted only at sea level (pressure and wind) and at 500 mb (height, temperature and wind). Furthermore, the total number of bogus inputs was limited to 100 reports at sea level and to 50 reports at 500 mb. This limit of fifty boguses at 500 mb proved a handicap in achieving the desired re-analysis at this level.⁶

Within these rules and restrictions, the following procedures were used to modify the original numerical analyses utilizing the weather-satellite data up to the equivalent real-time data cut-off point for each re-analysis:

- 1) The operational 0000/1200 GMT surface, 500 mb, 500 mb SR, 300 mb, and thickness (500 mb - 1000 mb) fields were considered the first guess fields.
- 2) SIRS 500 mb height data and ATS-1 300 mb wind data were plotted on the corresponding analyses, and significant differences noted.
- 3) All available satellite cloud pattern pictures were reviewed to gain a familiarity between cloud patterns and synoptic systems.

⁶The FNWC program has since been rewritten to accommodate 100 boguses at sea level, 500 mb and 300 mb (Mr. T. Hesse, FNWC, personal communication, August 1971).

4) Using the 500 mb SR analysis, spiral cloud centers and zero vorticity (SD zero-line) lines noted on the satellite views were plotted and the Nagle-Hayden statistical computations performed.

5) The FNWC surface and 500 mb analyses were subjectively changed to conform to the major features derived from the satellite data.

6) The next 0600/1800 GMT surface analysis was used to improve the sea-level modification.

7) A 1000 mb field was constructed from the modified surface charts, then a new thickness was manually generated.

8) The subjective thickness was compared to the numerical 12-hour history thickness. Any changes in the normally conservative thickness patterns were reconciled, with necessary adjustments made to the appropriate thickness pattern. From the changed thickness pattern, the surface and 500 mb analyses were adjusted to reflect the change and to ensure continuity of the pressure systems.

9) Bogus reports (see Appendix C) were prepared for the purpose of objectively duplicating the manually modified surface and 500 mb charts.

10) Analyses were then made of the surface and mandatory upper air levels using only the conventional data first (UNMOD ANALS), and then using both the conventional and bogus data (MOD ANALS).

11) The re-analyses were examined. If cloud-related synoptic features were not sufficiently delineated, new bogus data were fabricated, and a re-cycling performed until the modified fields appeared satisfactory (experience would tend to eliminate the re-cycling).

12) The primitive equation (PE) prognosis was run to 48 hours on both the unmodified and satellite-modified analysis fields, generating UNMOD and MOD PROGS.

13) Finally, error fields for the surface and 500 mb levels were generated for both sets of PE prognostics.

V. CASE STUDIES OF MODIFICATIONS TO ANALYSES

Synoptic times 0000 GMT 10 March through 1200 GMT 12 March 1971 were studied in detail, with modifications made to the respective sea level pressure and 500 mb fields. The dates of 1200 GMT 10 March and 0000 GMT 11 March 1971 were selected as initial times from which the current (July 1971) FNWC primitive equation (PE) five-layer prognostic model was run to 48 hours. Several changes had been made to the prognostic program since March 1971; therefore, to make a valid comparison of the UNMOD PROG and the MOD PROG, the UNMOD PROG was re-run.

Figures showing analyses follow immediately after the detailed description of the analysis modifications made in each case study. The vortices are labeled alphabetically from Eastern Pacific to Western Pacific as they made their appearance in time. In each case, the referenced positions are the 500 mb position unless otherwise stated. The dashed contours of the analyses are isolines of the UNMOD ANAL; they are superimposed on the neoteric MOD ANAL isolines to clearly illustrate the modifications effected by the inclusion of explicit satellite data and the implicit "values" of the satellite observations.

A. 0000 GMT 10 MARCH 1971 MODIFICATIONS TO ANALYSES

The 0000 GMT surface maps of the Pacific Ocean are based on a maximum number of ship reports because it is near midday over this region and therefore fits into the routine broadcast day. Video satellite pictures

are available at this time and are the basis of the following modifications to the sea level and 500 mb MOD ANALS (Figs. 6, 7 and 8):

1. Vortex A

Vortex A at 62N 134W is over British Columbia and is in the dissipation stage based on the fragmented appearance of its spiral cloud pattern.

2. Vortex B

Vortex B, near 51N 156W, is a weak trough on the UNMOD ANAL. In the video pictures, this vortex appears to be a classical mature cyclonic vortex associated with a major polar frontal band. Consequently, at 500 mb a low with a central value of 5000 m was introduced. Its associated trough was repositioned westward on the basis of the sharp dissipation of middle and high clouds in the frontal band and the curvature of the cloud lines.

3. Vortex C

Vortex C at 52N 179E, with a central value of 5072 m on the UNMOD ANAL, was relocated to 50N 176E based on the satellite picture of the center and lowered to 5000 m based on the computational values obtained. This is a mature cold vortex. Its trough was deepened to the south and southwest and the cyclonic curvature accentuated on the basis of the cloud band curvatures.

4. Vortex D

Vortex D, over the north tip of Honshu, is well defined by Japanese radiosonde reports. East of this vortex, the ridge along 155E

was increased slightly based on the anticyclonic cloud curvature and the clear area on the east side of the ridge.

5. Vortex F

A comma cloud (PVA Max) at 41N 177W located northwest of a major bulge in the frontal band, presages future development of a wave cyclone (vortex F). The trough and downstream ridge were enhanced slightly on the basis of the SD zero-line delineation and thickness pattern considerations.

6. Vortex G

Vortex G, over the northeast tip of Siberia, is defined by conventional radiosonde data; the video pictures contained too much snow and ice reflection to permit observation of the cloud systems.

B. 1200 GMT 10 MARCH 1971 MODIFICATIONS TO ANALYSES

The 1200 GMT sea level pressure map of the Pacific Ocean normally has few ship observations because it is near midnight (local time) over this region, and therefore most ships either do not record or do not transmit observations at 1200 GMT in the Pacific Ocean. Based primarily on the photo mosaic of ITOS 1 IR nighttime viewing, the following modifications were made to the sea level and 500 mb MOD ANALS (Figs. 9, 10 and 11):

1. Vortex B

Vortex B has passed through the mature stage based on the fracturing of the dry tongue and the gray tone of the encircling clouds in the IR data. However, it is still a well-defined closed system. The

original FNWC analysis rejected Ship Papa's 500 mb wind of 335 deg/38 kt, as it failed the consistency check between the 700 mb wind of 245 deg/46 kt and the 400 mb wind of 240 deg/36 kt. In the modification, the 500 mb wind was changed to 235 deg in consonance with the cloud pattern and the speed unchanged. Vortex B was positioned northwest of Ship Papa with an estimated central height of 4990 m. However, due to the difficulty encountered in bogusing (see discussion in Appendix C), the MOD ANAL value in the numerical analysis version is 5047 m. To maintain vertical consistency and continuity, the sea-level low was positioned beneath the 500 mb low and deepened from 980 mb to 971 mb. The 500 mb trough extending southeast from vortex B was deepened slightly in the vicinity of the jet maximum along the north boundary of the frontal band near 42N 140W.

2. Vortex C

Vortex C, south of Adak, Alaska, is probably nearing the dissipating stage as the brightest clouds (coldest temperatures) completely surround the center, and the cloud lines are generally fragmented and not bright, indicating stable mid- or low-level stratocumulus. Winds are missing from Adak's report (station 70454), but the clouds detected by the IR sensor indicate weak easterly flow. The 500 mb analysis was modified to show this closed circulation.

3. Vortex D

Vortex D, east of Hokkaido, has not intensified based on both conventional data and cloud patterns. The bright clouds nearly surrounding the center indicate this small system is in the mature stage.

4. Vortex E

A large, bright cloud mass southeast of vortex D, near 40N 158E, has separated from this vortex and is in the initial stage of surface cyclone development. Vortex E is not as well organized as vortex F at this time, but the photo of IR data clearly shows that this is the next unstable system upstream from vortex F. Consequently, at 500 mb the trough on the west side of the cloud mass was deepened and the ridge on the east side (near 162E) was enhanced by using the SD zero-line to derive 500 mb heights. However, the numerical MOD ANAL did not portray the short-wave character intended for this system.

5. Vortex F

The comma cloud noted in the 0000 GMT 10 March discussion has apparently joined with the convex bulge in the polar front near 42N 160W. This is between the two major vortices, B and C, in an area of maximum baroclinicity. The photo of IR values shows this cloud mass to be the whitest region of cloudiness in this portion of the ocean. A frontal wave which exhibits an area of cold temperatures (white) in the IR mode, suggesting strong ascending motion and falling sea level pressures, is indicative of a developing surface cyclone and is typical of the second stage of a rapidly developing system [15]. Cyclonic circulation is weakly evident, though the dry tongue is visible. This cloud pattern is nearly identical to the CP20 example of Nagle and Clark, which they describe as indicating a rapidly deepening system. Thus the pattern of IR values of vortex F implies a strong short-wave trough at 500 mb with a closed surface circulation.

It is interesting to note that the sea level pressure could not be properly ascertained in this area from conventional ship reports, the nearest reporting ship being over 500 nmi away. Thus the FNWC surface analysis has no indication of this developing system. Even the 1800 GMT 10 March surface analysis continued to show fairly zonal flow over the region. In fact, a key ship report (call sign JIVA) near 50N 150W reported a pressure of 984.5 mb and south-southwest wind of 40 kt. Its pressure was interpreted to belong in the pattern of vortex B to the northeast, though the wind indicated cyclonic development to the west of the ship. Unfortunately, no other ship observations were available so the FNWC duty officer attached a note to this report, "... in without wind," indicating that he considered the pressure correct, but the wind erroneous. Not until 0000 GMT 11 March did six ships near the storm send in their reports thereby pinpointing the storm's position and intensity (975 mb). The National Weather Service maps were equally vague in defining this system until 0000 GMT 11 March.

The Nagle-Hayden technique produced 500 mb values of 5320 m for the spiral cloud method, and 5370 m for the alternate method. Extrapolating back in time from a re-analysis of the 1800 GMT surface analysis indicates that the sea level pressure was below 996 mb at 1200 GMT, thus in hydrostatic agreement with the final subjective 500 mb height of 5340 m.⁷ The original analysis value at this point was 5460 m. In the

⁷Note that the 1800 GMT surface analysis is available prior to the update of the 1200 GMT analysis at FNWC.

modification, no attempt was made to close off a 500 mb cyclonic circulation. The 500 mb trough was re-positioned on the upstream edge of the cloud pattern associated with the developing vortex and deepened according to the height computation of 5340 m. The sea-level low was positioned by the apparent circulation center in the cloud patterns and deepened to a closed 995 mb. (Further discussion of this vortex is contained in Section VI.)

6. Vortex G

Vortex G at 62N 166E again is not distinguishable on the photo of IR data, probably due to very low clouds or an isothermal atmosphere, but was adequately covered by Russian radiosonde stations.

C. 0000 GMT 11 MARCH 1971 MODIFICATIONS TO ANALYSES

An excellent suite of video pictures for this period (1900 to 0200 GMT) was obtained from Naval Weather Service facilities and NESS. The NWSED Midway Island APT, and the NESS ATS-1 film loops and enlarged photographs were particularly useful in showing the rapid development of vortex F.

The following modifications were made to the surface and 500 mb analyses (Figs. 12, 13 and 14):

1. Vortex B

Vortex B in the Gulf of Alaska is considered to be in a late mature stage. Its frontal occlusion has separated from the vortex center, the dry tongue nearly encircles the center, and the feeder bands are short and diffuse.

Ship Papa's (50N 145W) wind direction at 500 mb is reported as 265 deg/54 kt, but the cloud streaks on the video pictures indicate west-northwesterly flow at mid-troposphere levels. An examination of the sounding showed a constant wind direction of 265 deg from 850 mb to 100 mb, which is not likely to occur. It was decided to insert a bogus west-northwesterly wind of 290 deg in the vicinity of Ship Papa. Since the conventional report could not be modified by the bogus method without rejecting the entire sounding, several bogus winds at 500 mb were injected to "override" (see Appendix C) the Papa report, however, the numerical MOD ANAL achieved only a westerly flow of 275 deg.

The desired 500 mb central value for Vortex B was 4980 m. Deliberate "overbogus" (see Appendix C) of four surrounding points brought the central value down to only 5061 m but achieved the desired cyclonic circulation. The associated trough was deepened to the southeast of the vortex as indicated by the cloud curvatures and SD zero-line computations.

2. Vortex C

The circulation associated with vortex C is well defined and covers a large area as it continues to drift eastward with minor intensification. The 500 mb center was closed off and the trough deepened, conforming to the cyclonic curvature of the cloud lines and to the change in cloud type (open cells on the west side and enhanced cloudiness on the east side of the trough line).

3. Vortex D

Vortex D has moved slowly eastward and has weakened, judging from the large dry tongue which completely encircles the center.

4. Vortex E

Vortex E has formed between vortex D and the large bright frontal cloud mass noted in the 1200 GMT 10 March discussion. As a result of the interaction between the comma cloud (PVA Max) and the enhanced convective activity along the frontal zone, wave development on the front is indicated in the vicinity of 40N 160E. The surface cyclone was deepened and separated from the surface cyclone associated with vortex D to the northwest to indicate its interpreted development. At 500 mb, the trough was deepened nearly 70 m and the downstream ridge was heightened 40 m. Eight 500 mb bogus wind reports were entered on the east side of this trough to attempt depiction of the strong southwesterly flow in this region, but again the numerical MOD ANAL could not incorporate this shortwave intensification as was desired.

5. Vortex F

As noted in the 1200 GMT 10 March discussion, vortex F, in the vicinity of 48N 155W, has undergone rapid intensification during the night. The first daylight pass of ESSA VIII (orbit #10233 at 1945 GMT 10 March) clearly shows the intense nature of this small system. The cloud pattern corresponds perfectly with the Nagle and Clark CP20 or "hammerhead" designation [5]. Vortex F must be considered fully occluded at this time, dictating a 500 mb closed low slightly northwest

of the sea-level low, flanked by strong ridges east and west, south of a vigorous trough in the cold air along 155W. Since the conventional analysis had a slight ridge in this vicinity and only minor troughing in the nearby systems B and C, considerable modification was required to fit the dynamics and flow pattern of vortex F. The 500 mb heights were deepened as much as 300 m in the trough. The 500 mb center was modified to show a closed circulation and a center value of 5090 m. The ridges upstream and downstream were heightened by using the SD zero-line computations.

6. Vortex G

Though Vortex G is extremely small, the video photo shows it to be a mature, intense system. Vortex G is moving southward, entering the Bering Sea east of the Kamchatka Peninsula in conformity with the spiral cloud pattern. The Russian data network measured this system very accurately and no modifications were required.

D. 1200 GMT 11 MARCH 1971 MODIFICATIONS TO ANALYSES

The 1200 GMT 11 March 1971 synoptic maps again illustrate the lack of conventional data in the North Pacific. Three station vessels, November, Papa, and Victor, were the only rawinsonde ships reporting over the entire oceanic expanse. Marcus, Wake, and Midway Islands were the only island stations in strategic locations; however, the 500 mb winds were missing in the reports from both Midway and Wake. Surface synoptic ship reports were equally sparse. In the eastern North Pacific

Ocean between 180 longitude and the west coast of North America, eleven ship reports were plotted on the NWS preliminary surface analysis, and eight ship reports were plotted on the FNWC operational surface analysis.

The photo mosaic of ITOS-1 IR nighttime viewing was the primary source for the following changes to the surface and 500 mb analyses (Figs. 15, 16 and 17):

1. Vortex B

Vortex B moved northwestward into the northern Gulf of Alaska and is well delineated by conventional rawinsonde observations at Kodiak (70350) and Anchorage (70273). It is poorly defined in the IR data values and is probably being absorbed into the major low pressure system over northern Alaska. Its trough extends southeastward and affects the circulation over Ship Papa which reported a 500 mb wind of 235 deg/14 kt. No modifications were required for vortex B.

2. Vortex C

The photo mosaic was badly blurred in the vicinity of vortex C. The trough position was discernible from the cloud patterns, but the center was not. Relying on continuity, vortex C was considered a 500 mb cyclone with a central height of 5000 m.

3. Vortex D

Vortex D, east of Hokkaido, was completely filled with gray clouds (low stratocumulus), indicating dissipation. The good data coverage of the surface specified a 1016 mb closed sea-level low. The surface analysis was not changed. Based on the observed cloud lines,

indicating primarily the orientation of thickness contours, the 500 mb analysis was modified slightly to enhance the cyclonic flow south and west of vortex D.,

4. Vortex E

Vortex E is the dominant mid-Pacific feature. The center is faintly discernible on the mosaics with a large, extremely wide dry tongue extending northeast. The stage of development is early maturity (occluding) or early CP 20 [5]. In the area of cold air advection (the dry tongue), large amounts of gray clouds are present, suggesting low cloud tops, stable conditions, and a small air/sea temperature difference. This would indicate that deepening is proceeding at a slow rate [13].

Vortex E is closed off with a 5160 m central value at 500 mb. The surface low is positioned to the southeast and deepened to 1004 mb. The ridge along 178E has begun to move in such a way as to increase the distance between it and vortex E. This ridge was enhanced to accommodate greater anticyclonic flow apparent from the cloud patterns.

5. Vortex F

Vortex F is the dominant East Pacific synoptic feature at this time. From the photo of IR values vortex F can be classified as a CP30 [5] or a mature storm with a secondary frontal wave [7]. Vortex F is approximately 350 nmi southeast of Ship Papa with the sea level pressure lowered to 964 mb based on the continuing development. The 500 mb center was lowered to 5040 m based on the quasi-objective computations.

6. Vortex G

Vortex G has moved further into the Bering Sea. The added moisture supply has clearly enhanced the cloud development seen in the ITOS IR depiction. Minor modifications were made at 500 mb to increase the cyclonic flow in the trough extending southwest of vortex G.

7. Vortex H

An incipient secondary frontal wave development (Vortex H) can be anticipated because of the enhanced comma cloud (PVA Max) near 40N 150W on the IR mosaic.

E. 0000 GMT 12 MARCH 1971 MODIFICATIONS TO ANALYSES

The excellent video coverage at this synoptic time permitted a detailed investigation of the synoptic patterns of the North Pacific Ocean. The following modifications were made (Figs. 18, 19 and 20):

1. Vortex B

Vortex B is poorly formed and the closed center has dissipated. No modifications were attempted on this system.

2. Vortex C

Vortex C appears diffuse. The 500 mb analysis was modified to reflect the phase and amplitude of the trough lying along 155W, as indicated by the open area to the west and enhanced cloudiness to the east.

3. Vortex D

Vortex D has continued to dissipate. The analysis was modified only to accentuate the ridging which contributes to the clear area in the photo noted at 40N between vortices D and E.

4. Vortex E

Vortex E is moving rapidly to the east northeast across the mid-Pacific Ocean at 45 kt. The cold dry tongue has changed slightly but the system has not intensified appreciably. It has deepened to 992 mb at sea level and, based on the ITOS video mosaic, the system's position was altered slightly westward and modified to obtain the closed circulation and a 500 mb height of 5160 m, for continuity.

5. Vortex F

Vortex F approaches the west coast of North America as a fully mature system with a cloud shield that covers the northwestern United States and Canada. The analysis was modified to maintain continuity in intensity and position based on the satellite pictures.

6. Vortex G

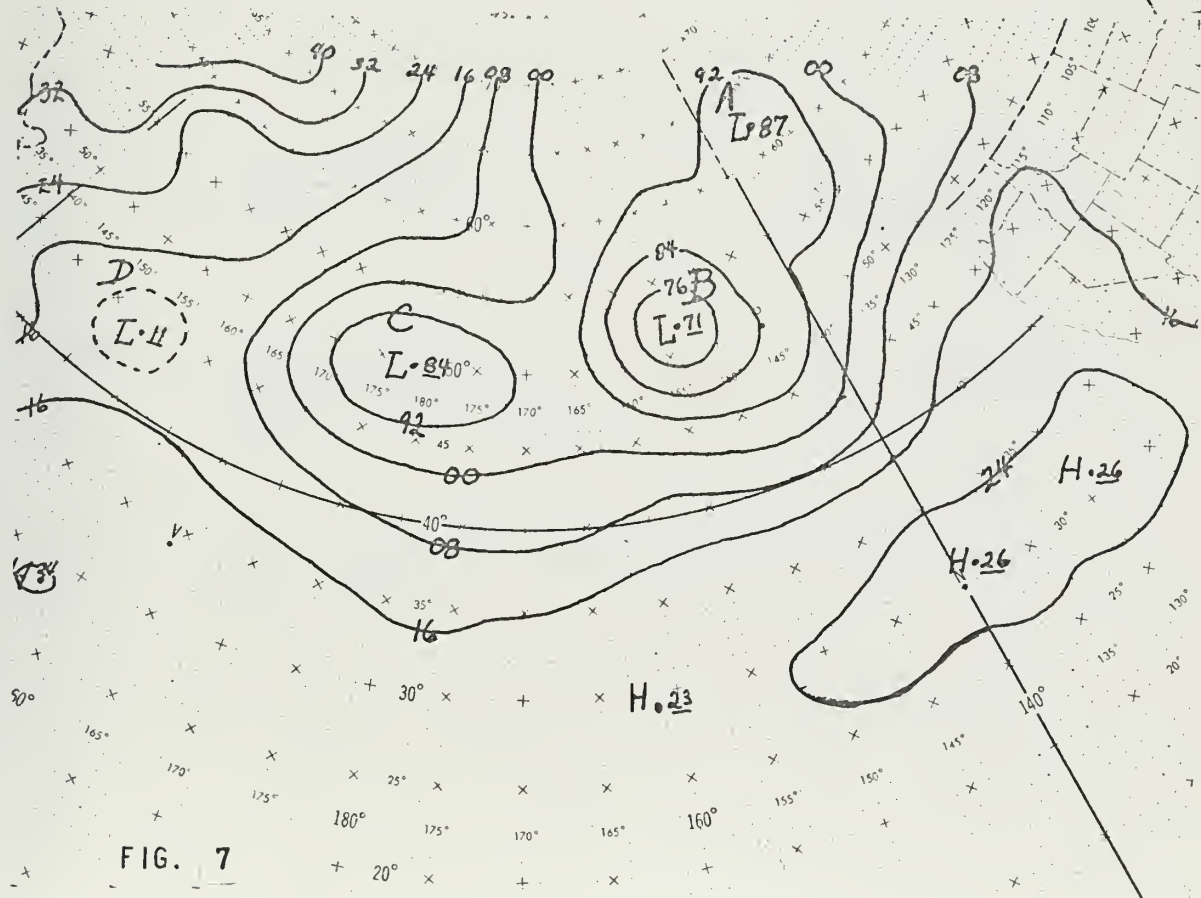
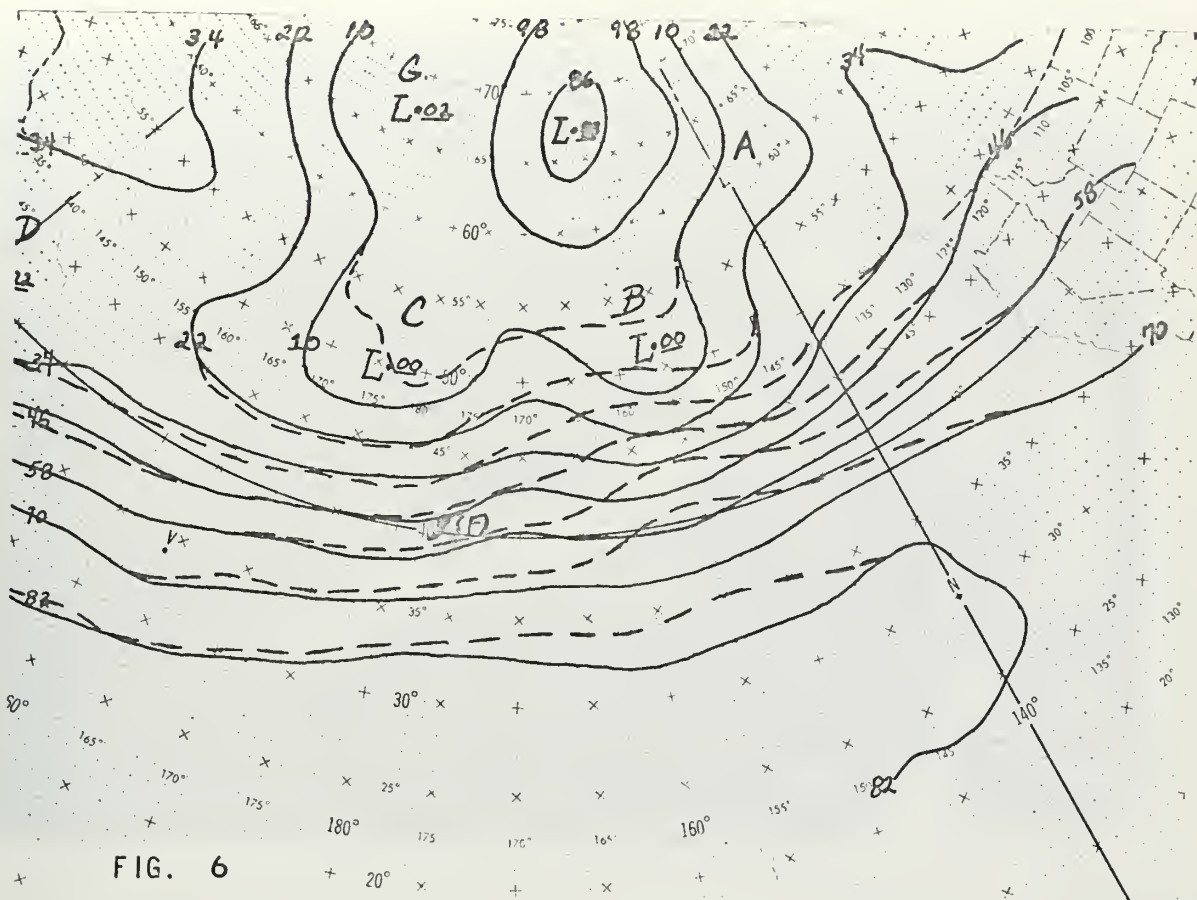
Vortex G is dissipating and no further modifications were attempted on this system.

7. Vortex H

Vortex H has developed rapidly since 1200 GMT 11 March and the video photo clearly displays the enhanced comma shaped cloud (PVA Max) which appears just ahead of the base of a short wave trough, indicated by the cloud-free subsiding air imbedded in the long wave ridge as it interacts with the frontal band. The analysis was modified to reflect the curvature and intensity associated with this secondary frontal wave.

The modification effort was successful with this short-wave feature as the numerical 500 mb MOD ANAL accepted bogus data that contoured the trough with deepening as much as 160 m in one location.

The associated ridge to the west was built into the trough of the UNMOD ANAL at 150W. To depict the increasing baroclinicity associated with this system, the gradient was tightened in the southeast quadrant of vortex H as far east as 125W.



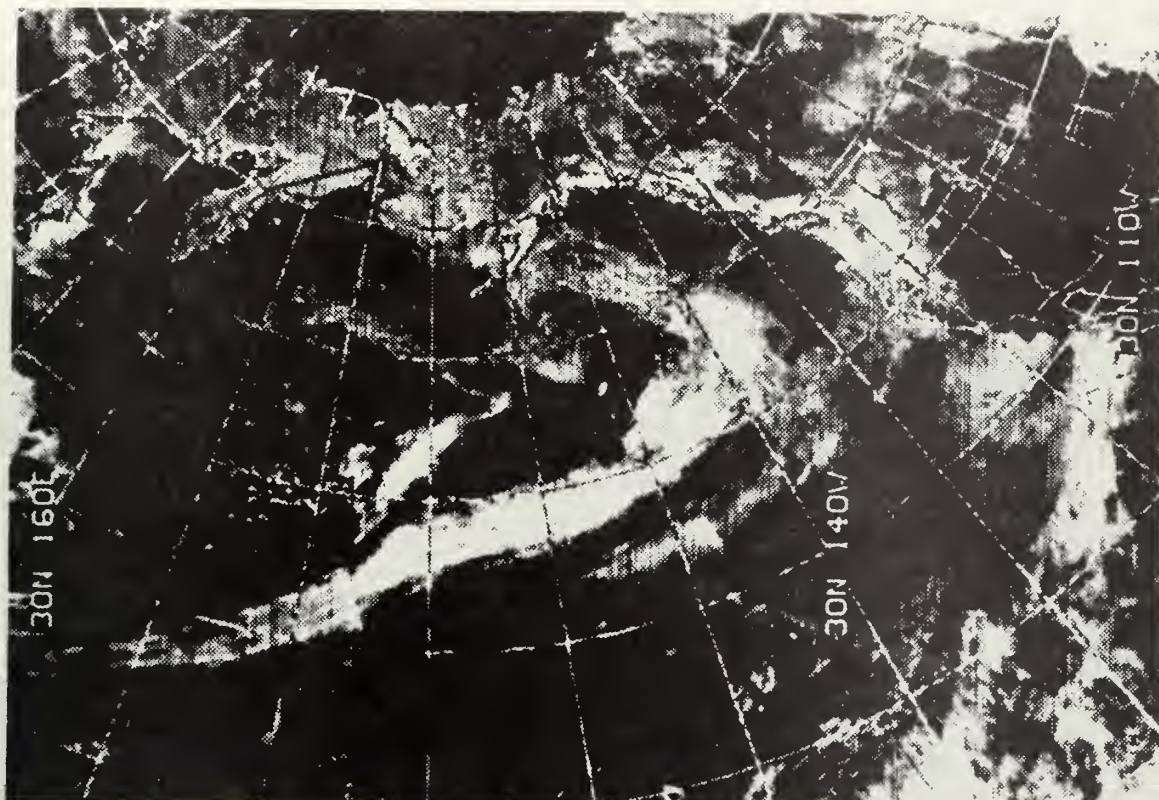


Fig. 8

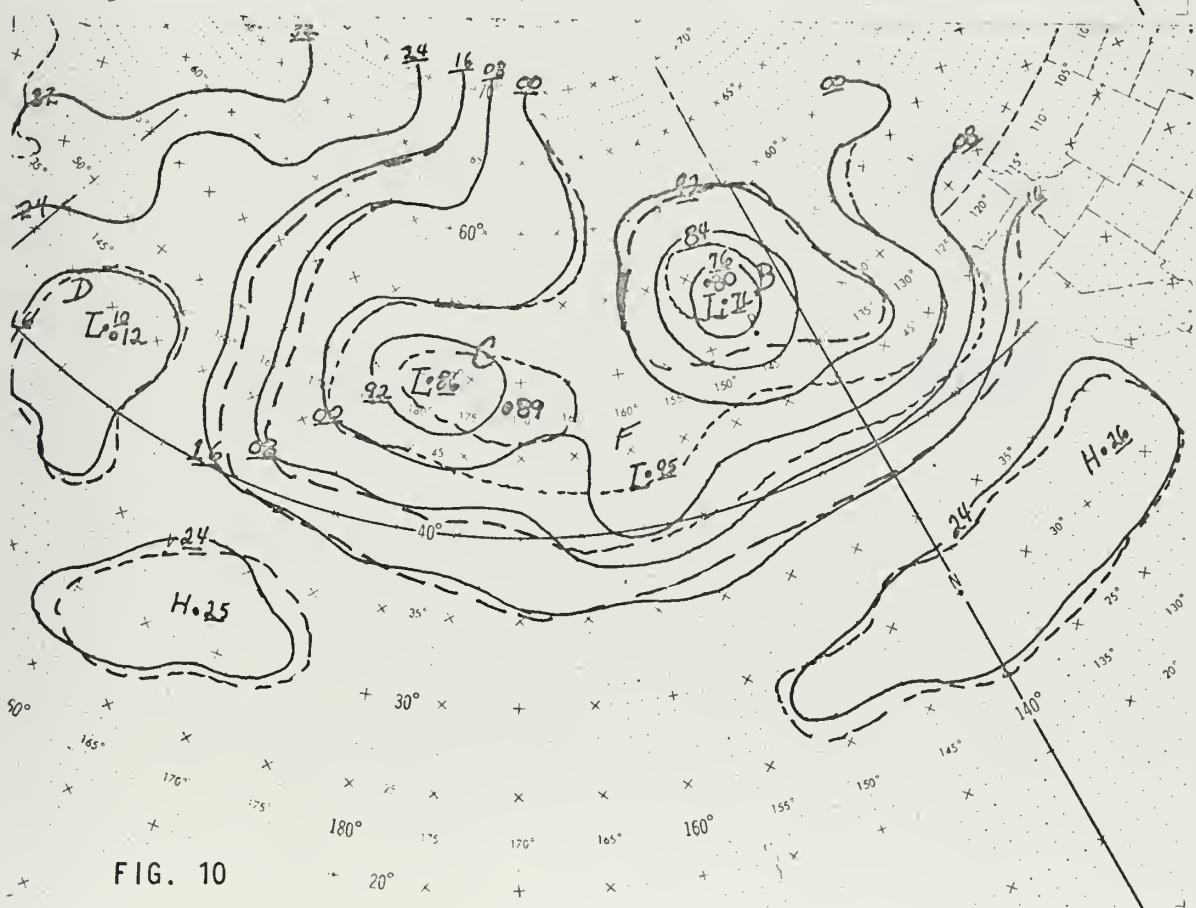
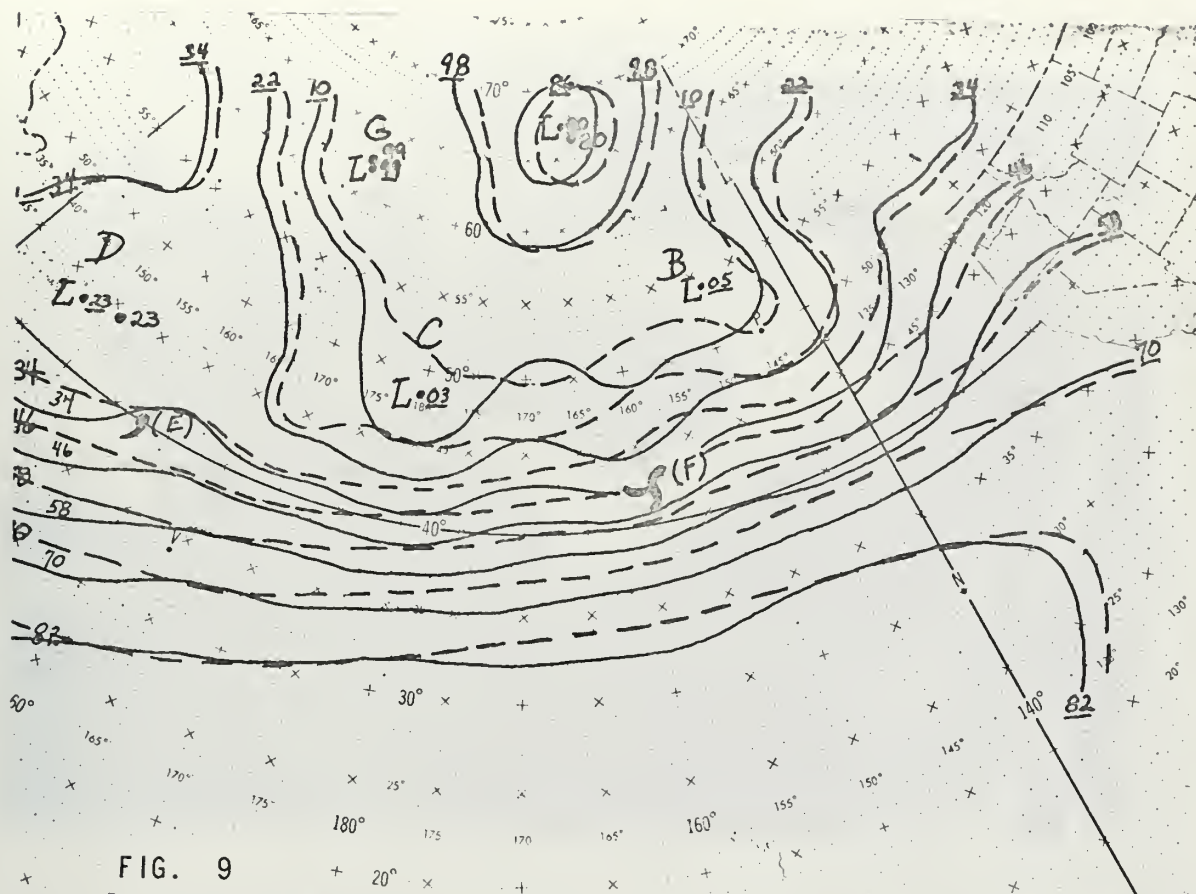
Fig. 6 500 mb analyses
0000 GMT 10 March 1971
Values are 5XX0 meters

—— UNMOD ANAL
—— MOD ANAL
(no modification made)

Fig. 7 Sea level analyses
0000 GMT 10 March 1971
Values are 10XX or 9XX mb

---- UNMOD ANAL
—— MOD ANAL

Fig. 8 ITOS-1 Video Mosaic for approximately 0000 GMT 10 March 1971 at 140W.



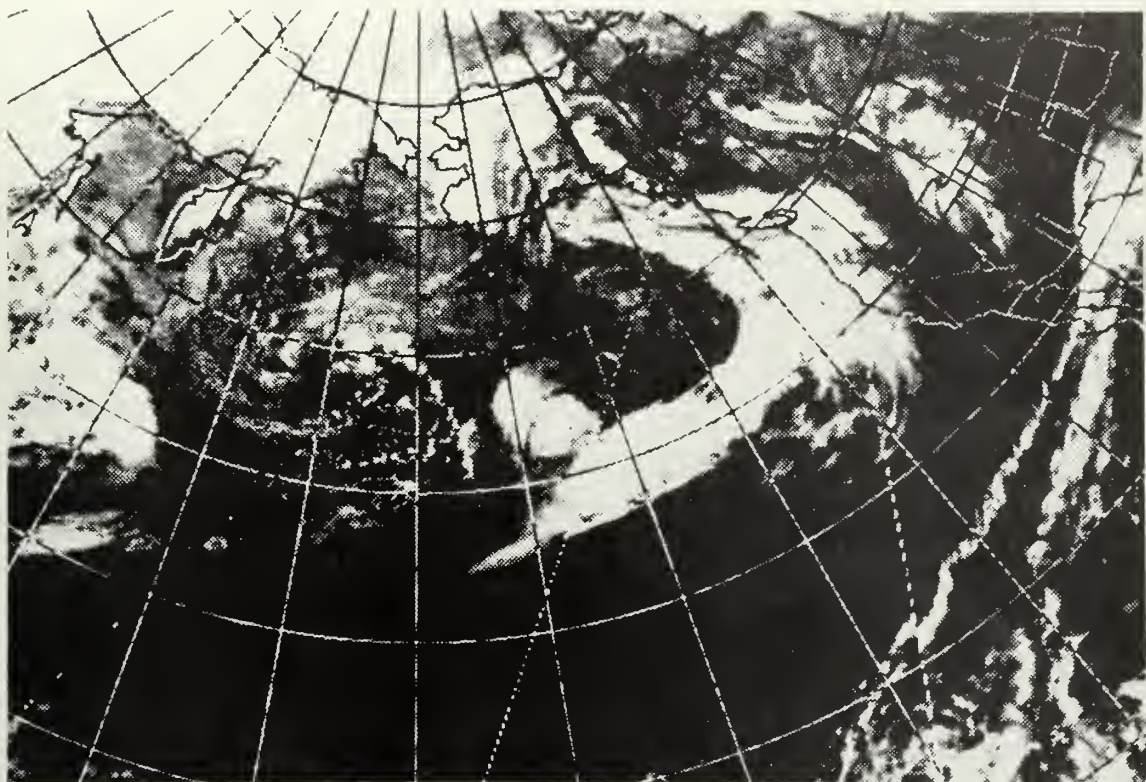


Fig. 11

Fig. 9 500 mb analyses
 1200 GMT 10 March 1971
 Values are 5XX0 meters

----- UNMOD ANAL
 ——— MOD ANAL

Fig. 10 Sea level analyses
 1200 GMT 10 March 1971
 Values are 10XX or 9XX mb

----- UNMOD ANAL
 ——— MOD ANAL

Fig. 11 Photo of ITOS-IR Mosaic for approximately 1200 GMT 10 March
 1971 at 140W.

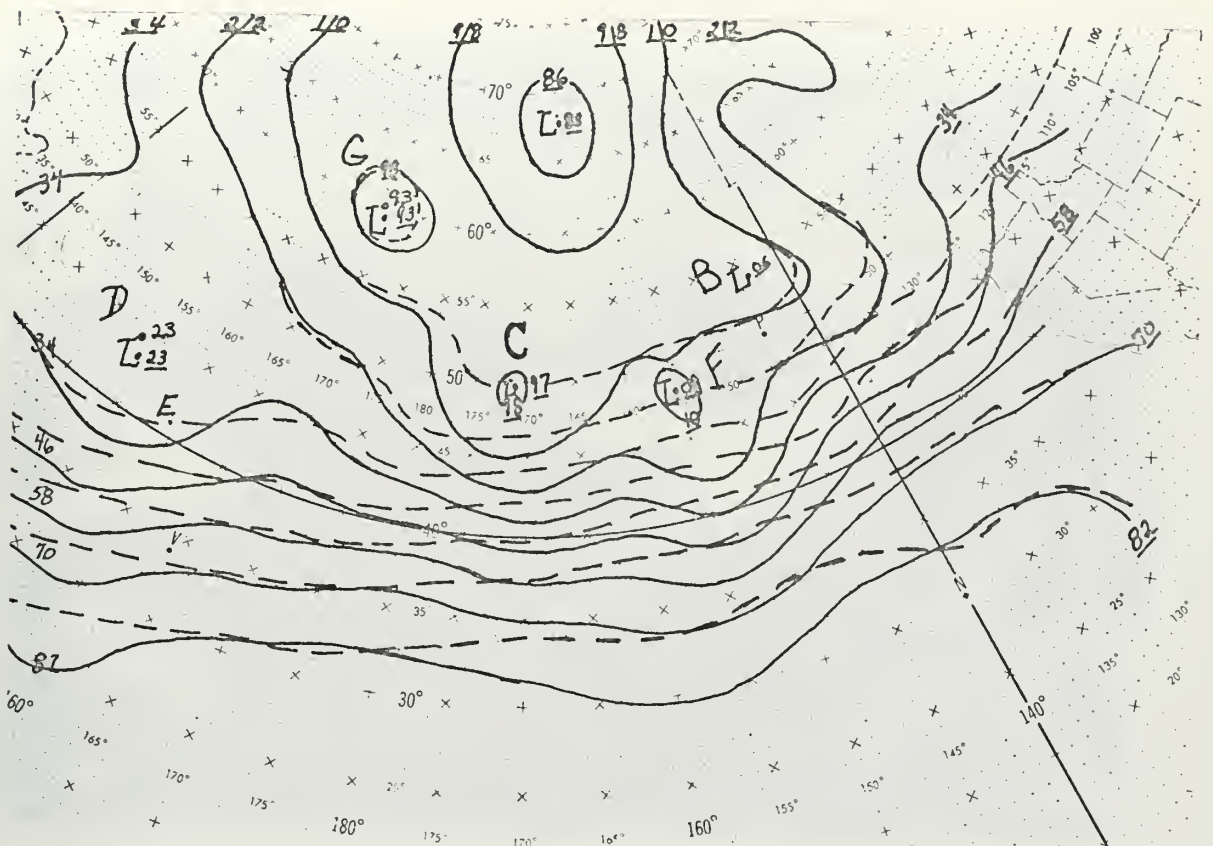


FIG. 12

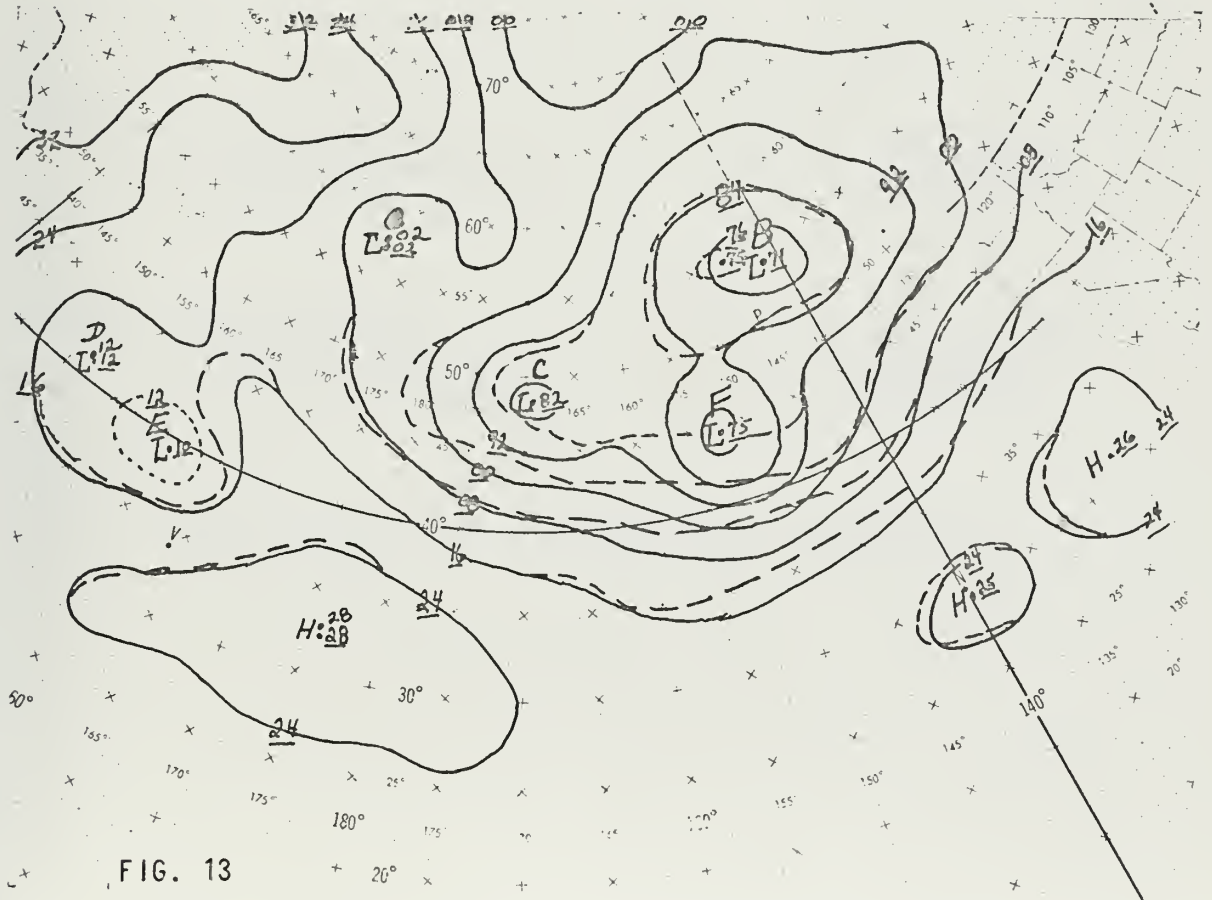


FIG. 13

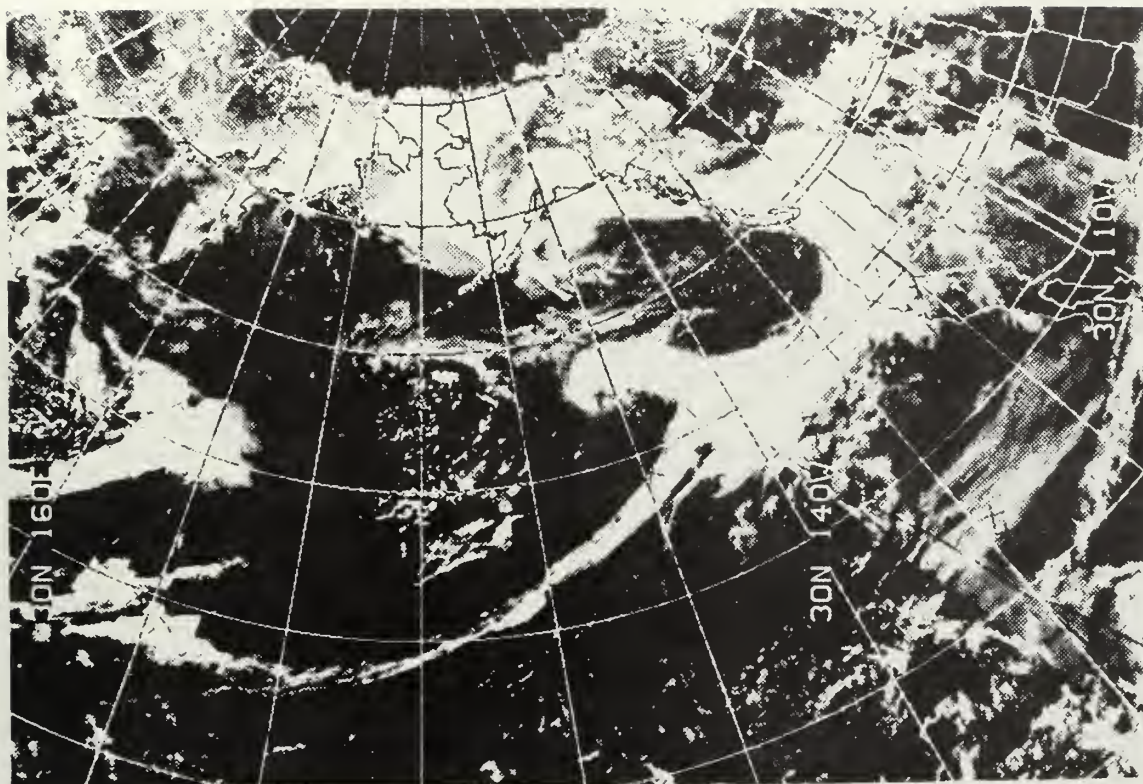


Fig. 14

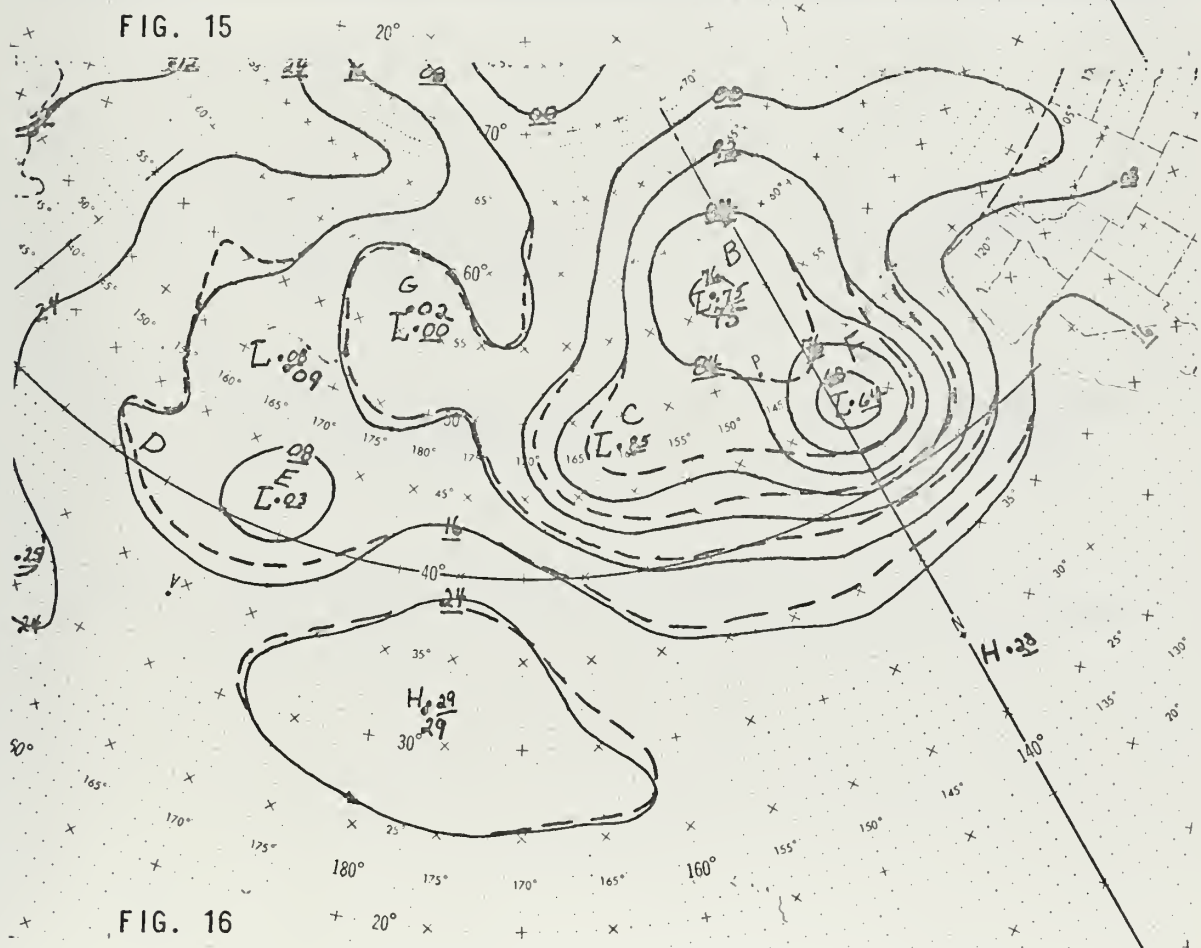
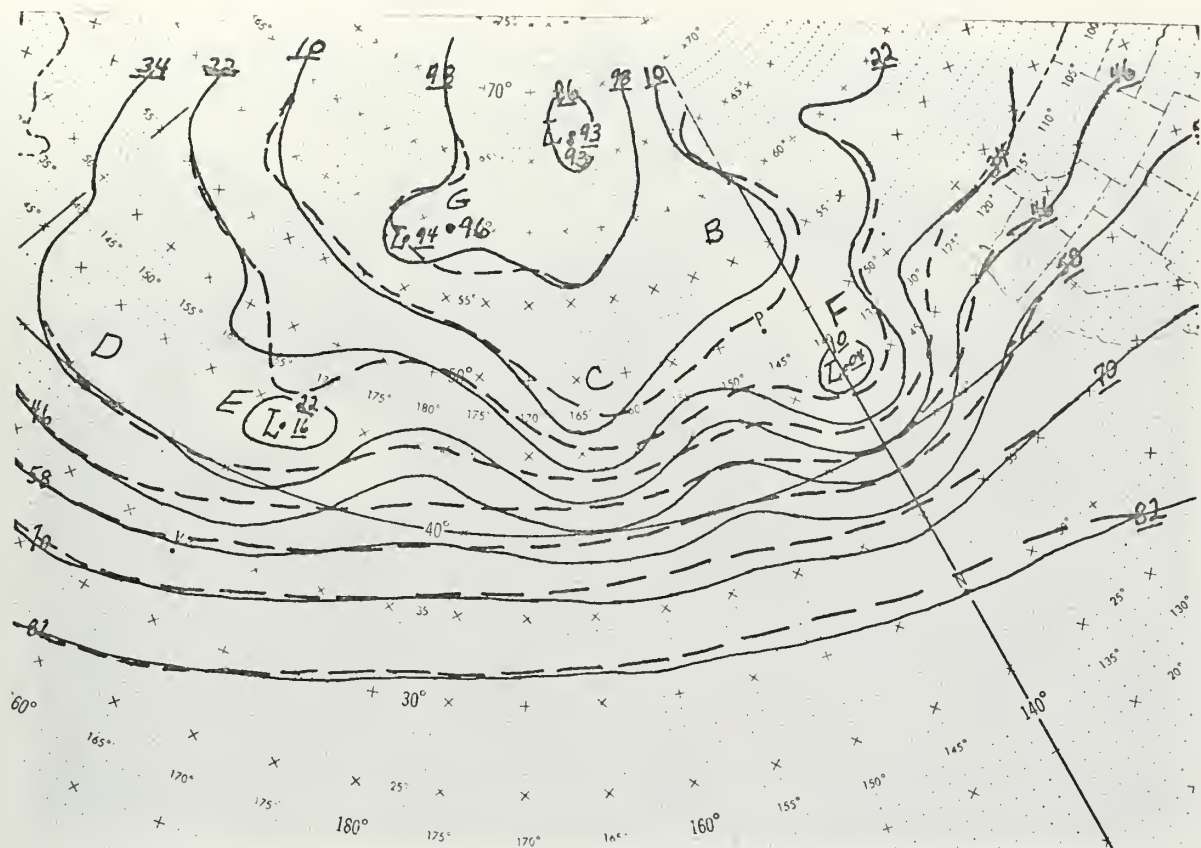
Fig. 12 500 mb analyses
0000 GMT 11 March 1971
Values are 5XX0 meters

----- UNMOD ANAL
—— MOD ANAL

Fig. 13 Sea level analyses
0000 GMT 11 March 1971
Values are 10XX or 9XX mb

----- UNMOD ANAL
—— MOD ANAL

Fig. 14 ITOS-1 Video Mosaic for approximately 0000 GMT 11 March 1971 at 140W.



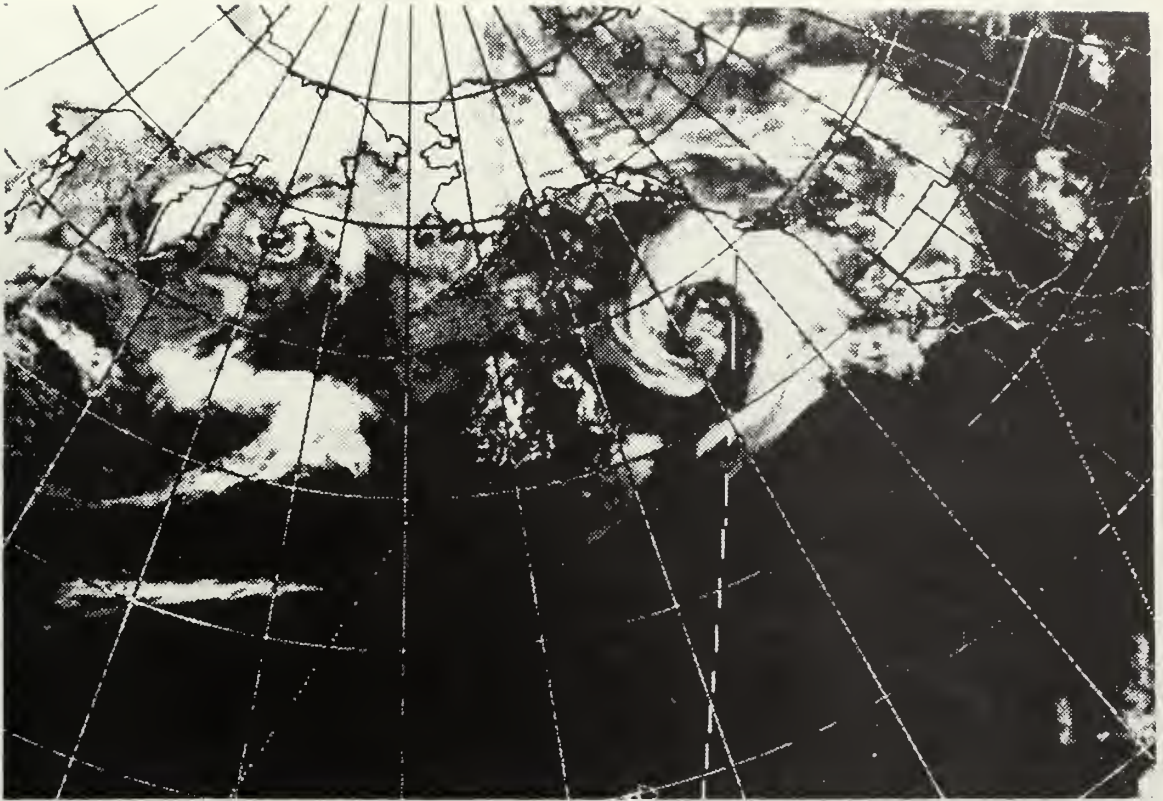


Fig. 17

Fig. 15 500 mb analyses
1200 GMT 11 March 1971
Values are 5XX0 meters

---- UNMOD ANAL
—— MOD ANAL

Fig. 16 Sea level analyses
1200 GMT 11 March 1971
Values are 10XX or 9XX mb

---- UNMOD ANAL
—— MOD ANAL

Fig. 17 Photo of ITOS-IR Mosaic for approximately 1200 GMT 11 March 1971 at 140W.

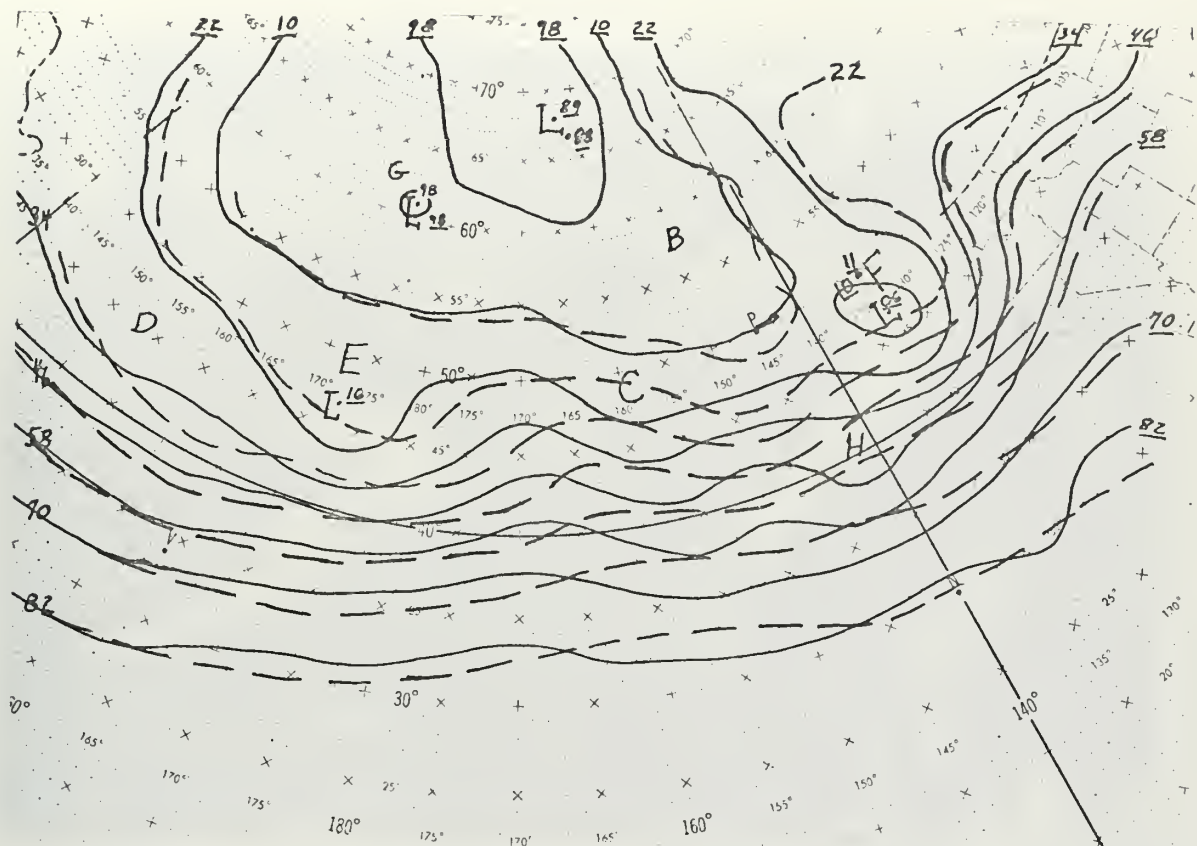
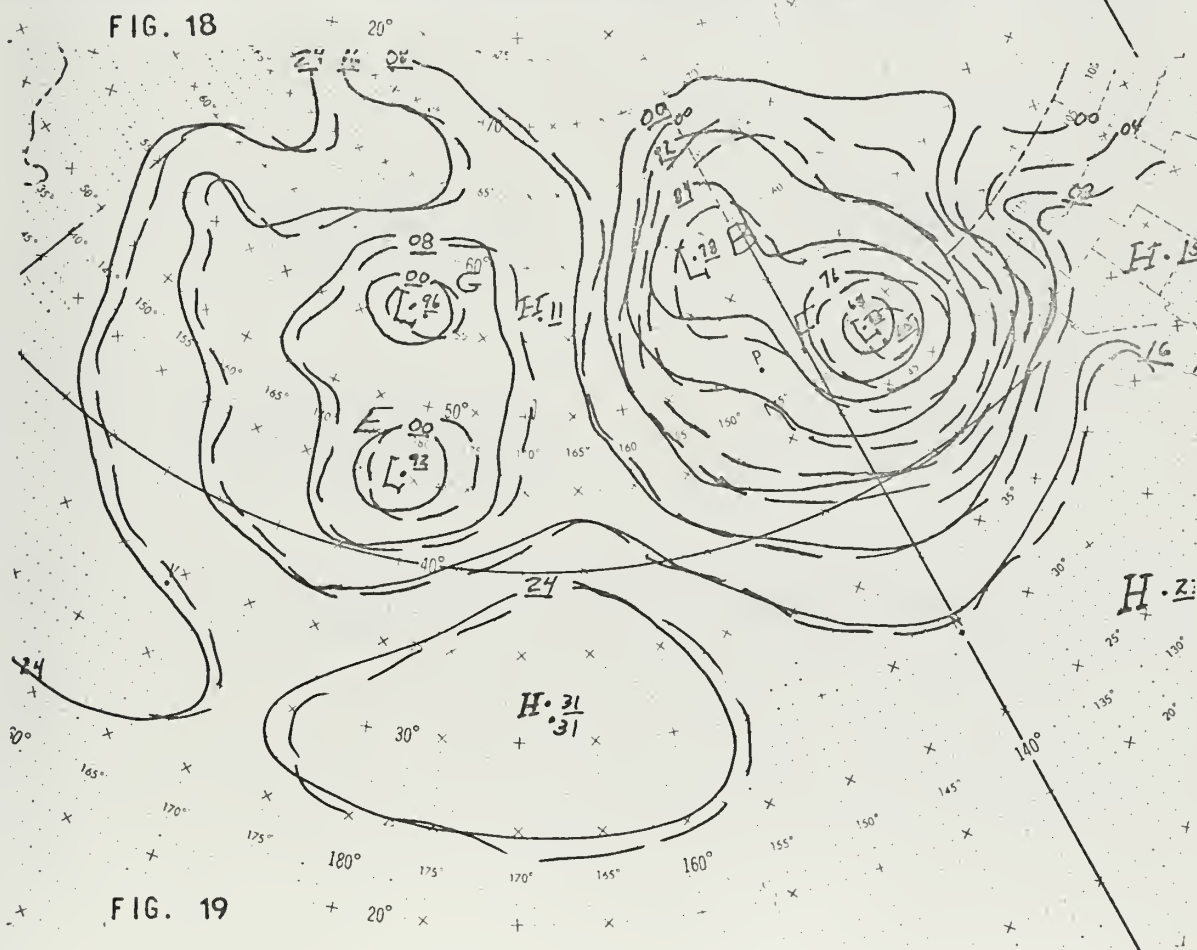


FIG. 18



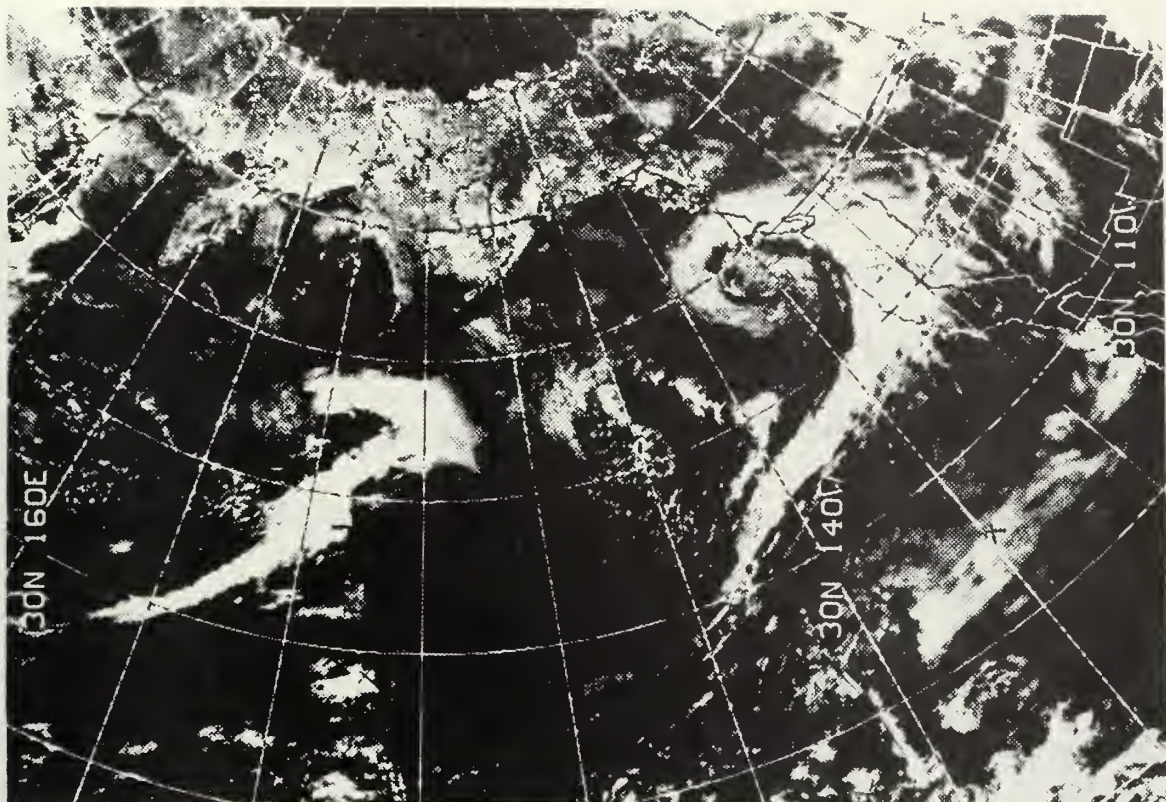


Fig. 20

Fig. 18 500 mb analyses
0000 GMT 12 March 1971
Values are 5XX0 meters

---- UNMOD ANAL
—— MOD ANAL

Fig. 19 Sea level analyses
0000 GMT 12 March 1971
Values are 10XX or 9XX mb

---- UNMOD ANAL
—— MOD ANAL

Fig. 20 ITOS-1 Video Mosaic for approximately 0000 GMT 12 March 1971 at 140W.

VI. RESULTS

To facilitate the discussion, the experiments in modifying the analyses and the effect on the attendant prognoses will be taken up separately. Comments concerning the utilization of the four techniques that resulted in the quantification of the satellite data will be included in the analysis discussion.

A. ANALYSIS

The results of the experimental 500 mb and sea level pressure modifications of the analyses (MOD ANALS) from 0000 GMT 10 March through 0000 GMT 12 March 1971, and the corresponding analyses from conventional data (UNMOD ANALS) are displayed opposite the applicable satellite pictures in section V. It must be pointed out that the desired degree of modification (see Appendix C) could not be objectively (numerically) reproduced in all cases. However, only the objectively modified analyses are presented in section V.

The influence of the satellite data on the analyses is readily apparent in each of the figures. As an example, Fig. 10 shows what is considered to be the most pronounced case of satellite modification made to the objective upper-air analyses for the particular period of time. The modification changes the analysis of zonal flow to a more meridional flow around short-wave troughs and ridges.

The rapid intensification of Vortex F between 10 and 11 March 1971 is an outstanding example of the situation encountered by the analyst (human or machine) working in the data sparse area of the North Pacific Ocean. Using the FWC Pearl Harbor manually analyzed sea-level pressure maps purely as an example, vortex F, when measured from the erroneously positioned peak of the frontal wave at 1200 GMT 10 March to its accurately specified position 12 hours later seemingly moved at the excessive speed of 80 kts across much-used shipping lanes, dropped 34 mb in pressure, and increased its wind from 10-15 kts to a storm-force intensity of 55 kt. Real-time availability of satellite photos or a nephanalysis at 0000 GMT and application of the satellite forecasting rule -- that a PVA maximum approaching a convex bulge in a trailing cold front may result in a rapidly deepening surface cyclone -- would have permitted a re-analysis of the position of the frontal wave and its potential for deepening. The photo of excellent ITOS-1 IR nighttime observations at 1246 GMT 10 March would have confirmed the presence of a deepening system, and the first daylight ATS-1 and ESSA-8 video pictures about 1800 GMT 10 March would have emphasized the need for a storm warning superseding previously issued gale warnings or heavy weather advisories.

Comments concerning the four data input methods of 1) subjective techniques, 2) vector winds, 3) the Nagle-Hayden technique, and 4) SIRS soundings, which were used in the modifications follow.

1. Subjective Techniques

Subjective methods of incorporating satellite data entered the modification efforts in a number of ways:

a. Revising Conventional Soundings

A revision of rejected and missing portions of conventional rawinsonde observations through comparison with satellite photos and SIRS soundings led to several significant improvements of the conventional data. For example, the Ship Papa 500 mb wind at 1200 GMT 10 March 1971 failed the FNWC Monterey consistency check and was rejected. (See 1200 GMT 10 March modification discussion.) It was a simple matter to compare the cloud patterns in the vicinity of Ship Papa with the winds reported on the sounding above and below the 500 mb level, determine the probable transmission garble, and correct it with a bogus wind report.

b. Determining Intensification of Synoptic Features

Two basic steps were followed in determining the amount of intensification undergone by a given synoptic feature from one map time to the next: 1) close surveillance, and 2) choosing a satellite photography analog.

Close surveillance was afforded by the outstanding collection of satellite photographs obtained from the various agencies noted in Table 1. The time lapse in photographic coverage was never greater than 12 hours. The photographs of nighttime IR values were particularly valuable since these mosaics nearly coincided with the 1200 GMT

synoptic time. Consequently, during the time frame of the study each synoptic feature, particularly the vortical systems, could be clearly followed.

Analogues were selected from the various satellite photography guidebooks [1, 7, 12, 14, 15, 17 and 26] which contain an excellent assortment of time-lapse photographs relating changes in cloud patterns to synoptic map changes for the given feature (i.e. wave cyclone, cold trough, etc.).

Using the analogue selected, and noting the changes in the individual cloud patterns, a qualitative decision was made concerning the sign of the intensity change since the last map time. The confidence level of the decision was strengthened by "looking ahead" to the next 0600 or 1800 GMT sea-level pressure analysis (see section IV for an explanation of this "updating" procedure). Next, tentative 500 mb height values were assigned to the feature on the basis of the 12-hour old value, the current operational analysis value, and the subjectively indicated change. This tentative value was then compared with the computation from the Nagle-Hayden technique and the SIRS values (if available) for a "best fit" with the conservative thickness pattern. This final value was then placed into the modification.

c. Tightening of Gradient in Proximity to Jet Streams

The 500 mb gradient was geostrophically corrected in the vicinity of the polar jet stream where clear-cut detection of jet stream cirrus was possible [15]. This method would have been more useful for modifying the 300 or 200 mb levels.

Several excellent satellite photographs of subtropical jet streams were noted during this period, but no attempt was made to modify the wind flow in the lower latitudes.

d. Modifying Thickness Contours near Fronts

After surface fronts were re-positioned on the basis of satellite interpretation, the 1000/500 mb thickness patterns were adjusted to conform to the standard model pattern of the National Weather Service [25]. After revising the surface analysis, if necessary, the 500 mb field was retrieved by graphical addition of the surface and thickness fields. This procedure proved quite simple and rapid to use in practice since the area of change was normally small. Furthermore, when used in conjunction with the Nagle-Hayden SD zero-vorticity line delineation, this technique invariably resulted in a more meridional trough to ridge flow than before at 500 mb over the associated surface cyclone feature.

2. Vector Winds

The ATS-1 wind reports recorded at NESS by computing the vector movement of cloud patterns recorded on film loops did not provide useful inputs during this particular period. The migratory pressure patterns were generally north of 40N, whereas vector winds were seldom computed north of 30N. These computations were restricted to the 300 mb level, though NESS does derive low-level (850 mb) winds on occasion. Unquestionably, low-level wind observations during the development of vortex F would have been extremely useful. Though the authors had access to the film loops, there was no vector equipment on hand.⁸

⁸Vector wind console and satellite picture equipment are scheduled for installation at the FNWC Monterey, by January 1972.

3. Nagle-Hayden Technique

The Nagle-Hayden technique for deriving 500 mb height values from the SR 500 mb field by using the geometry of certain types of observable cloud patterns proved extremely workable in practice. Once the authors became accustomed to the methods of delineating the SD zero-line and spiral cloud amplitude and diameter, the corresponding statistical heights for the North Pacific Ocean could be constructed in less than one hour. Presumably, a skilled analyst could perform this task in less than 30 minutes. With access to a CRT (cathode ray tube) console at a major computer center, the entire process is amenable to computerization, with the values being derived and incorporated automatically in a matter of minutes.

The zero-line technique was particularly useful in interpreting short-wavelength troughs and ridges. At each map time, this method was used to derive 500 mb heights along troughs and ridges across the entire ocean. Although some of the values were then changed subjectively, most of them could have been incorporated without change into the MOD ANAL if the FNWC restriction of 50 bogus points could have been expanded.

4. SIRS Data

The FNWC program restriction of fifty bogus points at the 500 mb level prohibited direct input of all the available SIRS soundings. The SIRS values for 500 mb were considered as data during the manual MOD ANAL effort and therefore did influence the bogus values used to achieve the desired objective MOD ANAL. Available SIRS coverage for the North

Pacific Ocean was poor on the 1200 GMT 10 March map (two reports), fair at 0000 GMT 11 March (11 reports) and 1200 GMT 11 March (10 reports), and good at 0000 GMT 10 March (19 reports) and 0000 GMT 12 March (21 reports). Of these soundings, many were located in the subtropical regions, and not used in the modification. The remaining soundings were useful in the re-positioning of troughs and ridges.

To cite an example, on a north-south oriented trough line along 155W at 0000 GMT 10 March, three SIRS heights of 5190 m, 5370 m, and 5680 m were recorded. The corresponding FNWC operational analysis values were 5310 m, 5520 m, and 5760 m. The input of the SIRS values would have improved the FNWC operational analysis of this short-wave trough. At 0000 GMT 12 March, in the vicinity of a deepening trough near 135W, two SIRS values of 5490 m and 5480 m compared with 5640 m and 5620 m, respectively, for the FNWC analysis.

In summary, the scanty amount of applicable SIRS 500 mb height values was used to great advantage in the re-positioning of short-wave troughs and ridges. The hemispheric coverage of SIRS 500 mb heights for this period is discussed in Appendix B.

B. PROGNOSSES

The FNWC primitive equation (PE) prediction model was used to generate 12, 24, 36, and 48 hour prognostic fields from the MOD and UNMOD ANALS of 1200 GMT 10 March and 0000 GMT 11 March 1971. The sea level and 500 mb MOD and UNMOD PROGS for each of the

four forecast intervals are displayed in Figs. 21 through 36, with MOD (solid lines) and UNMOD (dashed lines) versions superimposed.

1. Broad Aspects

Salient features of the prognoses are summarized below.

1) The MOD and UNMOD prognoses appear to converge to a similar pattern with increasing forecast interval; this fact becomes quite evident by the 48-hour prognosis. That is, the small-scale features appear to be smoothed out with time such that very similar large-scale patterns remain in both MOD and UNMOD versions by 48 hours.

2) Evidently, the FNWC PE model is very stable in the matter of handling bogused short wave features. No large errors were generated in any of the prognoses. Dispersion of energy from the new short wave features across the Northern Hemisphere is minimal. In fact, the comparable 48 hour prognoses were virtually identical in the regions not affected by the apparent propagation of the modified synoptic features. Fig. 37 illustrates this stability by showing a field of differences between the error fields of the 48 hour 500 mb MOD and UNMOD prognoses. The error fields were generated by verifying with the 500 mb STACK ANAL (SA).⁹ That is,

$$\text{Diff. Field} = [(\text{MOD PROG} - \text{SA}) - (\text{UNMOD PROG} - \text{SA})], \quad (6)$$

which is the same as taking the difference between the two prognoses.

Small differences in this field outside the area of interest indicate negligible side effects of using bogus data in the FNWC PE model.

⁹STACK ANAL = operational FNWC update analysis.

2. The Prognosis of Individual Synoptic Features

a. Discussion of 1200 GMT 10 March 1971 Prognoses

(Figs. 21 through 28).

(1) Vortex B. The MOD PROG moved vortex B very slowly to the northwest, and filled it 4 mb to a 976 mb sea-level value in 48 hours. At 500 mb there was only slight movement northward. The center dropped 30 m to 5050 m in the first 12 hours and remained at that height for the rest of the 48 hours.

In the UNMOD PROG the movement was slightly faster but the surface low remained in the Gulf of Alaska and deepened the center from 982 mb to 974 mb in 48 hours. A secondary cyclone is generated at the surface within 12 hours to the southeast of vortex B by both the MOD and UNMOD prognoses. The 24 hour MOD PROG moved this low inland and filled it. The UNMOD PROG retained this low and kept it quasi-stationary west of Vancouver Island, B. C., out to 48 hours. Its central pressure dropped from 989 mb to 978 mb. This UNMOD stationary feature coincided with the actual position of the fast moving vortex F at 1200 GMT 12 March and resulted in the 48 hour UNMOD PROG verifying well in this area. However, its quasi-stationary position during this prognosis is not verified by the spiral cloud patterns for this period of time.

(2) Vortex C. The cloud vortex is represented on the 500 mb MOD ANAL as a cyclone; its corresponding surface low repositioned westward 300 nmi for proper vertical alignment. The MOD PROG moved

this vortex eastward at 30 kt for the first 12 hours, and thereafter it averaged 20 kt out to 48 hours. Slight filling occurred in the first 12 hours but the closed system was retained at the surface out to 48 hours, having filled 3 mb at sea level and 130 m at 500 mb, where the trough is in evidence at 155W.

The UNMOD PROG moved this system eastward at 48 kt and filled it to where only troughs remained at both sea level and 500 mb by 36 hours, followed then by further damping of amplitude to 48 hours.

(3) Vortex D. This small, cold-core system is moved slowly eastward and filled by both MOD and UNMOD PROGS.

(4) Vortex E. This system is modified in the analysis at 500 mb and given a better trough-ridge configuration with a 60 m height change. MOD and UNMOD PROGS handled the movement of the sea-level system similarly with a northeastward movement at 13 kt. However, at the 500 mb level, only the MOD PROG retained this short-wave feature out to 36 hours. The UNMOD PROG version assimilated this feature after 12 hours.

(5) Vortex F. This closed circulation was placed into an existing sea level trough on the MOD ANAL but was lost on the 12 hour MOD PROG. However, the trough was retained in the MOD PROG but not in the UNMOD PROG. On the MOD PROG the trough moves to the northeast and deepens into a closed circulation in 48 hours. Though all the subsequent cloud patterns indicate this moving trough was continuously

a closed circulation, the movement in the MOD PROG appears good and verifies well in 48 hours. As mentioned earlier, the UNMOD PROG missed this moving system, but by coincidence the quasistationary sea-level low in the UNMOD PROG verifies very well on the 48 hour prognosis (but only on this prognosis) relative to the observed cloud patterns.

(6) Vortex G. This system was handled identically and fairly well by both MOD and UNMOD PROGS. It was moved too slowly at 500 mb causing the cyclone to develop some vertical tilt.

b. Discussion of 0000 GMT 11 March 1971 Prognoses (Figs. 29 through 36).

(1) Vortex B. The sea level MOD and UNMOD PROGS moved vortex B toward the north-northwest (NNW) with the UNMOD PROG fluctuating around 975 mb and the MOD PROG filling the center by 12 mb to 983 mb. The centers coincide in the northern Gulf of Alaska at 48 hours. As cyclone B moves towards the NNW, the troughs to the south-east of vortex B remained stationary on both the sea level and 500 mb UNMOD PROGS.

(2) Vortex C. The MOD PROG sea level/500 mb, 982 mb/4970 m low moves east-southeast (ESE) at 30 kt and fills to 987 mb/5040 m in 12 hours and slows to 20 kt while filling to 991 mb/5220 m in 48 hours. To the northeast at 500 mb, a short-wave ridge appears in the long-wave trough in 24 hours, but is absorbed in the large-scale flow by 48 hours.

The corresponding trough in the UNMOD PROG fills rapidly and is completely absorbed by the long-wave flow in 24 hours.

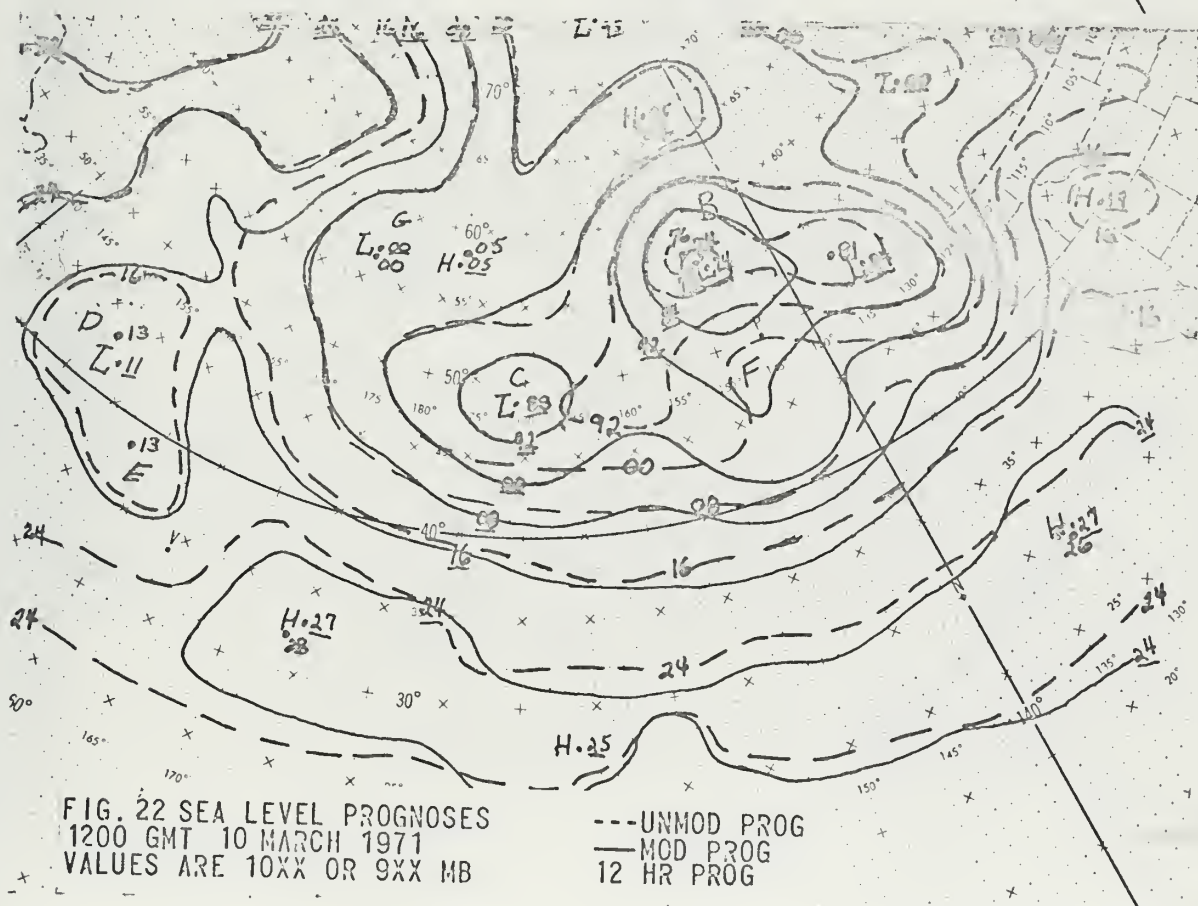
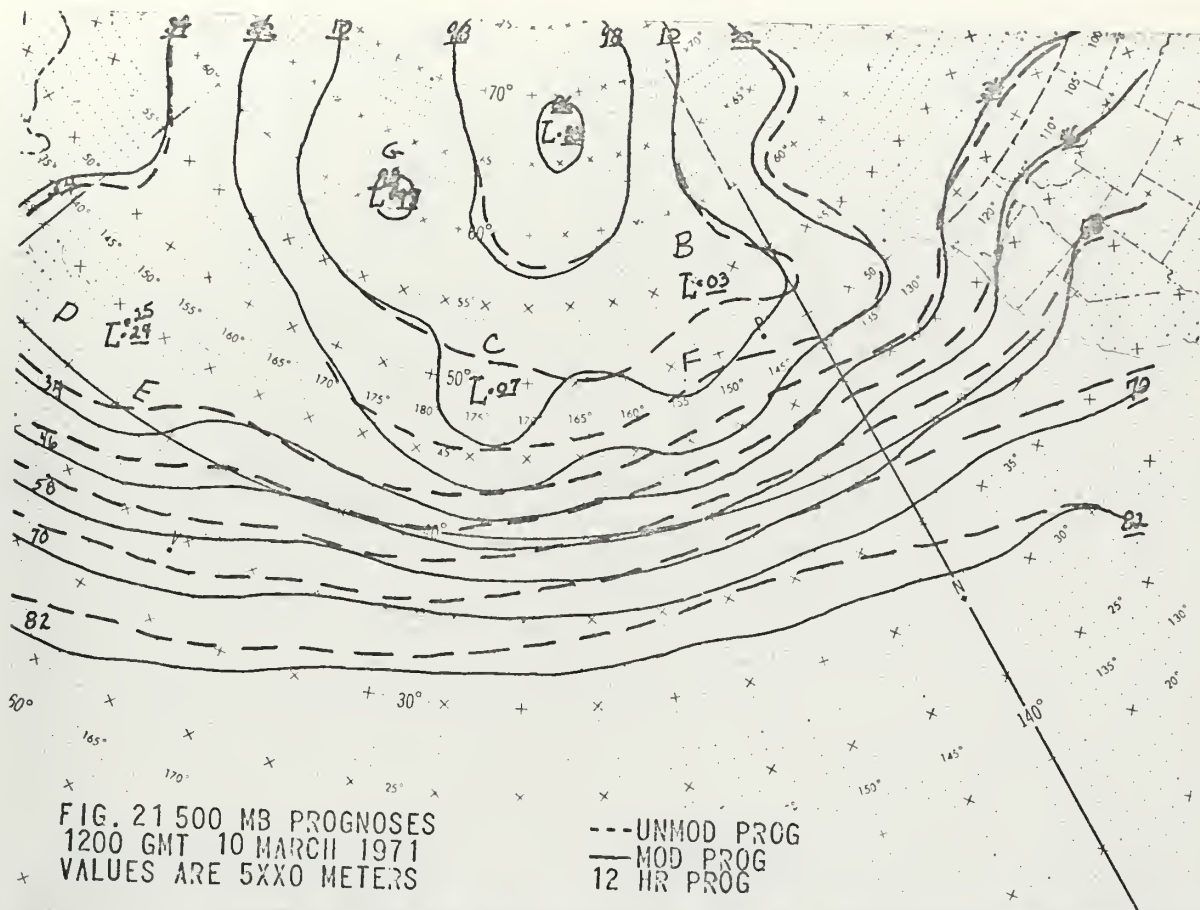
(3) Vortex D. This small system is handled well by both prognoses as it moved slowly eastward and dissipated.

(4) Vortex E. The MOD PROG moves this system at 20 kt toward the east-northeast and deepens it from 1010 mb to 990 mb at sea level in 48 hours. The associated 500 mb trough is continually broadened and sustained while the previously enhanced ridge to the east is completely smoothed into the long-wave pattern.

The UNMOD sea level trough moved eastward at 29 kt and the circulation intensified, but the center only deepened slightly. There is no 500 mb trough development associated with the sea level trough for this UNMOD PROG.

(5) Vortex F. This system existed only in the MOD ANAL and PROG. Considerable filling occurred in the first 12 hours with the sea-level/500 mb centers changing from 975 mb/5090 m to 982 mb/5160 m and retained only a weak trough. By 24 hours the sea level trough progressed northeast and blended with the stationary trough southeast of vortex B. Similarly at 500 mb, vortex F was no longer present as a distinctive feature, having merged into the long-wave trough dominating the region.

(6) Vortex G. This system was not modified and both prognoses handled it equally well, but excessive tilting of this system occurred with increasing forecast interval.



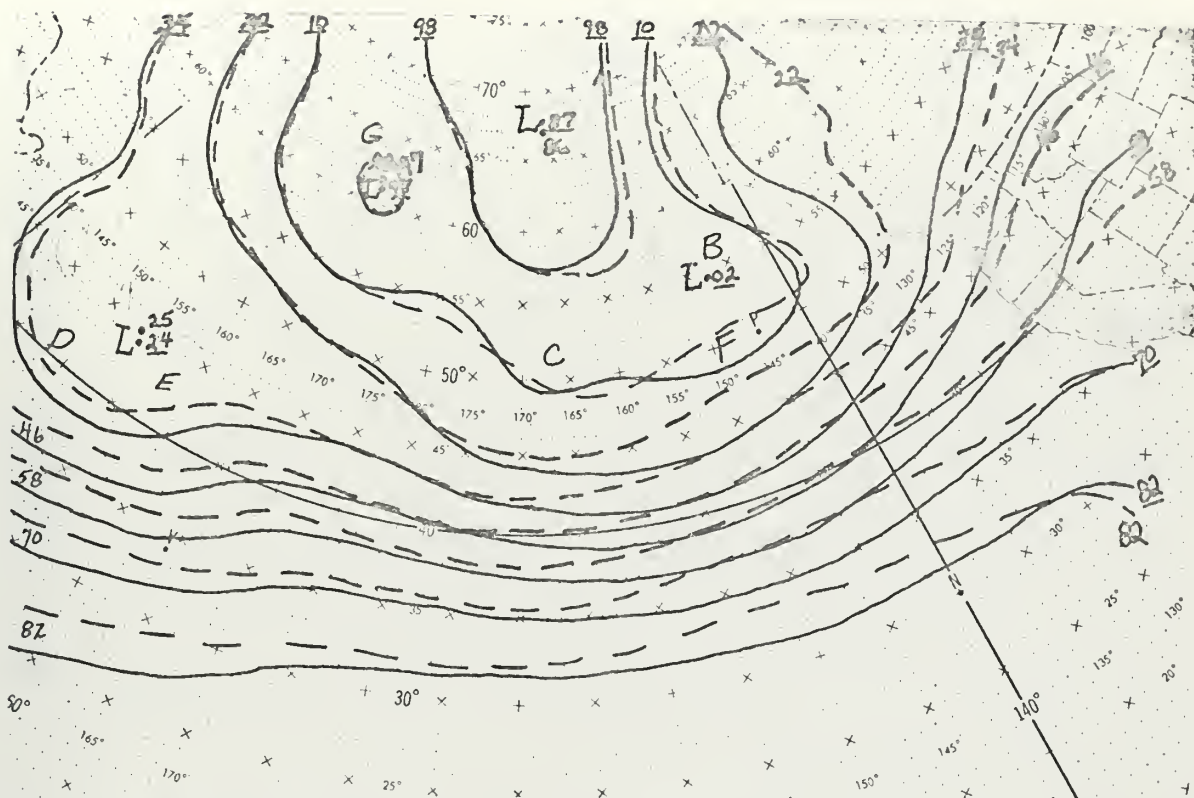


FIG. 23 500 MB PROGNOSSES
1200 GMT 10 MARCH 1971
VALUES ARE 5XX0 METERS

---UNMOD PROG
—MOD PROG
24 HR PROG

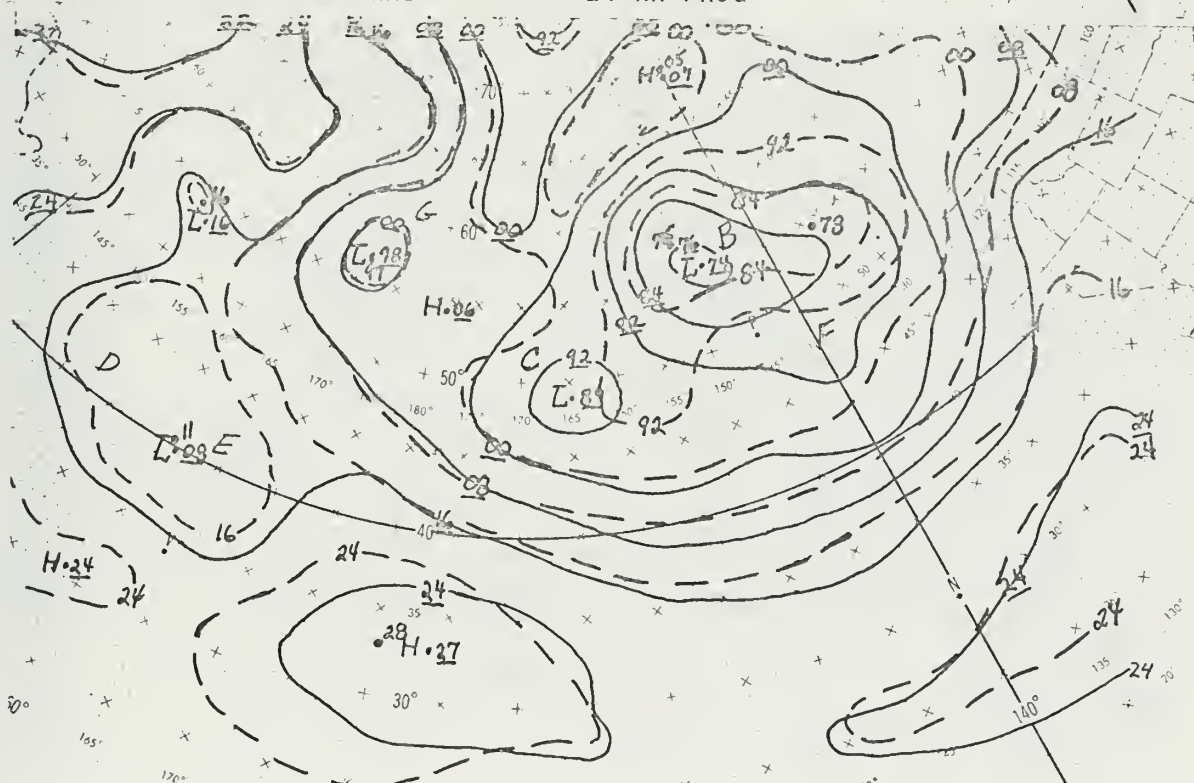


FIG. 24 SEA LEVEL PROGNOSSES
1200 GMT 10 MARCH 1971
VALUES ARE 10XX OR 9XX MB

---UNMOD PROG
—MOD PROG
24 HR PROG

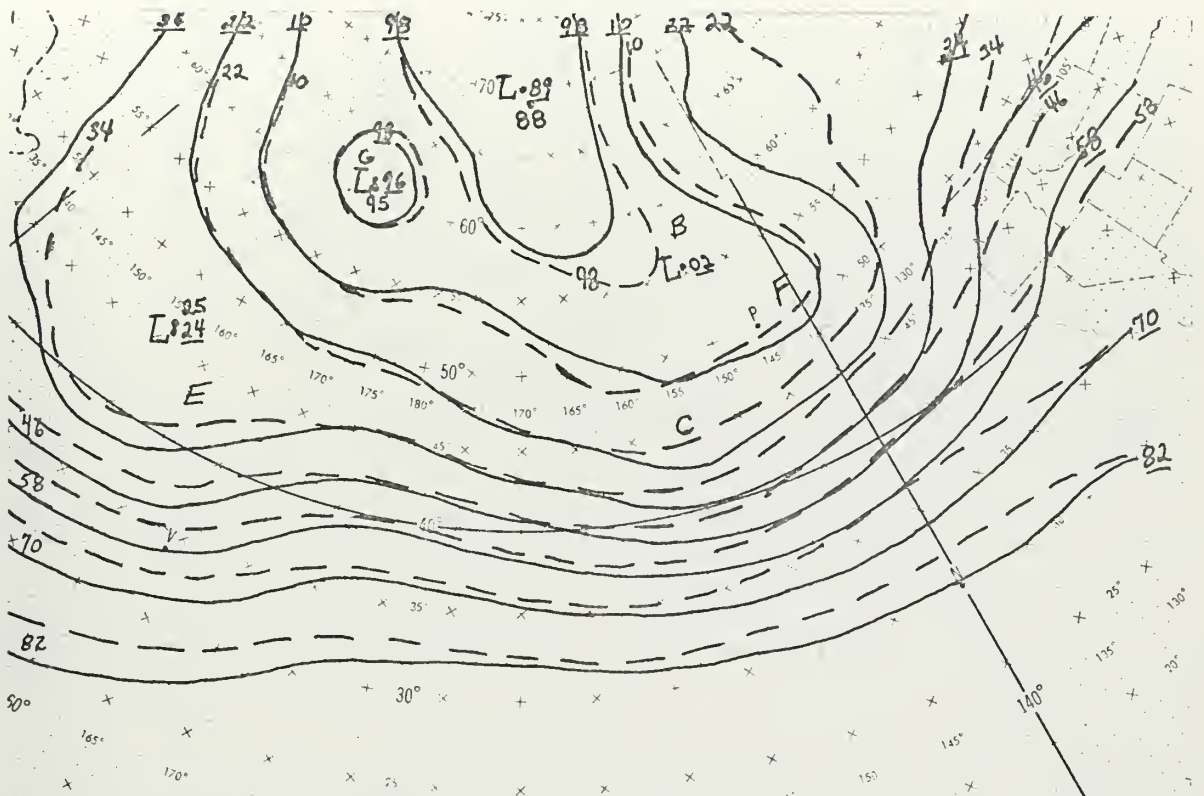


FIG.25 500 MB PROGNOSTIC
1200 GMT 10 MARCH 1971
VALUES ARE 5XX0 METERS

---UNMOD PROG
—MOD PROG
36 HR PROG

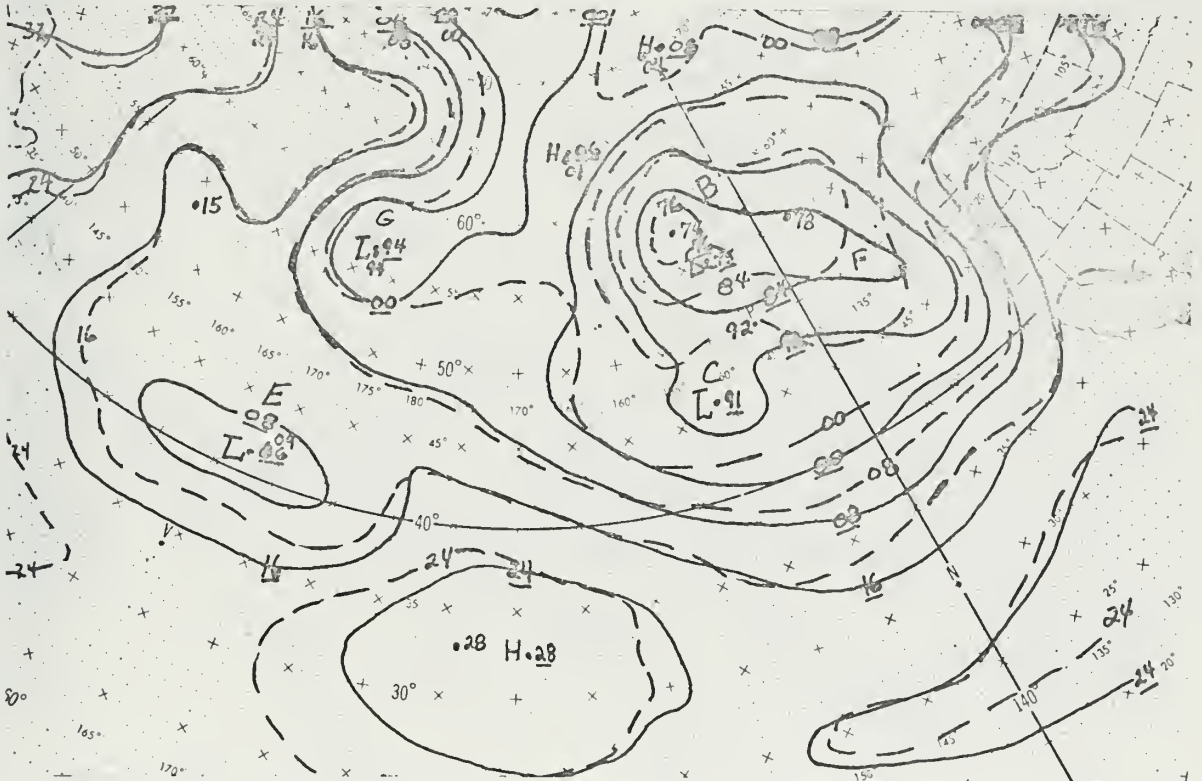
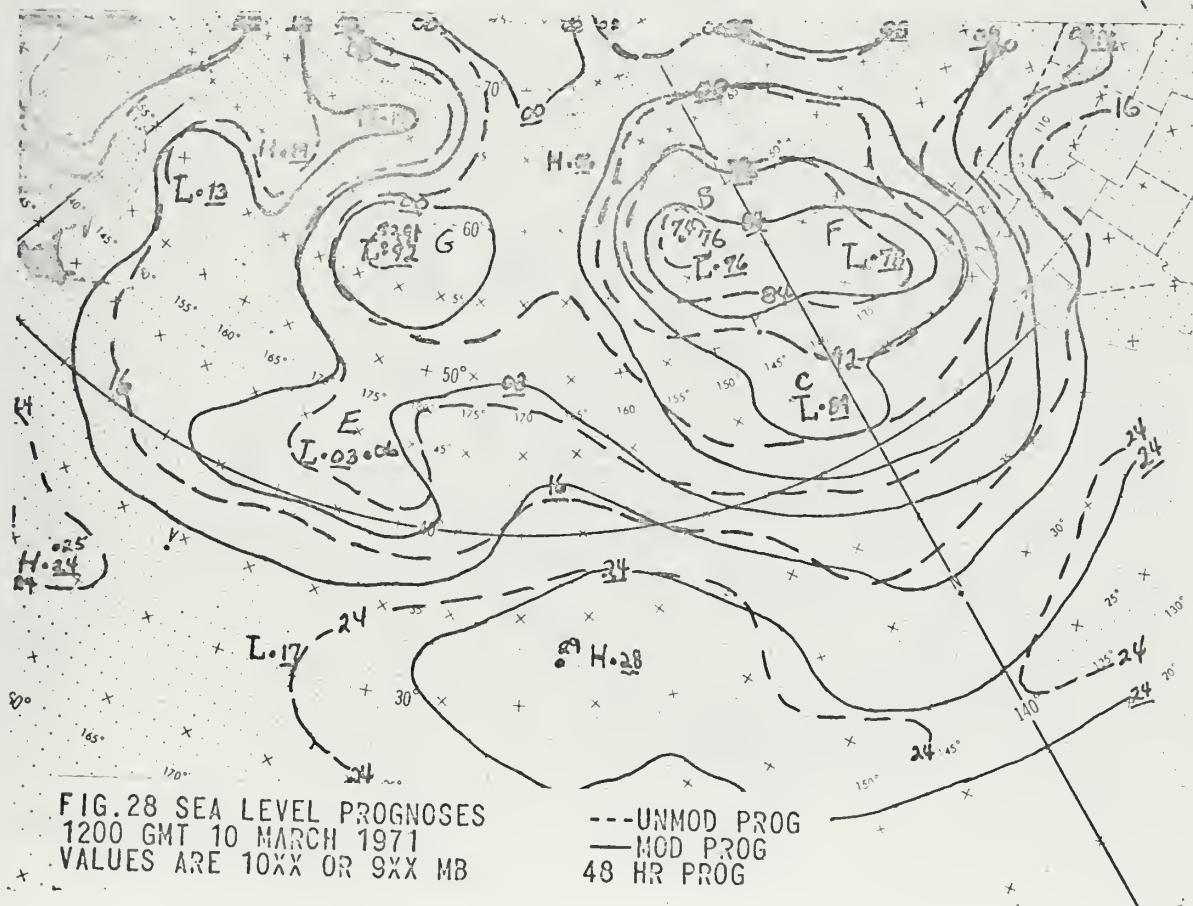
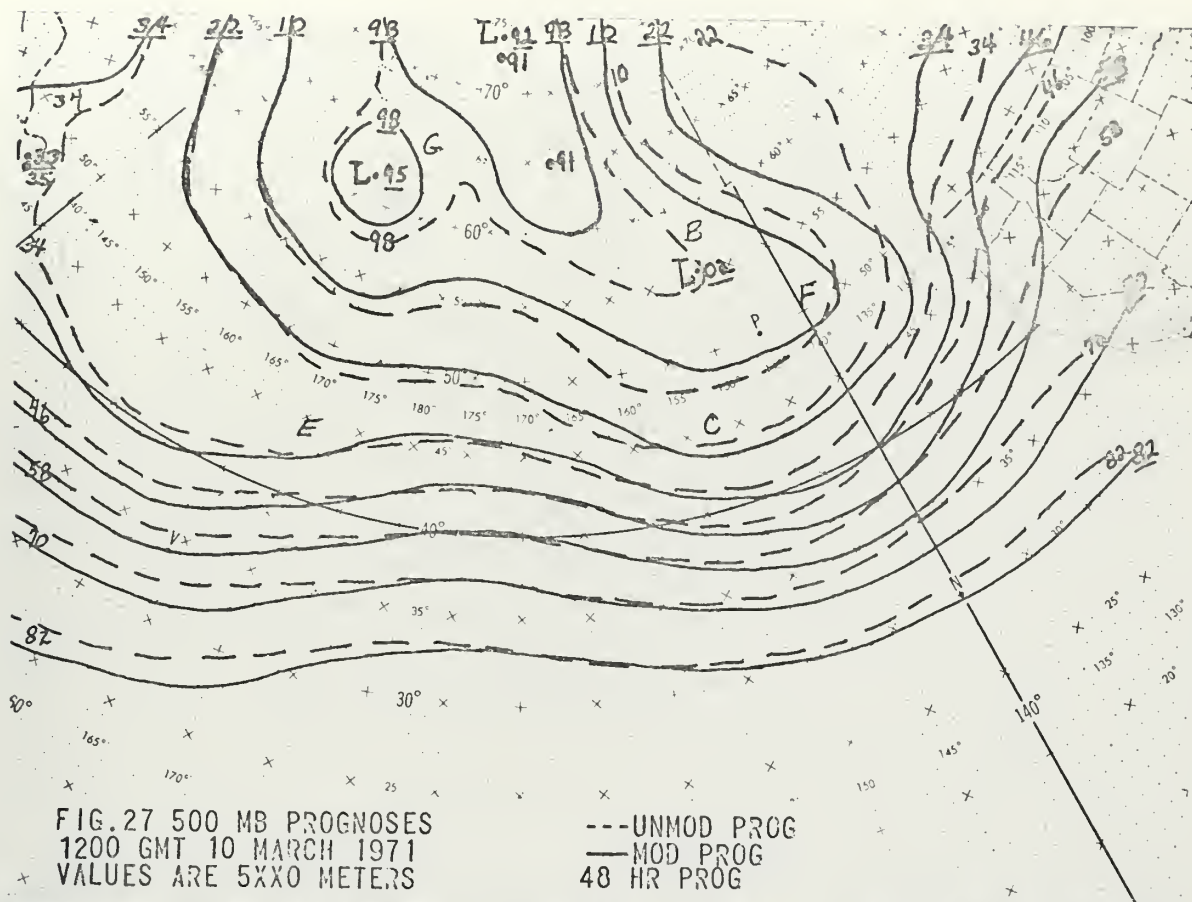


FIG.26 SEA LEVEL PROGNOSTIC
1200 GMT 10 MARCH 1971
VALUES ARE 10XX OR 9XX MB

---UNMOD PROG
—MOD PROG
36 HR PROG



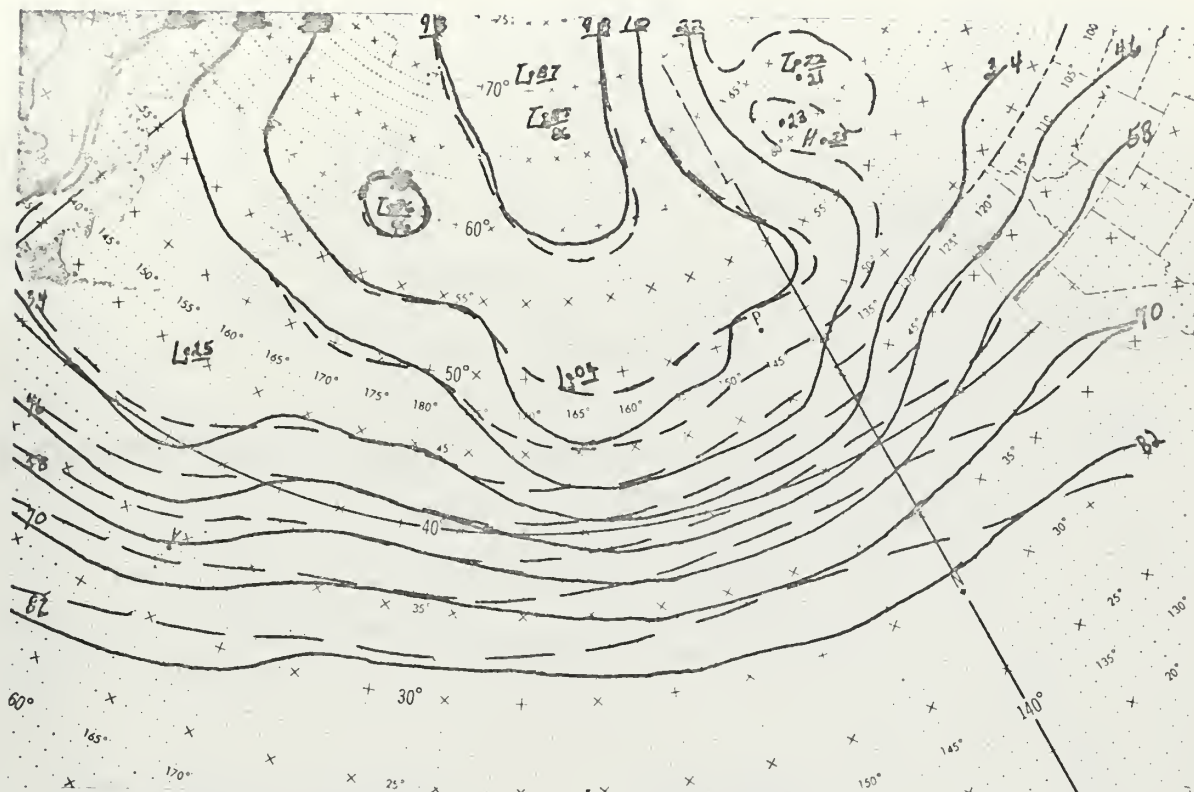


FIG. 29 500 MB PROGNOSTIC CHART
0000 GMT 11 MARCH 1971
VALUES ARE 5XX METERS

---UNMOD PROG
—MOD PROG
12 HR PROG

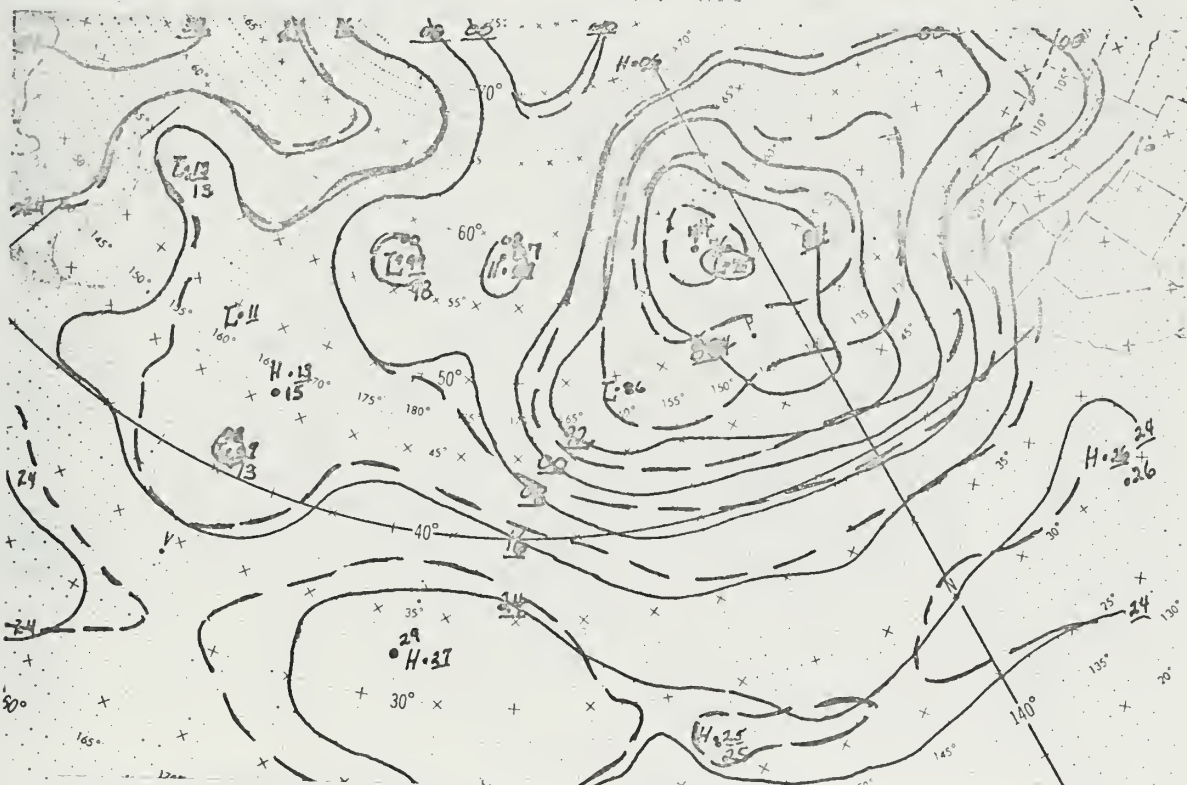


FIG. 30 SEA LEVEL PROGNOSTIC CHART
0000 GMT 11 MARCH 1971
VALUES ARE 10XX OR 9XX MB

---UNMOD PROG
—MOD PROG
12 HR PROG

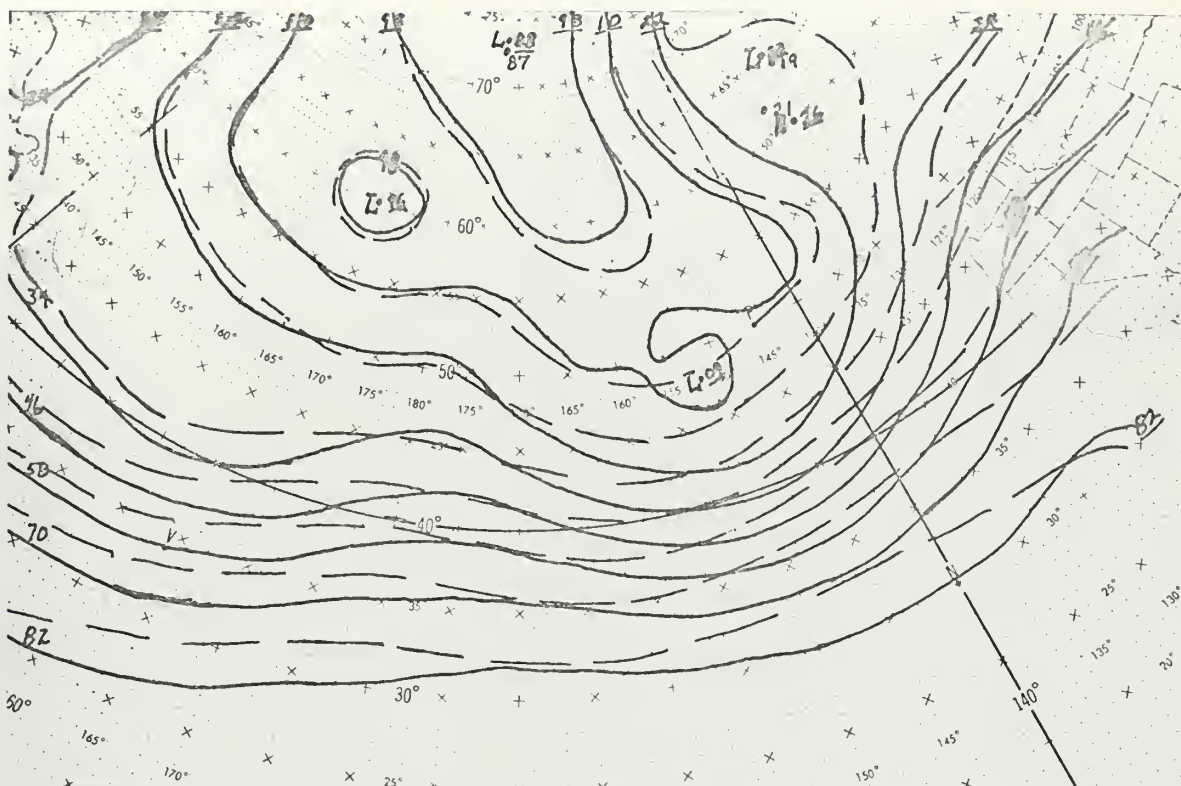


FIG.31 500 MB PROGNOSSES
0000 GMT 11 MARCH 1971
VALUES ARE 5XX0 METERS

---UNMOD PROG
—MOD PROG
24 HR PROG

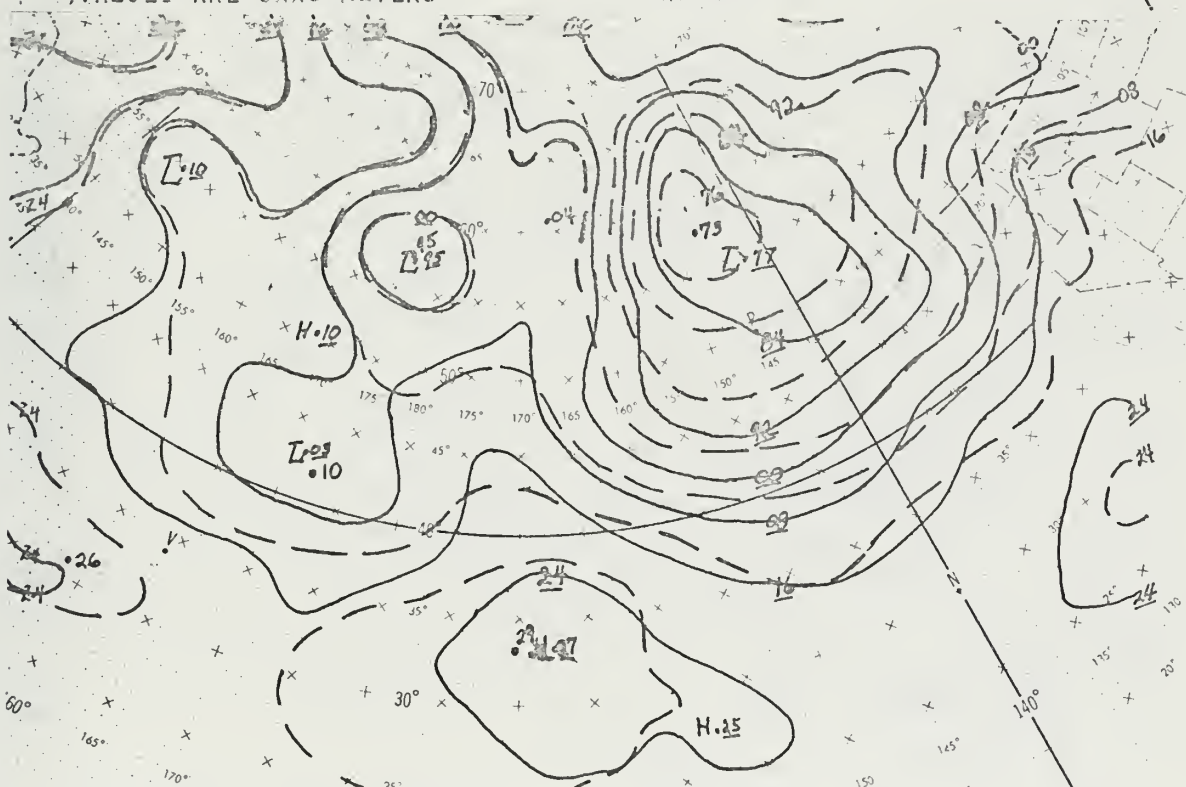
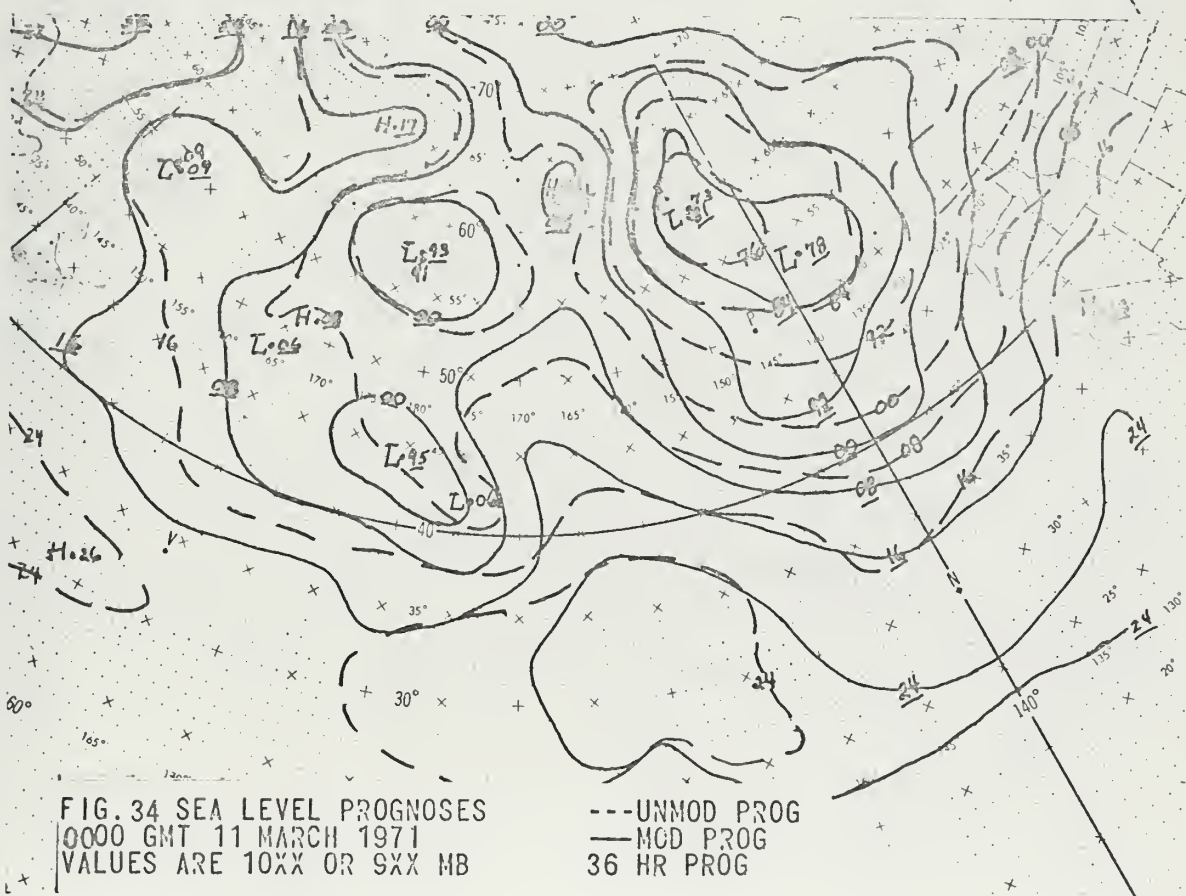
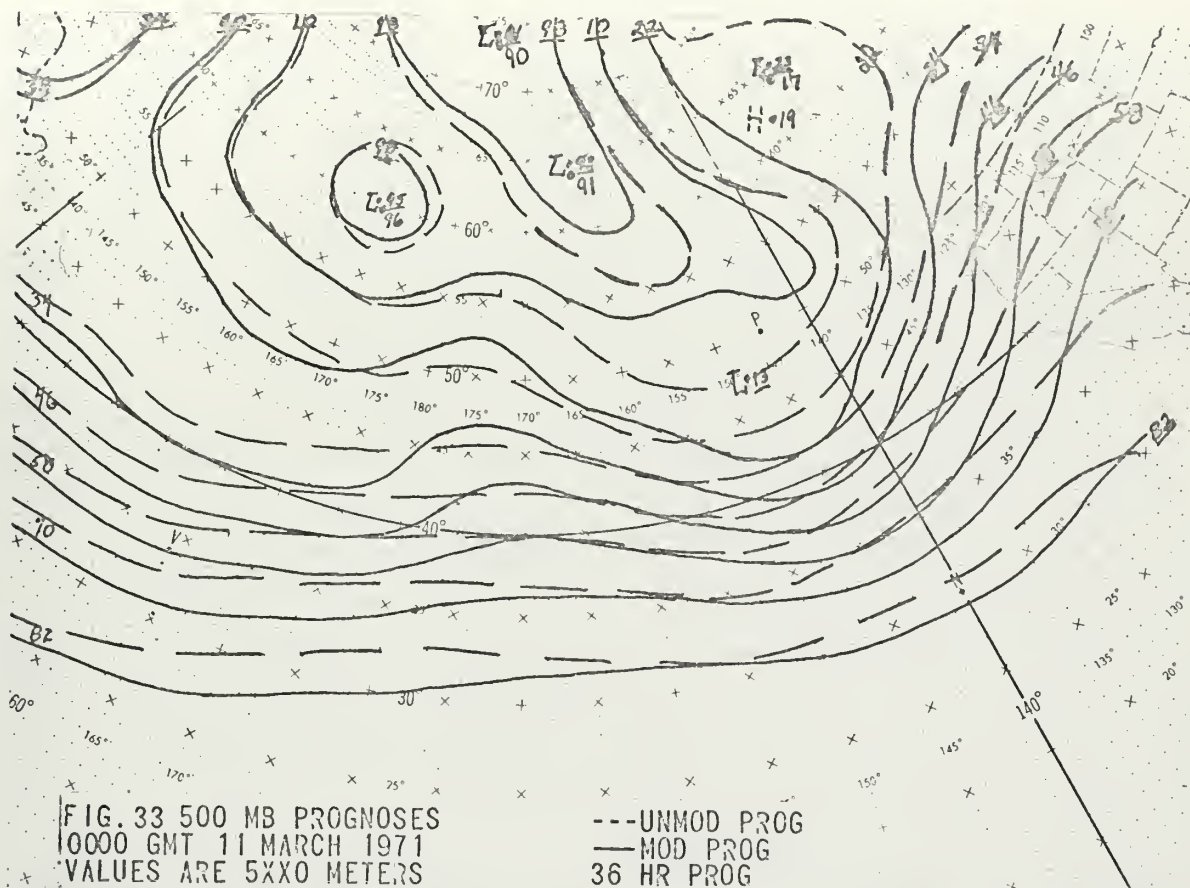


FIG.32 SEA LEVEL PROGNOSSES
0000 GMT 11 MARCH 1971
VALUES ARE 10XX OR 9XX MB



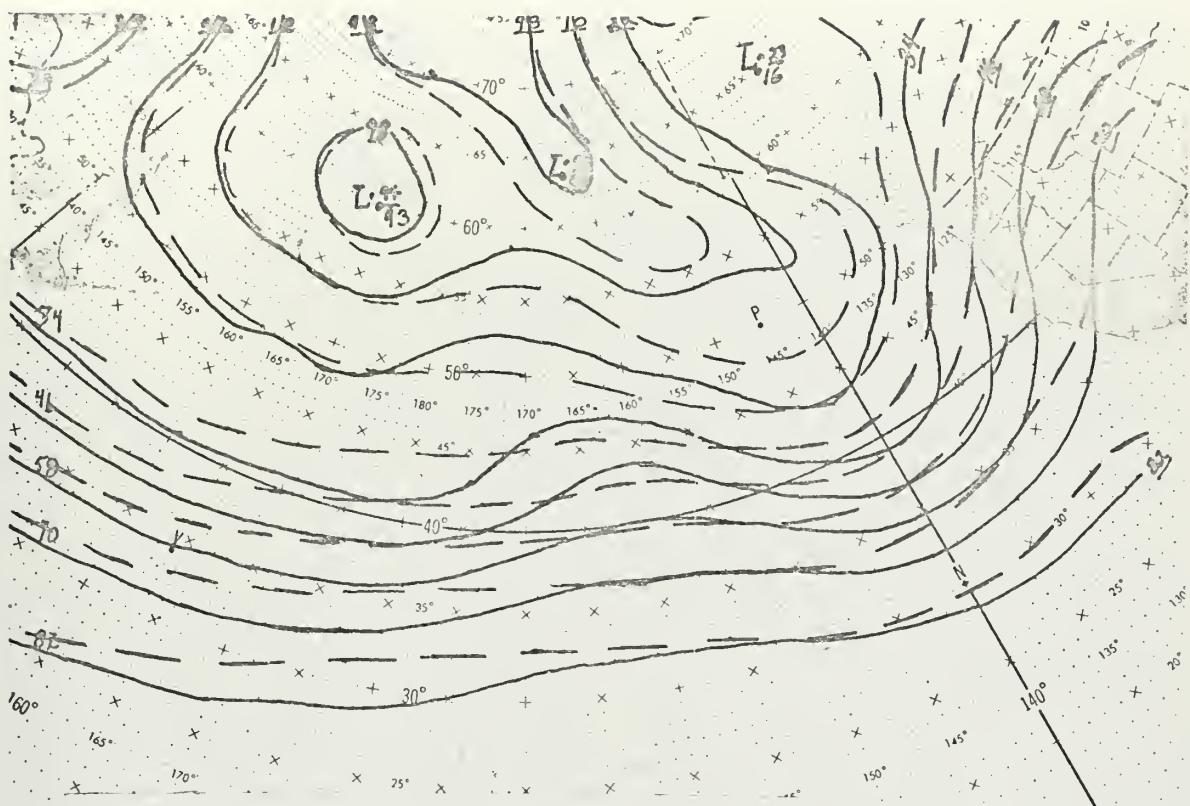


FIG.35 500 MB PROGNOSSES
0000 GMT 11 MARCH 1971
VALUES ARE 5XX0 METERS

---UNMOD PROG
—MOD PROG
48 HR PROG

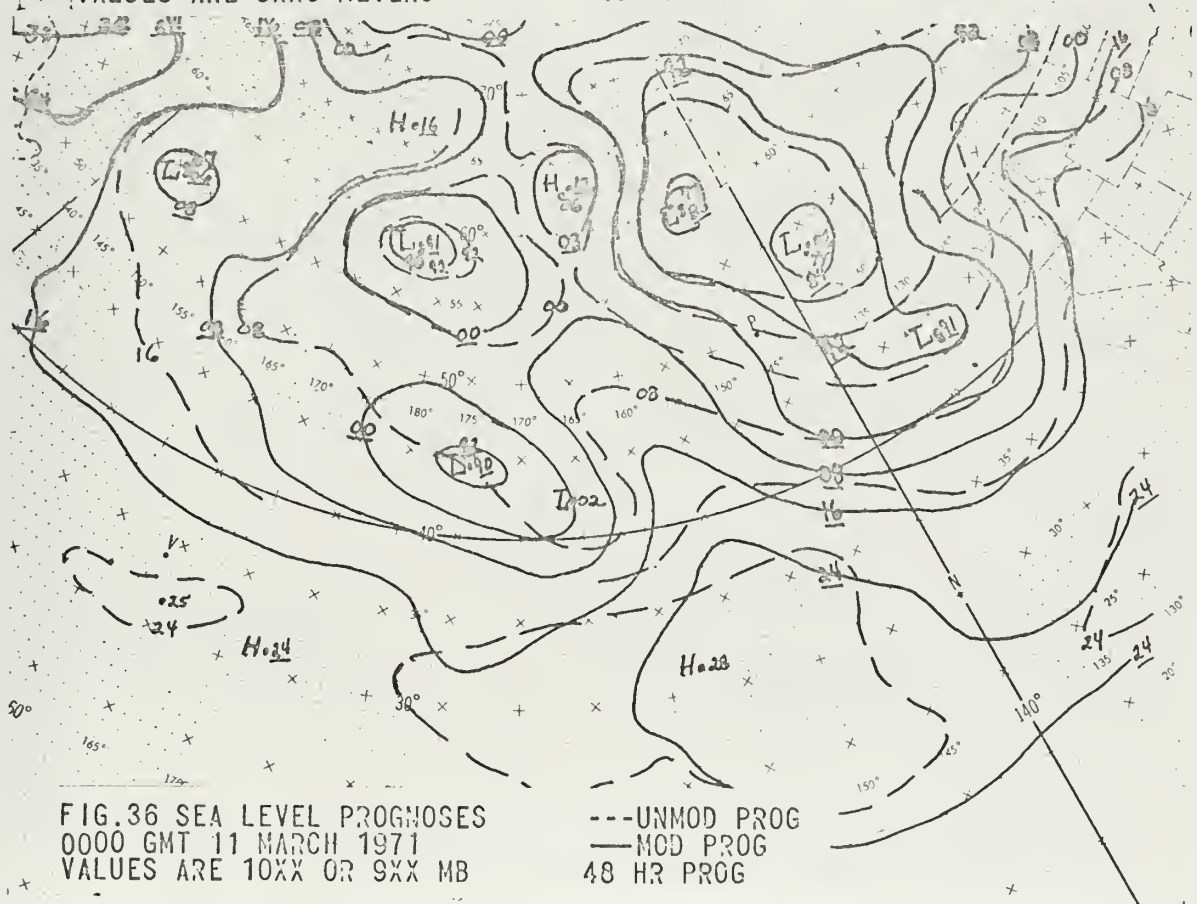


FIG.36 SEA LEVEL PROGNOSSES
0000 GMT 11 MARCH 1971
VALUES ARE 10XX OR 9XX MB

---UNMOD PROG
—MOD PROG
48 HR PROG

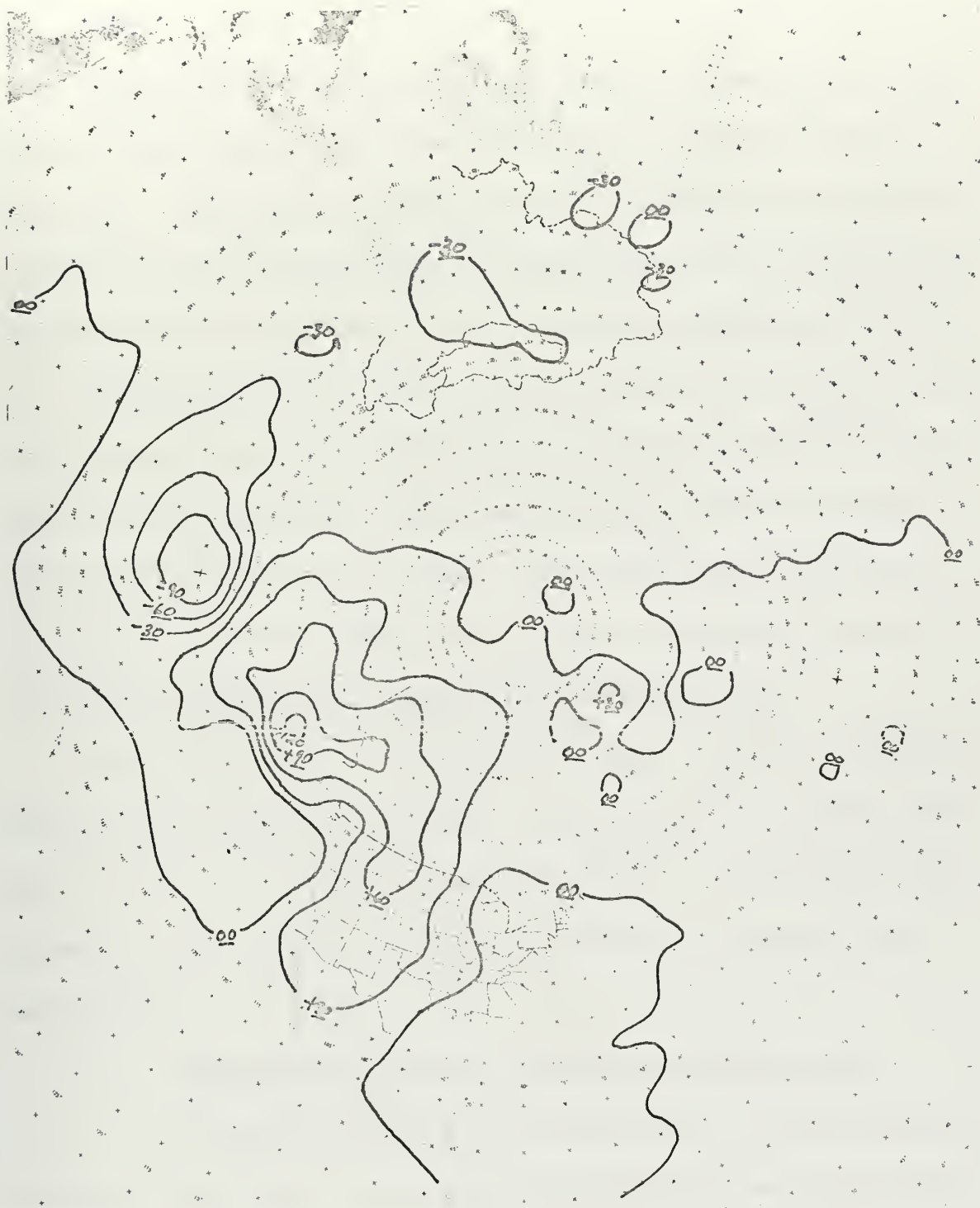


FIG. 37 500 MB.

PROJECTION: POLAR STEREOGRAPHIC—TRUE AT 60° NORTH LATITUDE
SCALE: 1:60,000,000

FLEET NUMERICAL WEATHER CENTRAL
MONTEREY, CALIFORNIA

CHART No 6B-1

Fig. 37 500 mb 48 hour Prognoses Differential Field obtained from the MOD and UNMOD PROG verification against the STACK ANAL.

C. VERIFICATIONS

The problem of selecting a suitable verification procedure for satellite-derived modifications has been stressed by many fellow workers [2, 4, 8]. This study emphasizes the use of satellite data for modifications to synoptic analysis over the sparse-data oceanic regions where cloud patterns are essentially void of complicating topographic effects.

The first part of the problem involves obtaining an accurate analysis of the oceanic atmosphere taken only from a broad base of conventional data over the North Pacific Ocean, against which the MOD PROGS and the UNMOD PROGS could be verified. The authors resolved this part of the problem by using the FNWC update analyses, henceforth referred to as the STACK ANALS which are largely free of satellite input.

The second part of the problem is the matter of obtaining the most accurate analysis using the maximum of conventional and satellite data for the basis of the analyses, against which only the MOD PROGS would be verified. This part of the problem is resolved by using the authors' MOD ANALS.

1. Description of Prognostic Verification Schemes Used

The initial evaluation of the prognoses is the difference fields between the MOD PROG and verifying STACK ANAL and the UNMOD PROG and the same STACK ANAL, as MOD PROG-STACK ANAL and UNMOD PROG-STACK ANAL (Figs. 38 through 53). With this comparison, the effects of initialization from both the modified and unmodified fields on the resulting prognoses will be measured against the best available verifying FNWC analyses.

The second evaluation of prognostic results considers a comparison of the following difference fields, MOD PROG-STACK ANAL and UNMOD PROG-MOD ANAL (Figs. 54 through 63).

Thus, the first evaluation assumes the STACK ANALs are the best available for verification while the second evaluation selects the best available corresponding analyses for verification of each prognosis.

2. Summary of Difference Field Evaluations

A study was performed on all difference fields generated. The patterns were evaluated and are discussed in three contexts. Absolute differences equivalent to or exceeding 4 mb at sea level and 60 m at 500 mb are considered significant for this evaluation. This criteria imposes a closer tolerance at sea level than at 500 mb.

a. General Overall Evaluation

The following comments apply to MOD and UNMOD PROGS in relation to both STACK and MOD ANALs.

The relative locations of major (two or more closed contours) difference centers dramatically and consistently reflect a high correlation with the position of analyzed low centers, troughs or ridges. (There were no major high centers in the study area.) In particular, the locations of the major negative-difference centers correlate with the analyzed positions of ridges while the locations of the major positive-difference centers correlate with the analyzed positions of low centers and troughs. This marked correlation strongly suggests that the short-wave-amplitudes in the prognoses have been damped. Wave-amplitude

damping of the short-wave features dominates the contributions to the difference patterns and, therefore, masks some phase difference contributions for these waves. However, there are detectable phase problems in the short-wave pattern which result from the prognostic model moving the short-wave trough-ridge systems too slowly compared to the verifying analyses. This contribution appears to increase with increasing forecast interval but remains a relatively minor contribution to the total difference field.

In addition, a qualitative evaluation shows that the magnitudes and areal coverage of major difference features are similar in the UNMOD and MOD PROG verifications.

b. Compiled Difference Field Results

Every difference field for which both MOD and STACK ANALS were available is compared and quasi-objectively evaluated on the basis of apparent forecast accuracy. The results, listing the prognoses that verify best, are shown in Table II.

PROG INTERVAL VERIFIED AGAINST		PROG from 1200 GMT 10 Mar			PROG from 0000 GMT 11 Mar	
		12	24	36	12	24
STACK	500 mb	UNMOD	MOD	UNMOD	UNMOD	UNMOD
ANAL	Sea Level	UNMOD	MOD	EQUAL	MOD	MOD
BEST	500 mb	MOD	UNMOD	UNMOD	UNMOD	UNMOD
CORRES						
ANAL	Sea Level	UNMOD	MOD	EQUAL	MOD	MOD

Table II. The results of a quasi-objective evaluation of all difference fields and selecting the best verification.

Interpreting the results of this evaluation indicates that the modifications improved the verification of the majority of sea level prognoses but did not improve the verification of the majority of the 500 mb prognoses against the STACK ANALS.

c. Salient Features

(1) Consistency in the Difference Patterns. Relative to the verifying analyses, there is a consistent tendency for the PE model to underforecast the amplitude of ridges and troughs, especially the short-wave features. Since this type of error becomes evident in the first 12 hours of prognosis, the major part of this problem may be related to the initialization of the PE model rather than its ability to handle short-wave features.

(2) Inconsistencies in the Difference Patterns. Possibly relating to initialization problems, the amount of difference occurring during the first twelve hours of prognosis was greater than the difference change during any other twelve hour interval. However, there is little consistency in the amount or sense of the differences generated during any twelve hour period. Likewise, there is no consistent pattern of generation of significant differences for a particular forecast interval (as 12, 24, 36, or 48 hours).

(3) Effects of Small-Scale Features. The difference fields reinforce the point noted in section VI. B, namely that many small-scale features were highly smoothed in 12 hours and completely obliterated

by 24 hours. This lack of ability to retain and develop the small-scale ridges and troughs accounts for a significant portion of each of the MOD PROG - MOD ANAL difference fields and neutralizes much of the effort made to modify the UNMOD ANALs. The small-scale features were the major modifications made to the analyses, especially at 500 mb. However, it should be emphasized that these small-scale features must still be regarded as synoptic scale in character and, therefore, desirable to include in analyses or prognoses.

(4) Effects of Using Bogused Reports. There are no indications that the use of bogus values to modify the analyses generates spurious errors in the prognoses, either in the general area of the initial modifications, or over the entire hemisphere, as seen in Fig. 37.

3. Comments Relating to the Difference Fields

Many aspects of a PE model, e.g., performance characteristics, formulations, and the assumptions made, are understood most clearly by those who designed the model. However, in some instances the model's behavior has not been fully documented. It is undoubtedly true that the forecaster in the field has the least insight into the complex non-linear interactions which take place in a primitive equation forecast [11].

In view of the above, this section is directed toward an increased understanding of the utility of satellite observations in relation to its potential in increasing the accuracy of forecasts from PE models.

(1) Causes Related to the PE Model and Initialization Process. Similar systematic error-pattern features from NMC PE prognostics were reported by Fawcett in 1969 [3]. He concluded that a consistent pattern of positive errors in monthly mean troughs and negative errors in monthly mean ridges does occur on the average. Further, this type of error pattern shows up in the daily prognostic charts as a lack of amplitude in short-wave troughs and ridges and an underforecast of the strength of the polar jet core. More recently a National Weather Service, Western Region, study pointed out the existence of "slowness of short-wave trough motion found in PE forecasts," [11].

The existence of both the damping and slowness of short-wave features has been noted in the 500 mb prognoses generated for this study. The significance of these model characteristics with regard to the analysis modifications applied to short-wave features cannot be explained in this research because the initialized fields were not retained. However, it is felt that the findings in this study corroborate the findings of the other recent aforementioned studies of the PE model [3, 11]. It is stated in [11] that, "In going from the analysis to the initialization, 30 percent of the energy may be lost."

(2) Causes Related to the Analysis and Bogus Techniques. The numerical damping and retarding of the short-wave features prompted further study of the manually produced MOD ANALS and the final numerically generated MOD ANALS. The numerical MOD ANALS, which were accepted by the authors, were achieved only after numerous attempts

at selecting the best bogus values and locations which would effectively result in the numerical MOD ANAL being in reasonable agreement with the manual MOD ANAL. It is noted that some inconsistencies do exist between the positions of the sea-level and 500 mb ridge lines in the final numerical MOD ANAL. This condition resulted from concentrating primary attention on selecting bogus values to properly locate troughs. It is difficult to completely assess the total effect of these inconsistencies on the resulting prognoses of short-wave features.

Another unknown factor is the effect of not explicitly modifying the soundings above 500 mb. In effect, the FNWC analysis program extrapolates both the 500 mb conventional and bogus data to 300 mb to be considered along with all other data for analysis at the latter level. From the 300 mb analysis, grid point values are then extrapolated back to 500 mb to aid in the final 500 mb analysis. Thus, the 300 mb analysis may affect the 500 mb analysis in such a way as to partially nullify the effect of the 500 mb bogus data. In summary, the effect of 500 mb bogus data cannot be readily determined beforehand.

The lack of consistent stratospheric data, conventional and bogus, will force the PE model to climatological values which imply stability and a possible damping effect on the desired unstable systems which could assist the development in the PE prognosis.



FIG. 38 500 MB VERIFICATIONS
1200 GMT 10 MARCH 1971 PROGNOSSES
12 HR PROG - STACK ANAL IN METERS. VT 00 00 GMT 11 MAR

---UNMOD
—MOD

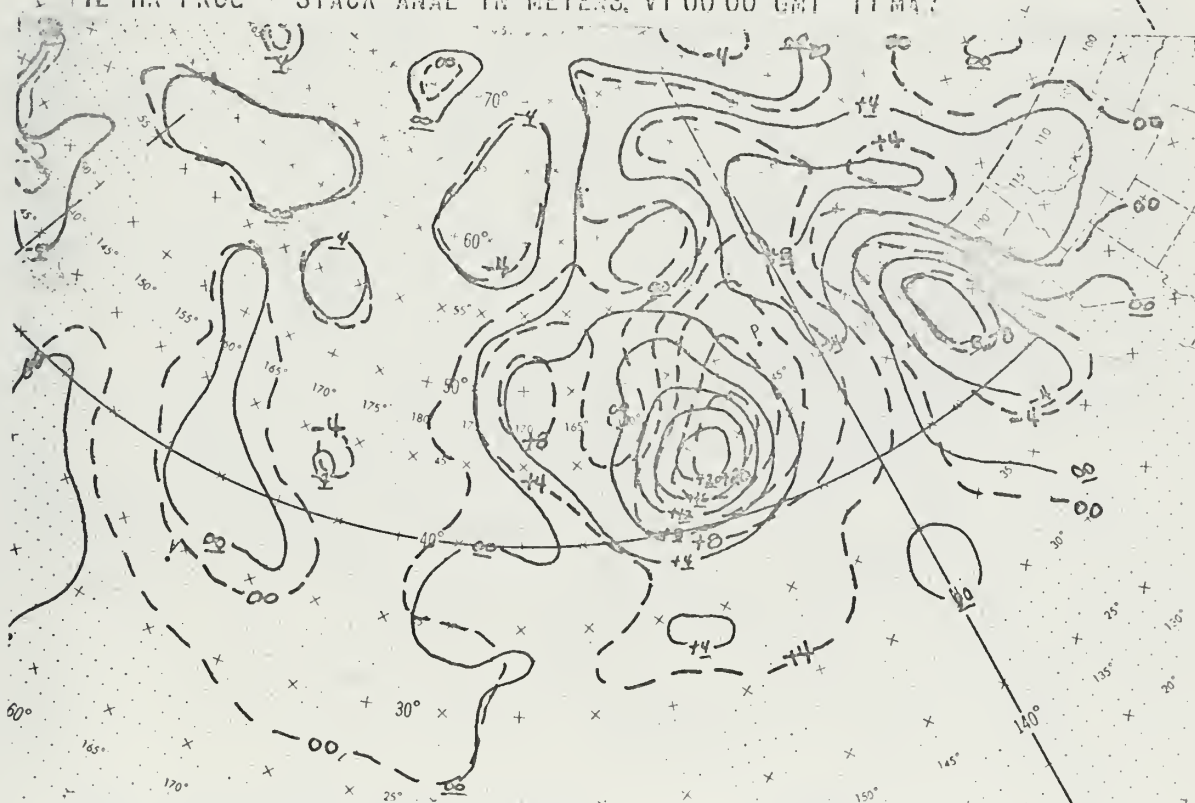


FIG. 39 SEA LEVEL VERIFICATIONS
1200 GMT 10 MARCH 1971 PROGNOSSES
12 HR PROG - STACK ANAL IN MB. VT 00 00 GMT 11 MAR

---UNMOD
—MOD

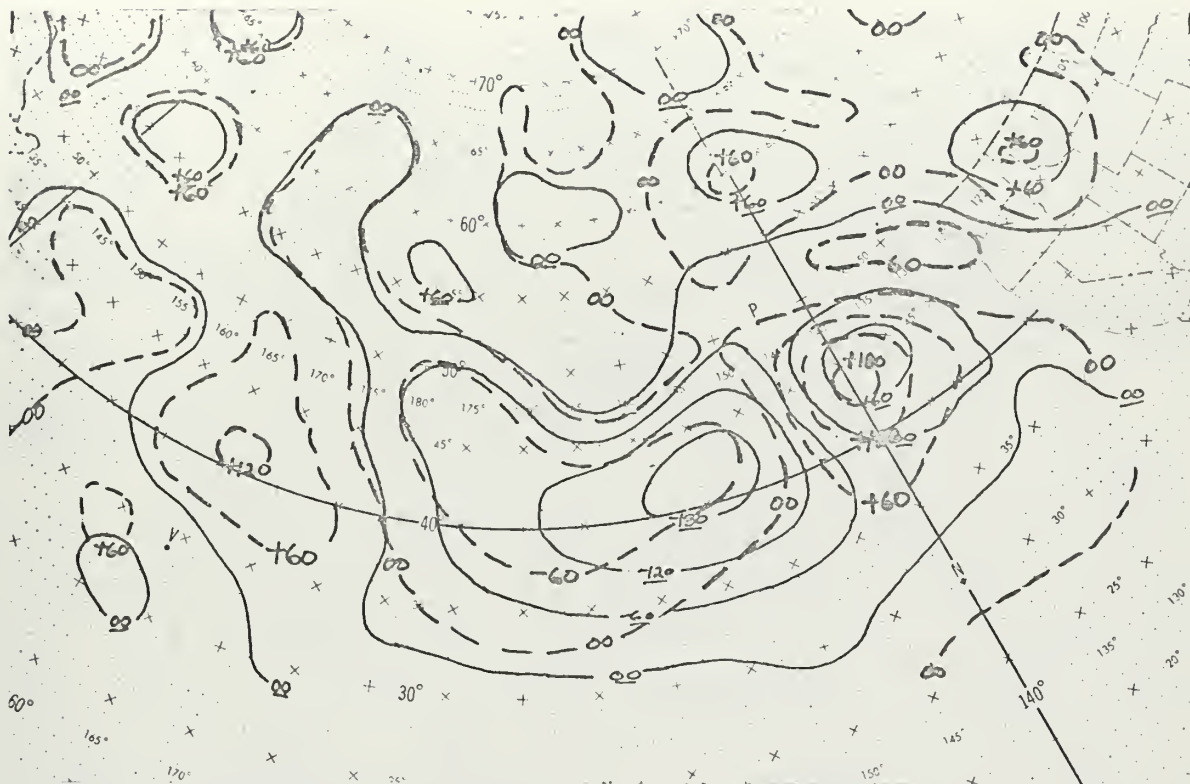


FIG. 40 500 MB VERIFICATIONS
1200 GMT 10 MARCH 1971 PROGNOSSES
24 HR PROG - STACK ANAL IN METERS. VT 1200 GMT 11 MAR

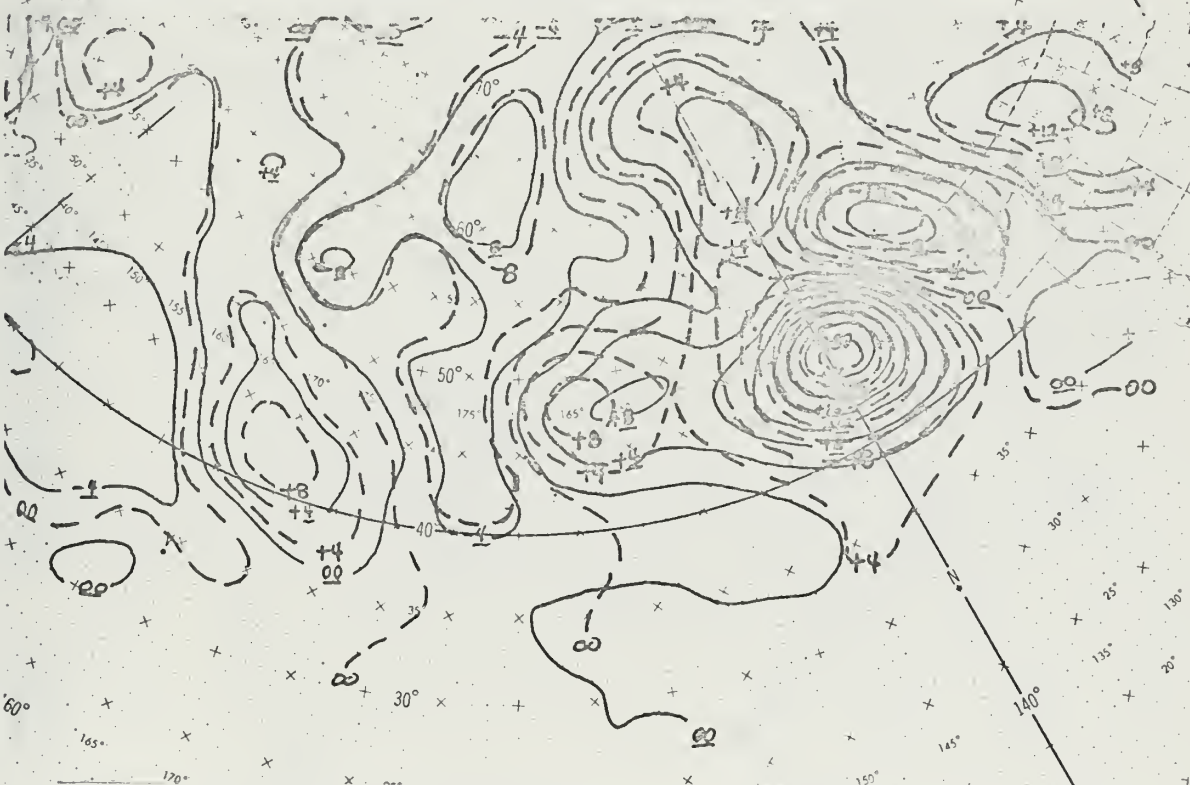


FIG. 41 SEA LEVEL VERIFICATIONS
1200 GMT 10 MARCH 1971 PROGNOSSES
24 HR PROG - STACK ANAL IN MB. VT 1200 GMT 11 MAR

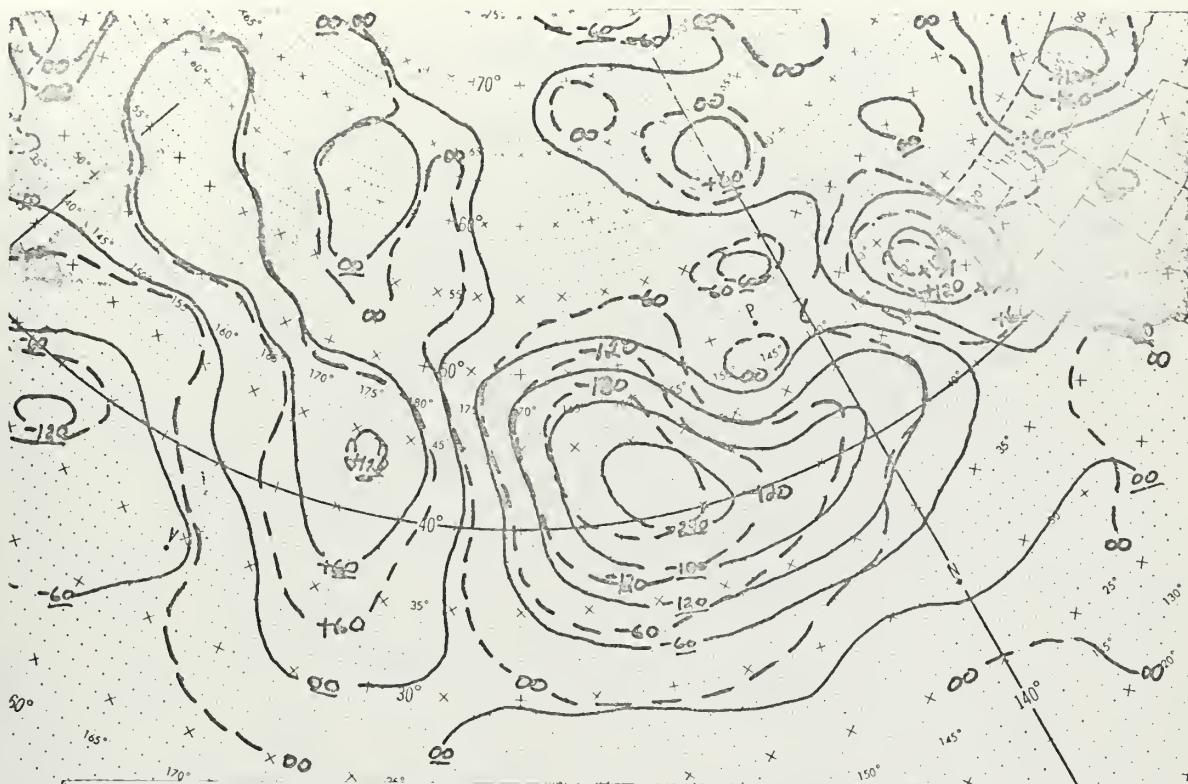


FIG. 42 500 MB VERIFICATIONS
 1200 GMT 10 MARCH 1971 PROGNOSSES
 36 HR PROG - STACK ANAL IN METERS. VT 0000 GMT 12 MAR

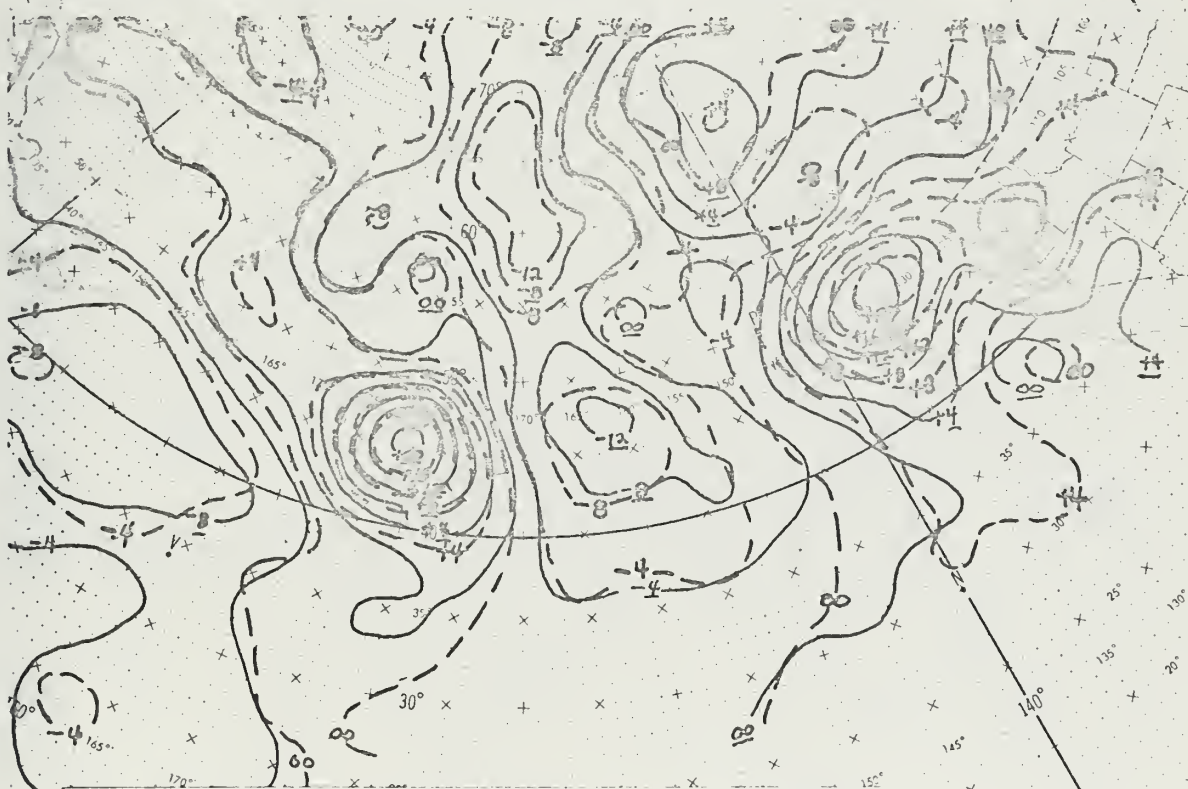


FIG. 43 SEA LEVEL VERIFICATIONS
 1200 GMT 10 MARCH 1971 PROGNOSSES
 36 HR PROG - STACK ANAL IN MB. VT 0000 GMT 12 MAR



FIG. 44 500 MB VERIFICATIONS
 12 00 GMT 10 MARCH 1971 PROGNOSSES
 12 00 GMT 12 MAR
 ---UNMOD
 —MOD
 48 HR PROG - STACK ANAL IN METERS. VT

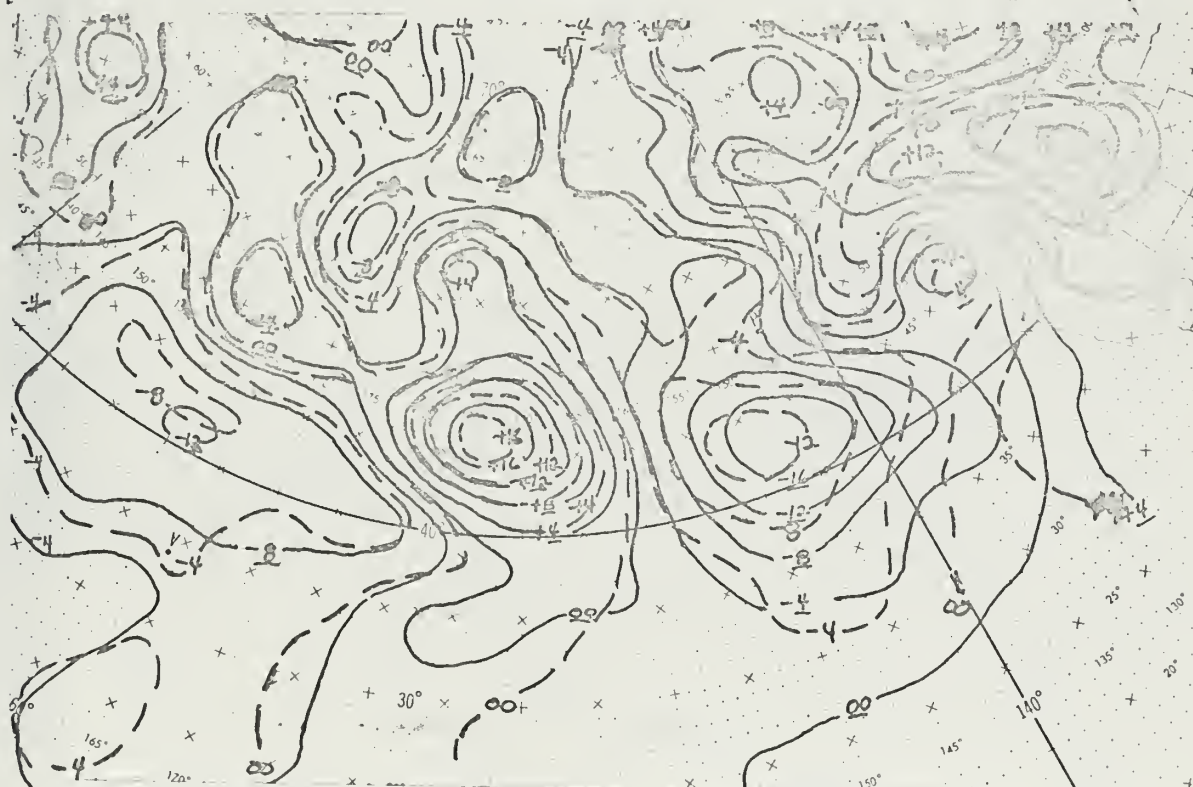


FIG. 45 SEA LEVEL VERIFICATIONS
 12 00 GMT 10 MARCH 1971 PROGNOSSES
 12 00 GMT 12 MAR
 ---UNMOD
 —MOD
 48 HR PROG - STACK ANAL IN MB. VT

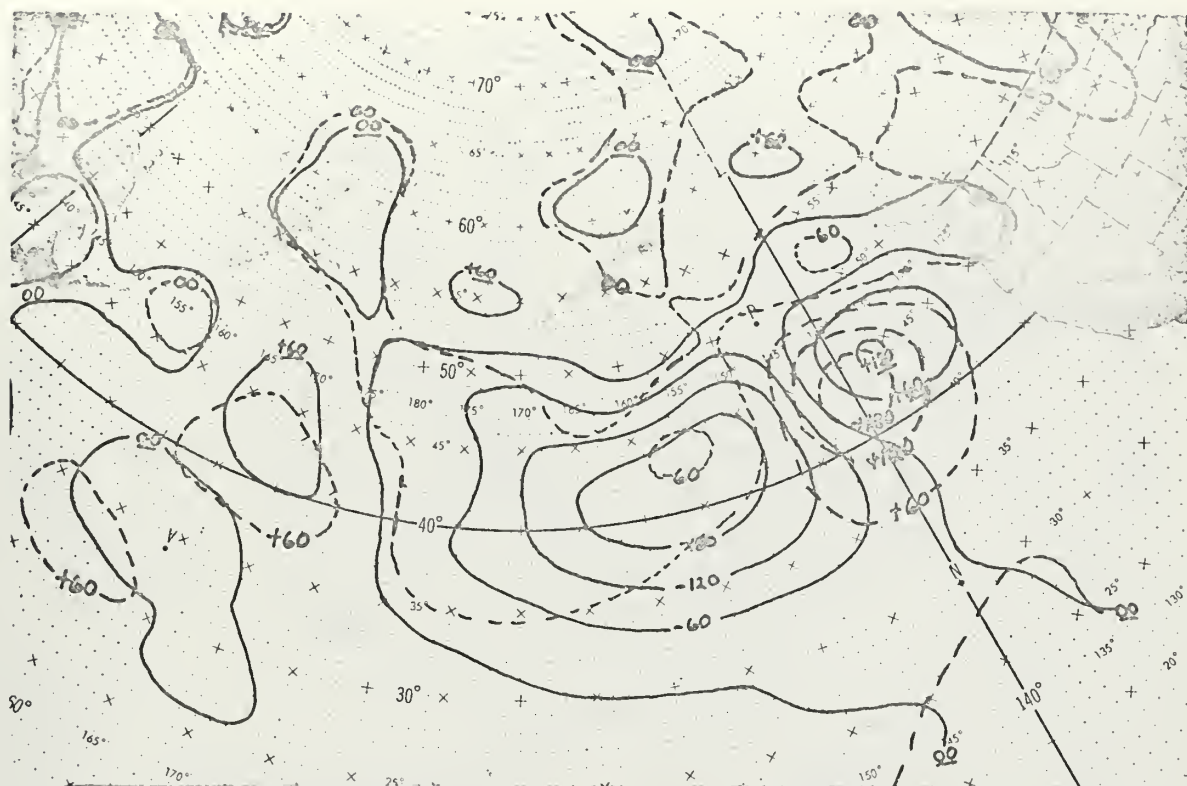


FIG. 46 500 MB VERIFICATIONS
0000 GMT 11 MARCH 1971 PROGNOSSES
12 HR PROG - STACK ANAL IN METERS. VT 1200 GMT 11 MAR



FIG. 47 SEA LEVEL VERIFICATIONS
0000 GMT 11 MARCH 1971 PROGNOSSES
12 HR PROG - STACK ANAL IN MB. VT 1200 GMT 11 MAR

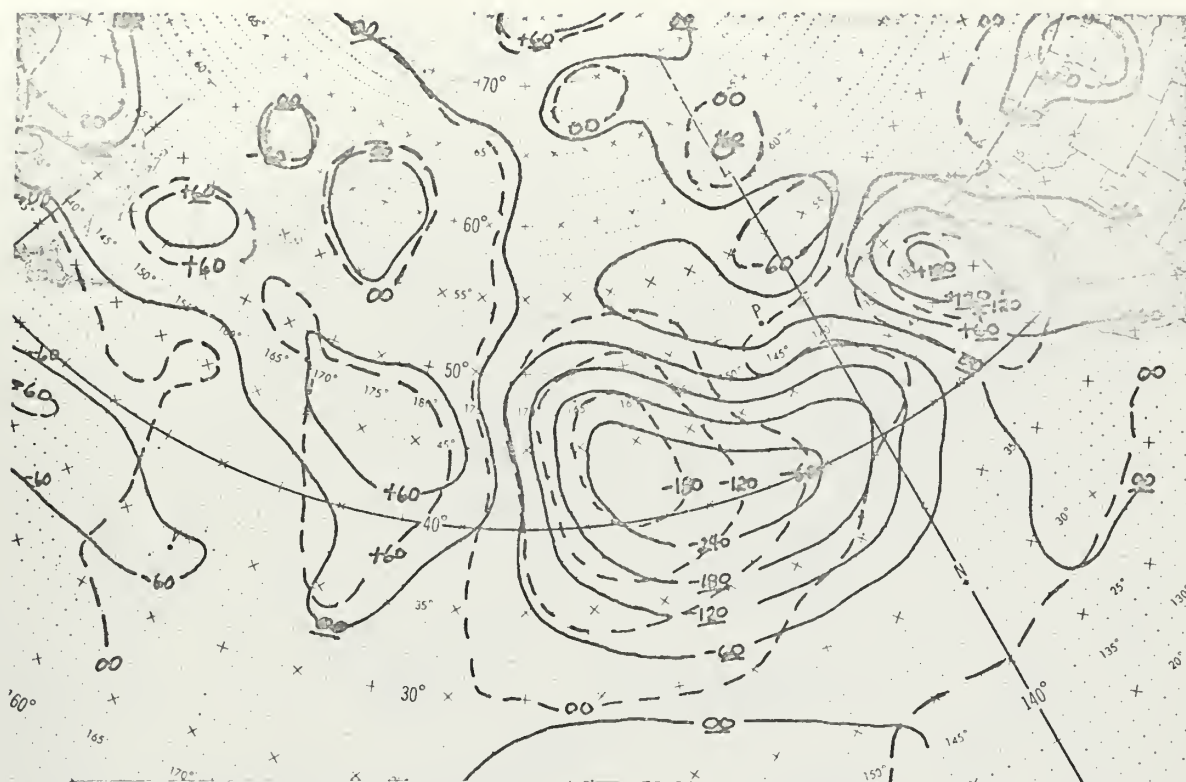


FIG. 48 500 MB VERIFICATIONS
 0000 GMT 11 MARCH 1971 PROGNOSSES
 124 HR PROG - STACK ANAL IN METERS. VT 0000 GMT 12 MAR

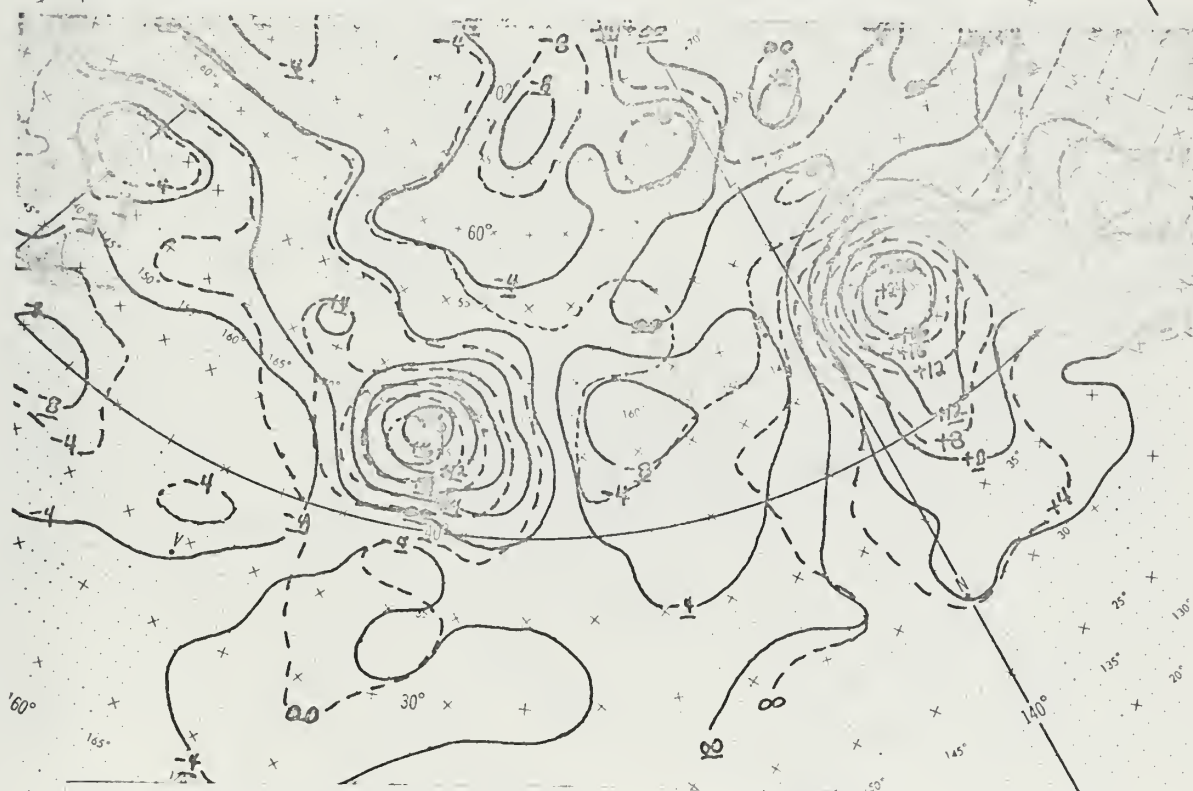


FIG. 49 SEA LEVEL VERIFICATIONS
 0000 GMT 11 MARCH 1971 PROGNOSSES
 124 HR PROG - STACK ANAL IN MB. VT 0000 GMT 12 MAR



FIG. 50 500 MB VERIFICATIONS
0000 GMT 11 MARCH 1971 PROGNOSSES
36 HR PROG - STACK ANAL IN METERS. VT 12 00 GMT 12 MAR

---UNMOD
—MOD



FIG. 51 SEA LEVEL VERIFICATIONS
0000 GMT 11 MARCH 1971 PROGNOSSES
36 HR PROG - STACK ANAL IN MB. VT 12 00 GMT 12 MAR

---UNMOD
—MOD



FIG. 52 500 MB VERIFICATIONS
 00 00 GMT 11 MARCH 1971 PROGNOSSES
 48 HR PROG - STACK ANAL IN METERS, VT 0000 GMT 13 MAR

---UNMOD
 —MCD

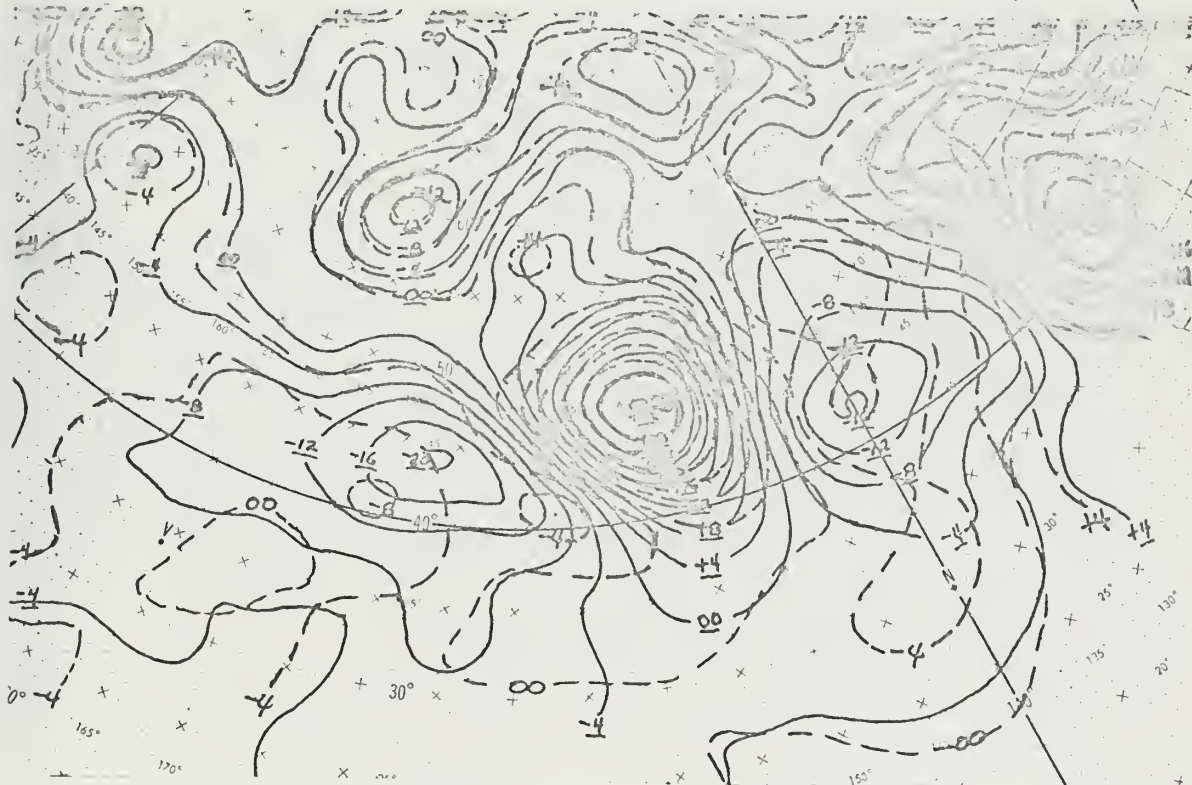


FIG. 53 SEA LEVEL VERIFICATIONS
 00 00 GMT 11 MARCH 1971 PROGNOSSES
 48 HR PROG - STACK ANAL IN MB, VT 0000 GMT 13 MAR

---UNMOD
 —MCD



FIG. 54 500 MB VERIFICATIONS ---UNMOD-STACK
1200 GMT 10 MARCH 1971 PROGNOSSES ---MOD - MOD
12 HR PROG - BEST CORRES ANAL IN METERS. VT 00 00 GMT 11 MAR

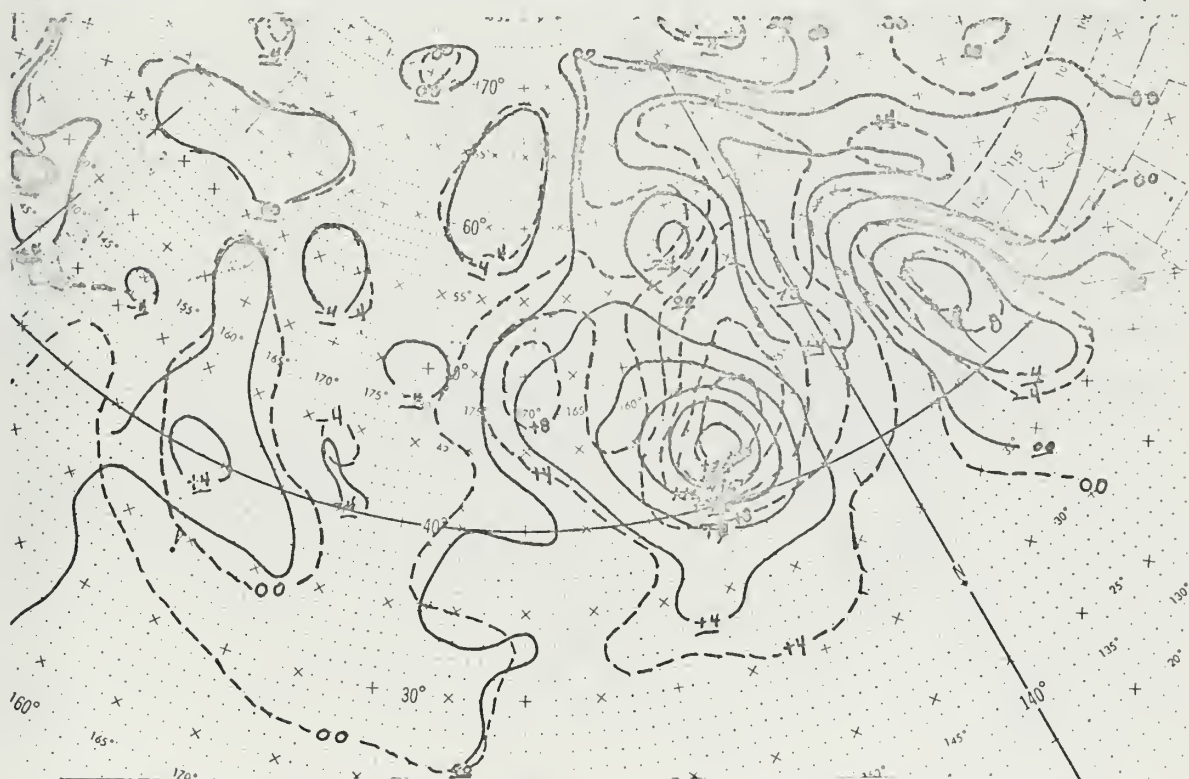


FIG. 55 SEA LEVEL VERIFICATIONS ---UNMOD-STACK
1200 GMT 10 MARCH 1971 PROGNOSSES ---MOD - MOD
12 HR PRGC - BEST CORRES ANAL IN MD. VT 00 00 GMT 11 MAR

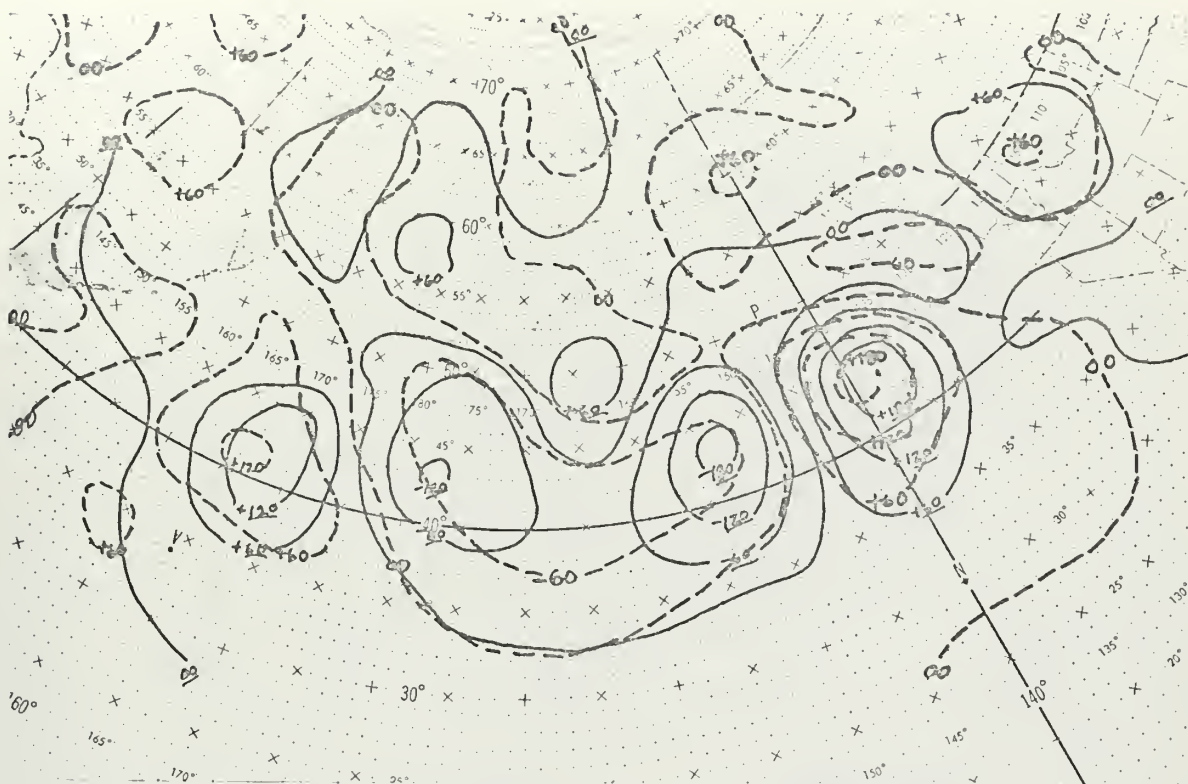


FIG. 56 500 MB VERIFICATIONS
 1200 GMT 10 MARCH 1971 PROGNOSSES
 24 HR PROG - BEST CORRES ANAL IN METERS. VT 1200 GMT 11 MAR

---UNMOD-STACK
 —MCD - MOD

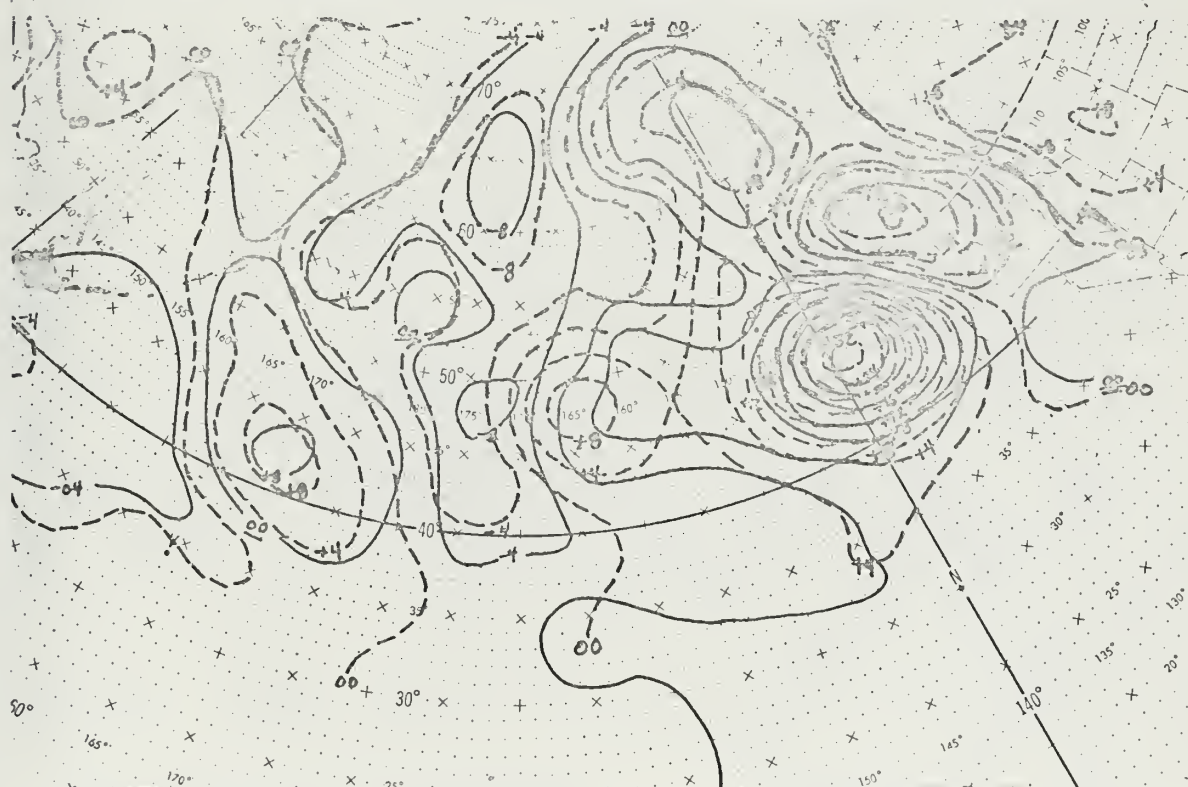


FIG. 57 SEA LEVEL VERIFICATIONS
 1200 GMT 10 MARCH 1971 PROGNOSSES
 24 HR PROG - BEST CORRES ANAL IN MD. VT 12 00 GMT 11 MAR

---UNMOD-STACK
 —MCD - MOD

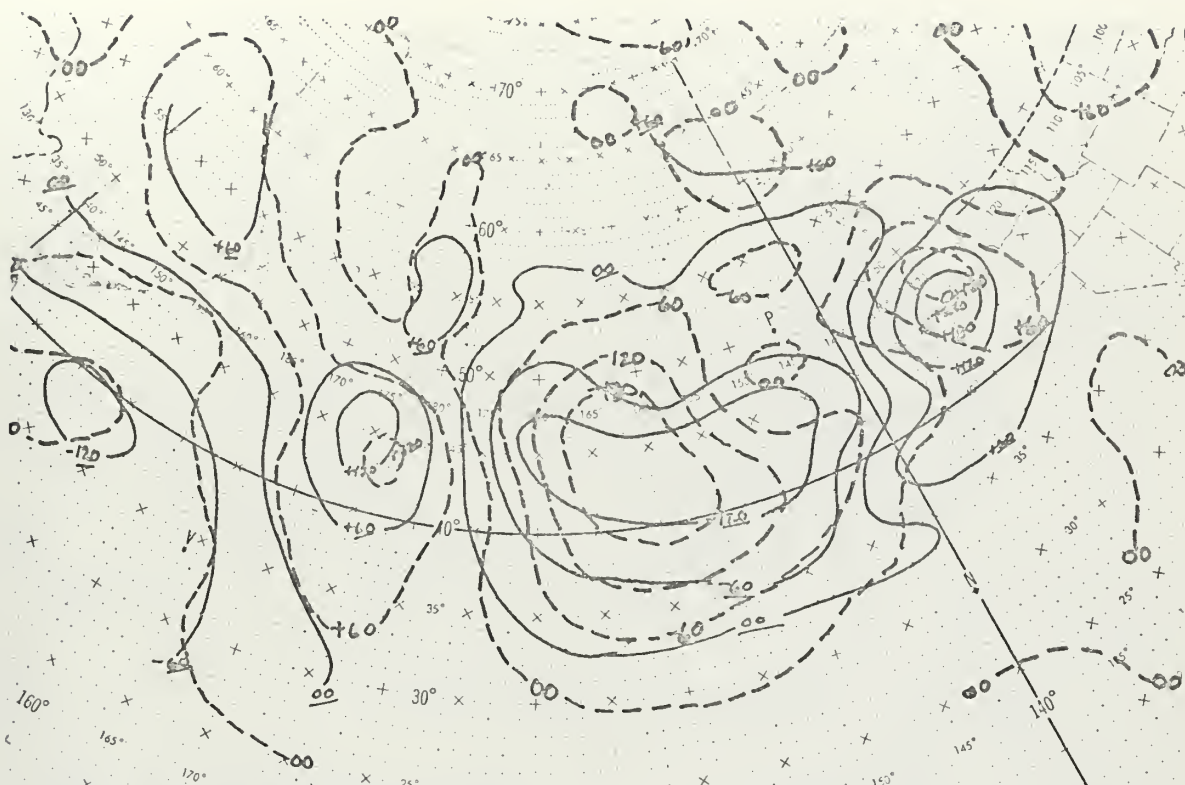


FIG. 58 500 MB VERIFICATIONS
 12 00 GMT 10 MARCH 1971 PROGNOSSES
 36 HR PROG - BEST CORRES ANAL IN METERS. VT 0000 GMT 12 MAR



FIG. 59 SEA LEVEL VERIFICATIONS
 12 00 GMT 10 MARCH 1971 PROGNOSSES
 36 HR PROG - BEST CORRES ANAL IN MB. VT 00 00 GMT 12 MAR

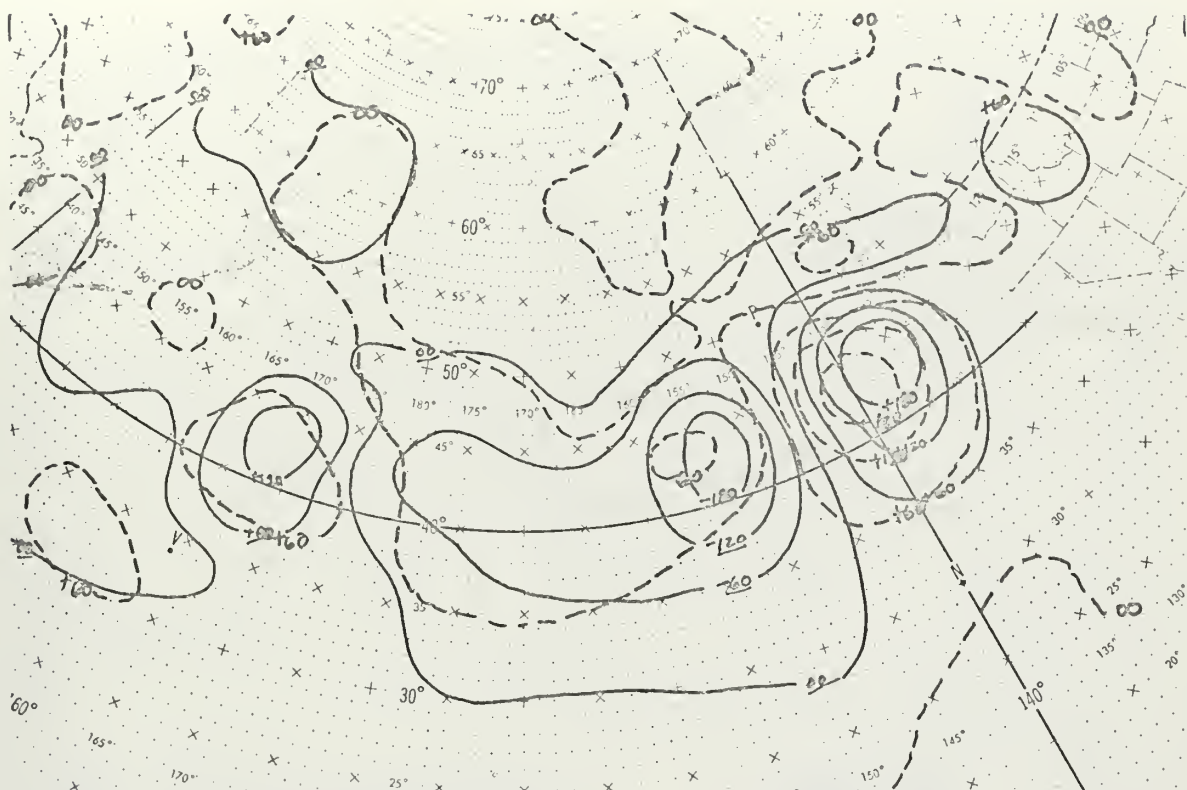


FIG. 60 500 MB VERIFICATIONS
0000 GMT 11 MARCH 1971 PROGNOSIS
12 HR PROG - BEST CORRES ANAL IN METERS. VT 1200 GMT 11 MAR

---UNMOD-STACK
—MOD - MOD



FIG. 61 SEA LEVEL VERIFICATIONS
0000 GMT 11 MARCH 1971 PROGNOSIS
12 HR PROG - BEST CORRES ANAL IN MD. VT 1200 GMT 11 MAR

---UNMOD-STACK
—MOD - MOD



FIG. 62 500 MB VERIFICATIONS
 0000 GMT 11 MARCH 1971 PROGNOSSES
 24 HR PROG - BEST CORRESPONDING ANAL IN METERS. VT 0000 GMT 12 MAR

---UNMOD-STACK
 —MOD - MOD



FIG. 63 SEA LEVEL VERIFICATIONS
 0000 GMT 11 MARCH 1971 PROGNOSSES
 24 HR PROG - BEST CORRESPONDING ANAL IN MD. VT 0000 GMT 12 MAR

---UNMOD-STACK
 —MOD - MOD

VII. CONCLUSIONS AND RECOMMENDATIONS FOR FURTHER STUDY

The design and execution of this experiment has resulted in several noteworthy findings and recommendations for workers pursuing further development in this area of numerically integrating conventional and satellite data.

Based on the availability of satellite data and the successful procedures developed, (as outlined in section IV), it is concluded that satellite data inputs to numerical analysis is operationally feasible and worthwhile. Furthermore, the modifications should be done by someone (or a group) who is familiar with the structure and behavior of both the numerical analysis scheme and the PE model. To retain the proper time and spatial continuity of developing systems, the modification procedures should be pursued on a continuous basis, not just "now and then." Likewise, the technique should be applied over the entire numerical grid and not just in one area.

The completely objective SIRS values should be either automatically processed along with conventional data or be assigned the first priority for bogus input and be weighted nearly the same as conventional data. The quasi-objective ATS winds near 300 mb and the Nagle-Hayden technique 500 mb height values for spiral cloud centers are reliable for use in the sparse data regions and should be treated with second priority for bogus input. The other subjective pattern-recognition techniques can produce a large quantity of approximate 500 mb height values that are

useful for sparse data regions and should be considered as tertiary priority for bogus input.

It is recognized that the ultimate effect of the satellite-improved MOD ANALS to generate conclusively favorable prognoses at the surface and 500 mb was not achieved. However, the MOD PROGS cannot be considered conclusively unfavorable either in view of the fact that there is definite time and space continuity in the prognosis of those pressure systems introduced in the analysis through satellite observations, although such systems were significantly damped early in the prognostic process. Further, the merits of the satellite-generated modifications may be heavily screened by behavioral characteristics of both the initialization procedures and the PE model.

It is also noteworthy that the incorporation of a considerable amount of carefully estimated bogus values did not result in the FNWC PE prognostic model generating any spurious errors a considerable distance downstream of the modified analysis area.

Finally, the reader is cautioned against making sweeping generalizations from the limited results reported on here. Only further testing will determine the universality of conclusions as drawn from the small-sample case study presented.

APPENDIX A

COMPUTER RECTIFIED PHOTOGRAPHS OF ATS-1 OBSERVATIONS;
1800 GMT 9-12 MARCH 1971

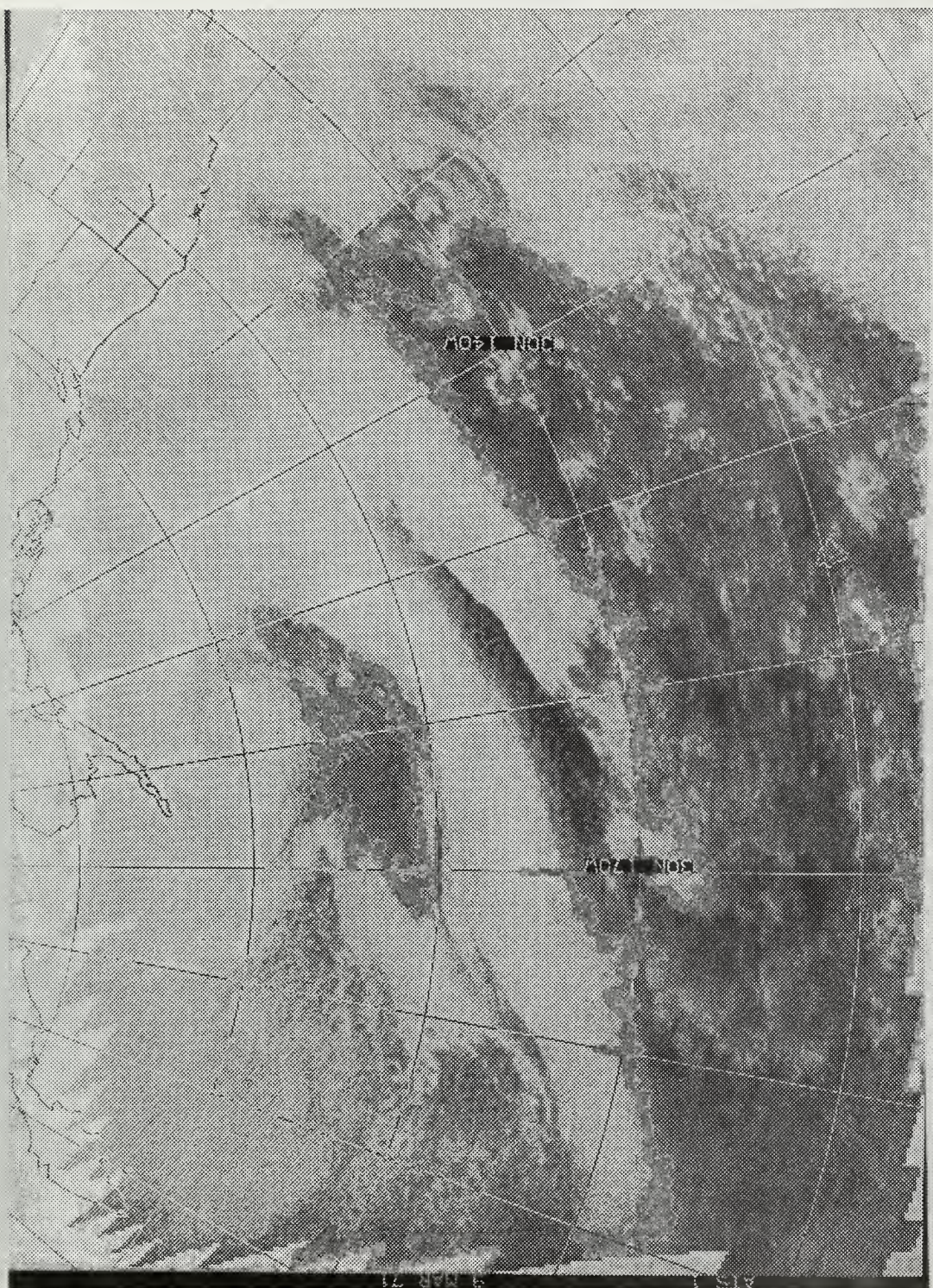


Fig. 64 Computer rectified photograph of ATS-1 observations about 1800 GMT 09 March 1971



Fig. 65 Computer rectified photograph of ATS-1 observations about 1800 GMT 10 March 1971

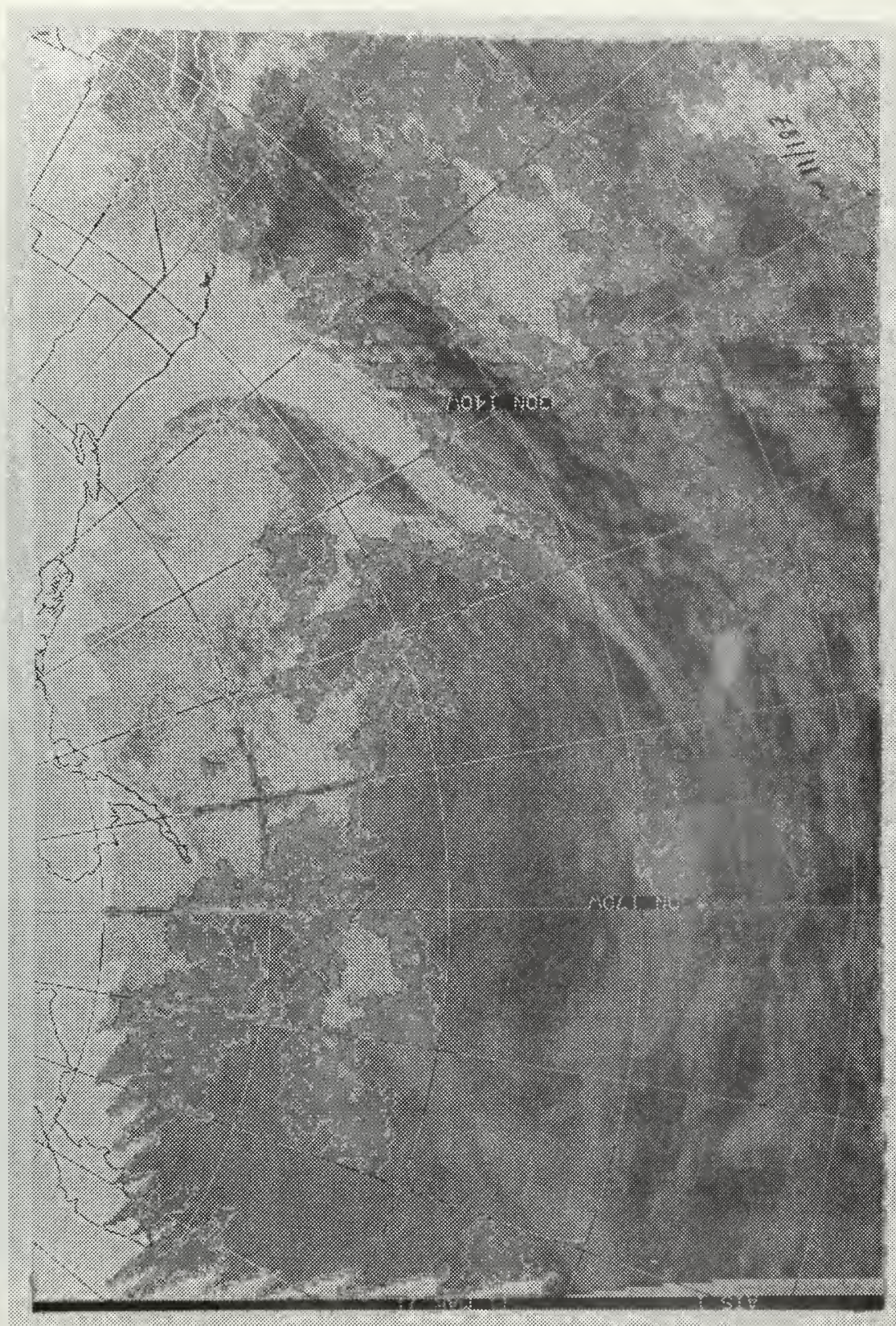


Fig. 66 Computer rectified photograph of ATS-1 observations about 1800 GMT 11 March 1971



Fig. 67 Computer rectified photograph of ATS-1 observations about 1800 GMT 12 March 1971

APPENDIX B

COMPARISON OF NORTHERN HEMISPHERE SIRS 500 mb HEIGHTS AND FNWC MONTEREY 500 mb ISOHYPTIC ANALYSES FOR 9 - 14 MARCH 1971

During the period 9 - 14 March 1971, SIRS 500 mb height data coverage over the North Pacific Ocean was insufficient to give a perspective of the accuracy and potential value of this data source. To provide a better study, all the Northern Hemisphere SIRS 500 mb values for 9-14 March were plotted on blank charts, overlain on the corresponding FNWC 500 mb operational contour analysis maps, and the FNWC contour height compared with the SIRS height. This approach differs considerably from the study of Nilsestuen [16] where the SIRS soundings were compared with actual radiosonde profiles from the same time and vicinity. Since a SIRS value does represent a sampling of a large area (a square 120 NM on a side), a comparison with the 500 mb contour analysis is perhaps more valid than that with a radiosonde height which is a discrete air sample, microscopic in size.

SIRS soundings north of 70N are classified by NESS as "unreliable," and used as an input at NMC with lesser "weight" (analysis significance). SIRS soundings south of 70N are given the same reliance as conventional soundings in the NMC objective analysis. This study considered SIRS values north of 70N separately to give some measure of their reliability.

Two tolerance checks were tabulated in this study: 1) Category 1 -- greater than 30 m difference, and 2) Category 2 -- greater than 60 m difference. SIRS sounding values which fell into the second category (> 60 m) are included in the first category (> 30 m).

Table III sums up the accuracy of SIRS soundings when compared with the conventional data analysis, on a hemispheric basis. For the eleven map times (09/0000Z - 14/0000Z March 1971), an average of 56 soundings per synoptic time went into the update NMC 500 mb analysis. The average number of conventional soundings at synoptic map time is approximately 575; so, the NMC use of SIRS data represents an increase of 10 per cent coverage. As to its accuracy, this brief study showed that an average of five of the 56 reports differed from the FNWC conventional data analysis values by more than 60 m. The modification effort made by the authors in the North Pacific supports a tentative conclusion that the accuracy of these differing reports is in favor of the SIRS data.

The results for the polar region (north of 70N) lend minor credence to the present NESC classification of "unreliable" for the SIRS data. An average of two out of eleven reports were greater than 60 m different from the FNWC analysis values. However, considering the scarcity of reliable conventional reporting stations in the polar region, 11 SIRS soundings represent a major increase in coverage.

Synoptic Map Time	Location N = North S = South of 70° N. Lat.	Total Number of SIRS Values	Category 1 No. of cases of SIRS - FNWC differing by more than 30 meters	Category 2 No. of cases of SIRS - FNWC differing by more than 60 meters	ABS HT Differences in meters SIRS - FNWC	
					MAX Cat.2	AVG Cat. 2
0000 GMT 09 Mar 71	N	9	1	1	100	100
	S	<u>21</u>	<u>2</u>	<u>0</u>		
	Sum	30	3	1		
1200 GMT 09 Mar 71	N	11	4	1	130	112
	S	<u>82</u>	<u>21</u>	<u>5</u>		
	Sum	93	25	6		
0000 GMT 10 Mar 71	N	19	6	2	150	116
	S	<u>49</u>	<u>7</u>	<u>3</u>		
	Sum	68	13	5		
1200 GMT 10 Mar 71	N	6	4	1	100	94
	S	<u>31</u>	<u>6</u>	<u>4</u>		
	Sum	37	10	5		
0000 GMT 11 Mar 71	N	13	5	3	90	77
	S	<u>34</u>	<u>9</u>	<u>3</u>		
	Sum	47	14	6		
1200 GMT 11 Mar 71	N	2	0	0	170	120
	S	<u>47</u>	<u>7</u>	<u>2</u>		
	Sum	49	7	2		
0000 GMT 12 Mar 71	N	19	9	6	160	124
	S	<u>43</u>	<u>8</u>	<u>5</u>		
	Sum	62	17	11		
1200 GMT 12 Mar 71	N	5	5	0	150	95
	S	<u>47</u>	<u>12</u>	<u>8</u>		
	Sum	52	17	8		
0000 GMT 13 Mar 71	N	6	1	0	120	77
	S	<u>43</u>	<u>10</u>	<u>3</u>		
	Sum	49	11	3		
1200 GMT 13 Mar 71	N	11	4	3	100	90
	S	<u>64</u>	<u>8</u>	<u>0</u>		
	Sum	75	12	3		
0000 GMT 14 Mar 71	N	17	11	3	90	74
	S	<u>42</u>	<u>7</u>	<u>2</u>		
	Sum	59	18	5		
TOTALS	N	118	50	20		
	S	<u>503</u>	<u>97</u>	<u>35</u>		
	Sum	621	147	55		
AVERAGES	N	10.7	4.5	1.8		
	S	<u>45.7</u>	<u>8.8</u>	<u>3.2</u>		98.1
	Sum	56.4	13.3	5.0		

Table III. A comparison of SIRS 500 mb heights to FNWC 500 mb analyzed heights for the Northern Hemisphere; 9-14 March 1971.

APPENDIX C

COMMENTS ON PROCEDURES USED TO DETERMINE BOGUS DATA

Pursuant to the desired numerical MOD ANAL is the development of procedures for utilizing all available options for obtaining a numerical MOD ANAL which is a duplicate of the manually-derived MOD ANAL. Bogus values of pressure or height, and wind to modify existing centers, troughs and ridges, can be positioned at any geographic coordinates and injected into the analysis scheme at sea level (100 points) and 500 mb (50 points), with priority over most rejection criteria. (A greater number of bogus values will be acceptable at other levels in the FNWC program in the near future.)

Bogus values that blend without conflicting with the conventional data do produce good numerical MOD ANALs. If the desired MOD ANAL values were not achieved on the first attempt, the pressure or height values assigned to the bogus positions in the unacceptable area required a compensation called "overbogus" which is, in effect, applying the necessary adjustment in pressure or height to force the analysis toward the desired MOD ANAL value as it smooths the data.

When the "overbogus" technique was not successful, it was necessary to "override" the erroneous conventional data by saturating a specific area with numerous bogus values, which was uneconomical in view of the limit set on the number of bogus data points allowed for this study.

Particular cases were encountered where neither one nor both of these techniques used together was sufficient to achieve the desired MOD ANAL values over the area of concern due to the limit of points, inexperience of the authors and design criteria.

BIBLIOGRAPHY

1. Air Weather Service Technical Report 212, Application of Meteorological Satellite Data in Analysis and Forecasting, by R. K. Anderson, and others, June 1969.
2. Casimes, T. C. and Swor, J. G., An Experiment in Modifying Objective 500 mb Contour Analyses Using TIROS IX Nephanalyses, M. S. Thesis, Naval Postgraduate School, Monterey, Calif., 1965.
3. Fawcett, E. G., "Systematic Errors in Operational Baroclinic Prognoses at the National Meteorological Center," Monthly Weather Review, Vol. 97, No. 9, September 1969.
4. Hayden, C. M. and Wiin-Nielsen, A. C., The Utility of Satellite Cloud Photographs in Objective Analysis of the 500 mb Height Field, University of Michigan (ORA Project 08203), Ann Arbor, Michigan, February 1968.
5. Meteorology International, Inc., Final Report, Contract No. E-93-67 (N), An Approach to the SINAP Problem: A Quasi-Objective Method of Incorporating Meteorological Satellite Information in Numerical Weather Analysis, by Nagle, R. E. and Clark, J. R., 1968.
6. Meteorology International, Inc., Technical Memo No. 3, Scale and Pattern Spectra and Decompositions, by Holl, M. M., 1963.
7. National Environmental Satellite Center, ESSA Direct Transmission System Users Guide, 1969.
8. National Environmental Satellite Center, ESSA Technical Report NESC-41, The SINAP Problem: Present Status and Future Prospects, by McClain, E. P., October 1967.
9. National Environmental Satellite Center Meteorological Satellite Laboratory Report 36, Experimental Use of Satellite Pictures in Numerical Prediction, Part III, Broderick, H. J., McClain, E. P., and Ruzecki, M. A., January 1966.
10. National Oceanic and Atmospheric Administration (NOAA) Technical Report NESS-5, The Use of Satellite-Observed Cloud Patterns in Northern Hemisphere 500 mb Numerical Analysis, by Nagle, R. E. and Hayden, C. M., 1971. (Unpub.)

11. National Weather Service Western Region Headquarters Technical Attachments No. 7-14, Systematic Errors of Numerical Progs, 26 January 1971 and No. 71-38, LFM (Limited-Area Fine-Mesh Model) Versus PE (Primitive Equation) Forecast, September 7, 1971.
12. Naval Air Systems Command Project FAMOS Research Report (4-67) Guide for Interpretation of Satellite Photography and Nephanalysis, August 1967.
13. Naval Air Systems Command Project FAMOS Field Memo (1-69), Cyclone Movement and 500 mb Wind Speed from Satellite Photographs, 31 March 1969.
14. Navy Weather Research Facility Report 33-1169-148, The Use of Satellite Pictures for Surface and 500 mb Chart Analysis, November 1969.
15. Navy Weather Research Facility Report F-0970-158, Guide for Observing the Environment with Satellite Infrared Imagery, by Bittner, F. E. and Ruggles, K. W., September 1970.
16. Navy Weather Research Facility Technical Paper No. 25-67, A Comparison of Maritime Vertical Temperature Profiles, Radiosonde Versus Satellite Infrared Spectrometer (SIRS), by Nilsestuen, R. M., October 1969.
17. Office of Naval Research Technical Report ONRL-44-66, Operational Guide to Synoptic Applications of Meteorological Observations from Satellites, by Hamilton, H. D., November 1966.
18. Project FAMOS Research Report 1-68, Techniques for the Objective Assembly of Meteorological Satellite Data, by Nagle, R. E. and Clark, J. R., 1968.
19. Serebreny, S. M., and Evans, W. E., Construction of ATS Cloud Console, Stanford Research Inst., Menlo Park, Calif., December 1969.
20. Serebreny, S. M. and others, Comparison of Cloud Motion Vectors and Rawinsonde Data, Stanford Research Inst., Menlo Park, Calif., July 1969.
21. Serebreny, S. M., Wiegman, E. J., and Hadfield, R. E., Further Comparison of Cloud Motion Vectors with Rawinsonde Observations, Stanford Research Inst., Menlo Park, Calif., 21 August 1970.

22. Shuman, F. G. and Hovermale, J. B., "An Operational Six-Layer Primitive Equation Model," Journal of Applied Meteorology, Vol. 7, No. 4, August 1968.
23. Shenk, W. E., "Meteorological Satellite Infrared Views of Cloud Growth Associated with the Development of Secondary Cyclones," Monthly Weather Review, V. 98, No. 11, p. 861-868, November 1970.
24. Smith, W. L., Wolf, H. M. and Jacob, W. J., "A Regression Method for Obtaining Real-Time Temperature and Geopotential Height Profiles from Satellite Spectrometer Measurements and Its Application to NIMBUS III 'SIRS' Observations," Monthly Weather Review, Vol. 98, No. 8, p. 582-603, August 1970.
25. Weather Bureau Forecasters Handbook No. 1, Office of Meteorological Operations, Environmental Science Services Administration (ESSA), December 1967.
26. World Meteorological Organization Technical Note No. 75, The Use of Satellite Pictures in Weather Analyses, by Anderson, R. K., Ferguson, E. W., and Oliver, V. J. 1966.

INITIAL DISTRIBUTION LIST

		No. Copies
1.	Library, Code 0212 Naval Postgraduate School Monterey, California 93940	2
2.	CDR H. D. Hamilton, Code 51Ho Department of Meteorology Naval Postgraduate School Monterey, California 93940	1
3.	Professor Robert J. Renard, Code 51Rd Department of Meteorology Naval Postgraduate School Monterey, California 93940	19
4.	LCDR T. J. Mantei PATRON THIRTY-ONE Naval Air Station Moffett Field, California 94035	2
5.	LCDR C. E. Workman Fleet Numerical Weather Central Monterey, California 93940	2
6.	Commanding Officer Fleet Numerical Weather Central Monterey, California	2
9.	Officer in Charge Environmental Prediction Research Facility Monterey, California 93940	1

DOCUMENT CONTROL DATA - R & D

(Security classification of title, body of abstract and indexing annotation must be entered when the overall report is classified)

1. ORIGINATING ACTIVITY (Corporate author) Naval Postgraduate School Monterey, California 93940		2a. REPORT SECURITY CLASSIFICATION Unclassified	
		2b. GROUP	
3. REPORT TITLE Experimental Use of Satellite-Derived Data in Numerical Analysis and the Effect on a Primitive Equation Prediction Scheme			
4. DESCRIPTIVE NOTES (Type of report and inclusive dates) Master's Thesis; December 1971			
5. AUTHOR(S) (First name, middle initial, last name) Thomas Joseph Mantei and Charles Edwin Workman			
6. REPORT DATE December 1971		7a. TOTAL NO. OF PAGES 119	7b. NO. OF REFS 26
8a. CONTRACT OR GRANT NO.		9a. ORIGINATOR'S REPORT NUMBER(S)	
b. PROJECT NO.			
c.		9b. OTHER REPORT NO(S) (Any other numbers that may be assigned this report)	
d.			
10. DISTRIBUTION STATEMENT Approved for public release; distribution unlimited			
11. SUPPLEMENTARY NOTES		12. SPONSORING MILITARY ACTIVITY Naval Postgraduate School Monterey, California 93940	
13. ABSTRACT The results of an experiment to test the utility of satellite-observed data for enhancing the accuracy and detail of numerical analyses and its effect on the attendant primitive equation (PE) prognoses is presented. The test, carried out in the framework of Fleet Numerical Weather Central's system, employed SIRS data and various quasi objective techniques to establish bogus pressure/height and wind data at sea level/500 mb over the North Pacific Ocean area. The resulting satellite-modified analyses for five synoptic times, in the period 10-12 March 1971, were used to generate PE prognoses from 1200 GMT 10 March and 0000 GMT 11 March 1971. Comparison with PE prognoses from analyses dependent only on conventional data indicated relatively more improvement at sea level than at 500 mb. The complex results are interpreted in terms of the initialization of the analyzed fields, known behavioral characteristics of the PE model, the mechanics of the modification procedures and the experience level of the analysts.			

KEY WORDS

LINK A

LINK B

LINK C

ROLE

WT

ROLE

WT

ROLE

WT

Numerical Weather Analysis and Prediction

Weather Satellite Observational Data

SIRS Data

Surface and 500 mb Analysis

BINDERY

Thesis

130814

M334 Mantei

c.1

Experimental use of
satellite-derived data
in numerical analysis and
the effect on a primitive
equation prediction
scheme.

BINDERY

TH
M3
C

Thesis

130814

M334 Mantei

c.1

Experimental use of
satellite-derived data
in numerical analysis and
the effect on a primitive
equation prediction
scheme.

thesM334

Experimental use of satellite-derived da



3 2768 002 04259 0

DUDLEY KNOX LIBRARY